United States
Environmental Protection
Agency

Office of Mobile Sources
Emission Control Technology Division
2565 Plymouth Road
Ann Arbor, Michigan 48105

EPA 460/3-86-001
March 1986

Air

EPA

Photochemical Modeling of Methanol-Use Scenarios in Philadelphia

EPA 460/3-86-001

Photochemical Modeling of Methanol-Use Scenarios in Philadelphia

by

G.Z. Whitten
N. Yonkow
T.C. Myers

Systems Applications, Inc.
101 Lucas Valley Road
San Rafael, California 94903

Contract No. 68-02-3870
Work Assignment 6

EPA Project Officer: Thomas N. Braverman
Technical Representative: Penny M. Carey

Prepared for

U.S. ENVIRONMENTAL PROTECTION AGENCY
Office of Mobile Sources
Emission Control Technology Division
2565 Plymouth Road
Ann Arbor, Michigan 48105

March 1986

This report was furnished to the Environmental Protection Agency by Systems Applications, Inc., 101 Lucas Valley Road, San Rafael, California, in fulfillment of Work Assignment 6 and 2- of Contract No. 68-02-3870. The contents of this report are reproduced herein as received from Systems Applications, Inc. The opinions, findings, and conclusions expressed are those of the authors and not necessarily those of the Environmental Protection Agency. Mention of company product names is not to be considered as an endorsement by the Environmental Protection Agency.

Publication No. 460/3-86-001

CONTENTS

ILLUSTRATIONS

TABLES

ABSTRACT

A photochemical modeling study was conducted to estimate the impact on smog production resulting from the substitution of methanol fuel for gasoline and diesel fuel in Philadelphia in the year 2000. Three photochemical models were used: a comprehensive grid model adapted from the Urban Airshed Model (UAM), a four-cell trajectory model (a Lagrangian version of the UAM), and a single-cell box model. All three models used identical chemical mechanisms and input data based on observations for two days in July of 1979. Emission rates, initial conditions, and boundary values were forecast to the year 2000. Mobile sources and stationary sources related to mobile source emissions were estimated to make up 20 percent of the total volatile organic (VOC) inventory for 2000. At the 20 percent methanol substitution level, i.e., complete substitution of mobile source VOC with 90 percent methanol/10 percent formaldehyde, methanol-related emissions show little or no impact on smog formation unless methanol is also substituted for 20 percent of the initial and boundary concentrations. Model sensitivity tests indicate that methanol substitution above 20 percent of the overall VOC inventory may significantly inhibit smog formation, but the reduction also depends strongly on other factors such as formaldehyde emissions, methanol carryover from upwind sources or previous days, and NO_x levels. Whereas formaldehyde emissions tend to accelerate ozone formation, methanol carryover and NO_x emissions tend to decrease ozone formation.

SECTION 1

INTRODUCTION

This report discusses the investigation of the potential impact of methanol fuel substitution in Philadelphia based on scenarios for the year 2000. The work was performed by Systems Applications, Inc. under the sponsorship of the Office of Mobile Sources (OMS) of the U.S. Environmental Protection Agency. Previous research has shown that methanol can be used as an alternative to gasoline and diesel fuels. The results of studies by Whitten and Hogo (1983) and Pefley, Pullman, and Whitten (1984) in Los Angeles indicate that conversion to methanol fuel on a large scale could reduce ozone levels and that methanol-fueled vehicles, which emit volatile organics (VOC) with lower reactivity than that of gasoline-fueled vehicles thus produce less photochemical smog.

In the previous study by Whitten and Hogo (1983), the Systems Applications trajectory model, which uses inputs common to both the Urban Airshed Model (UAM) and EKMA, was used to predict ozone reduction resulting from methanol fuel use in Los Angeles. The EKMA model can utilize alternative chemical reaction schemes as input, whereas in the UAM, the chemical mechanism is fixed to the computer code. The purpose of the study reported here was to investigate the effects of methanol substitution in a major urban area other than Los Angeles using the Urban Airshed Model (UAM), which is a preferred EPA model, in addition to the Systems Applications trajectory model and a single-cell box model. Because the substitution of methanol for gasoline involves a kinetic mechanism for methanol chemistry and also emphasizes the chemistry of formaldehyde (its main oxidation product), for the study reported here, a new UAM computer code was prepared based on an updated and expanded chemical mechanism featuring explicit formaldehyde and methanol chemistry. The methanol component of this new mechanism has been recently validated in a smog chamber study by Pefley, Pullman, and Whitten (1984).

Sections 2 and 3, respectively, describe the computer models and the input data used in this study. Section 4 contains a discussion of the results; Section 5 presents the summary and conclusions.

SECTION 2

DESCRIPTION OF MODELS USED

Three atmospheric models (a four-cell trajectory, a single-cell box model, and the Urban Airshed Model (UAM)) were used in this study. All three models contain the same chemical submodel, or mechanism, which is based on the Carbon-Bond III Mechanism (CBM-3), but which contains an explicit treatment of formaldehyde and methanol. The trajectory model and the box model are linked to the UAM grid model in the following manner: the trajectory model shares input files and computer algorithms with the UAM and is, in essence, a pilot cell for tracing a key trajectory path through the gridded framework of the UAM. The box model uses averaged inputs developed from the trajectory model. Because the box model is capable of generating isopleth diagrams, sensitivity tests can easily be implemented. The basic chemistry submodel, or mechanism, common to all three models used in this study, is described, followed by a description of each model.

CHEMICAL SUBMODEL

The substitution of methanol for gasoline as a transportation fuel changes the atmospheric chemistry of an urban airshed. Therefore, the chemical mechanism used to simulate the atmospheric chemistry of an urban area is of primary importance in assessing the effect of this substitution on oxidant formation. For this project, the primary urban atmospheric chemical reactions were simulated with a modified version (CBM-3M) of the Carbon-Bond III Mechanism (CBM-3). The unmodified version, CBM-3, is currently approved for oxidant assessment and State Implementation Plan (SIP) preparation by the U.S. Environmental Protection Agency (EPA, 1984). Technical descriptions of this mechanism and its use in atmospheric oxidant modeling can be found in Killus and Whitten (1984) and EPA, (1984).

The CBM-3 was designed to simulate typical gasoline-influenced urban atmospheres and not for the specific task of simulating methanol-related impacts. Because the reactivity of methanol to hydroxyl radical reaction is similar to that of the species PAR in the CBM-3, the unmodified CBM-3

may actually be suitable for methanol assessment. However, in this project the actual concentrations of methanol and, perhaps even more important, the concentrations of formaldehyde, as well as their chemistries, are essential in understanding the overall impact of methanol fuel substitution. Formaldehyde is the main oxidation product of methanol in both combustion and atmospheric photooxidation:

$$OH + CH_3OH \longrightarrow CH_2OH + H_2O \quad , \qquad (1)$$

$$CH_2OH + O_2 \longrightarrow HO_2 + HCHO \quad . \qquad (2)$$

Because water is not a significant direct product of methanol photochemistry, and because the second reaction is extremely fast and the sole pathway of CH_2OH loss, the entire chemistry of methanol can be condensed to one reaction, which produces formaldehyde and the hydroperoxyl radical:

$$CH_3OH + OH \longrightarrow HCHO + HO_2$$

The hydroxyl and hydroperoxyl radical species are central to the atmospheric chemistry of ozone formation and are treated explicitly in all current atmospheric chemical mechanisms. However, in the CBM-3 mechanism, formaldehyde is treated as part of a generalized lumped species for all carbonyl compounds (CARB). Hence, the main modification to the CBM-3 for this project was the addition of an explicit treatment of formaldehyde chemistry. Tables 1 and 2, respectively, present the CBM-3 described in Killus and Whitten (1984) and the modified version (CBM-3M) used for this project, which involved the addition of the reaction for methanol and an explicit treatment of formaldehyde.

As can be seen in Table 2, there are several points in the CBM-3M mechanism where formaldehdye is produced. This "delumping" of formaldehyde represents an improvement over the CBM-3 since the species CARB is parameterized to account for formaldehyde plus all other carbonyl species in CBM-3, whereas in the CBM-3M, the CARB parameters relating to formaldehyde have been eliminated or reduced.

Modifications that improve the chemical accuracy of the CBM-3M have been made to reactions 21, 25, 27, 28, 43, 44, 60, and 61. In the CBM-3, as shown in Table 1, all these reactions lead to the species CARB when formaldehyde is known to be a product. Thus, the subsequent chemistry of

TABLE 1. CARBON-BOND MECHANISM III

	Reaction	Rate Constant at 298K ($ppm^{-1}min^{-1}$)	Activation Energy (K)
1	$NO_2 \rightarrow NO + O$	*	0
2	$O + (O_2) + (M) \rightarrow O_3$	4.40×10^{6}†	0
3	$NO + O_3 \rightarrow NO_2 + O_2$	26.6	1450
4	$NO_2 + O_3 \rightarrow NO_3 + O_2$	0.048	2450
5	$NO_2 + O \rightarrow NO + O_2$	1.3×10^{4}	0
6	$OH + O_3 \rightarrow HO_2 + O_2$	100	1000
7	$HO_2 + O_3 \rightarrow OH + 2O_2$	2.40	1525
8	$OH + NO_2 \rightarrow HNO_3$	1.60×10^{4}	0
9	$OH + CO \xrightarrow{O_2} HO_2 + CO_2$	440	0
10	$NO + NO + (O_2) \rightarrow NO_2 + NO_2$	1.50×10^{-4}†	0
11	$NO + NO_3 \rightarrow NO_2 + NO_2$	2.80×10^{4}	0
12	$NO_2 + NO_3 + H_2O \rightarrow 2HNO_3$	§	-1.06×10^{4}
13	$NO + HO_2 \rightarrow NO_2 + OH$	1.20×10^{4}	0
14	$HO_2 + HO_2 \rightarrow H_2O_2 + O_2$	1.50×10^{4}	0
15	$X + PAR \rightarrow$	10^{5}	0
16	$OH + PAR \xrightarrow{O_2} MEO_2 + H_2O$	1300	560
17	$O + OLE \xrightarrow{O_2} MEO_2 + ACO_3 + X$	2700	325
18	$O + OLE \rightarrow CARB + PAR$	2700	325
19	$OH + OLE \xrightarrow{O_2} RAO_2$	3.70×10^{4}	-540

(continued)

TABLE 1.

	Reaction	Rate Constant at 298K ($ppm^{-1}min^{-1}$)	Activation Energy (K)
20	O_3 + OLE → CARB + CRIG	0.008	1900
21	O_3 + OLE → CARB + MCRG + X	0.008	1900
22	O + ETH $\xrightarrow{O_2}$ MEO_2 + HO_2 + CO	600	800
23	O + ETH → CARB + PAR	600	800
24	OH + ETH $\xrightarrow{O_2}$ RBO_2	1.20×10^4	-382
25	O_3 + ETH → CARB + CRIG	0.0024	2560
26	NO + ACO_3 $\xrightarrow{O_2}$ NO_2 + MEO_2	1.04×10^4	0
27	NO + RBO_2 $\xrightarrow{O_2}$ NO_2 + CARB + HO_2 + CARB	1.20×10^4	0
28	NO + RAO_2 $\xrightarrow{O_2}$ NO_2 + CARB + HO_2 + CARB	1.20×10^4	0
29	NO + MEO_2 $\xrightarrow{O_2}$ NO_2 + CARB + MEO_2 + X	3800	0
30	NO + MEO_2 $\xrightarrow{O_2}$ NO_2 + CARB + HO_2	7700	0
31	NO + MEO_2 → NRAT	500	0
32	O_3 + RBO_2 → CARB + CARB + HO_2 + O_2	5.0	0
33	O_3 + RAO_2 → CARB + CARB + HO_2 + O_2	200	0
34	OH + CARB → CRO_2 + X	500	0
35	OH + CARB $\xrightarrow{O_2}$ HO_2 + CO	7000	0
36	OH + CARB $\xrightarrow{O_2}$ ACO_3 + X	6000	0
37	CARB → CO + H_2	($\approx$0.001 K_1)*	0
38	CARB + (O_2) $\xrightarrow{O_2}$ 2/3 ($2HO_2$ + CO) 1/3 ($2MEO_2$ + CO + 2X)	($\approx$0.002 K_1)*	0

(continued)

TABLE 1.

	Reaction	Rate Constant at 298K ($ppm^{-1}min^{-1}$)	Activation Energy (K)
39	$NO_2 + ACO_3 \rightarrow PAN$	7000	0
40	$PAN \rightarrow ACO_3 + NO_2$	0.022	1.35×10^4
41	$HO_2 + ACO_3 \rightarrow$ Stable products	1.50×10^4	0
42	$HO_2 + MEO_2 \rightarrow$ Stable products	9000	0
43	$NO + CRIG \rightarrow NO_2 + CARB$	1.20×10^4	0
44	$NO_2 + CRIG \rightarrow NO_3 + CARB$	8000	0
45	$CARB + CRIG \rightarrow$ Ozonide	2000	0
46	$NO + MCRG \rightarrow NO_2 + CARB + PAR$	1.20×10^4	0
47	$NO_2 + MCRG \rightarrow NO_3 + CARB + PAR$	8000	0
48	$CARB + MCRG \rightarrow$ Ozonide	2000	0
49	$CRIG \rightarrow CO + H_2O$	670**	0
50	$CRIG \rightarrow$ Stable products	240**	0
51	$CRIG \xrightarrow{O_2} HO_2 + HO_2 + CO$	90**	0
52	$MCRG \rightarrow$ Stable products	150**	0
53	$MCRG \xrightarrow{O_2} MEO_2 + OH + CO$	340**	0
54	$MCRG \xrightarrow{O_2} MEO_2 + HO_2$	425**	0
55	$MCRG \xrightarrow{O_2} CARB + HO_2 + CO + HO_2$	85**	0
56	$OH + ARO \xrightarrow{O_2} RARO + H_2O$	8000	600
57	$OH + ARO \xrightarrow{O_2} HO_2 + OPEN$	1.45×10^4	400
58	$NO + RARO \xrightarrow{O_2} NO_2 + PHEN + HO_2$	4000	0

(continued)

TABLE 1.

	Reaction	Rate Constant at 298K ($ppm^{-1}min^{-1}$)	Activation Energy (K)
59	$OPEN + NO \xrightarrow{O_2} NO_2 + DCRB + X + APRC$	6000	0
60	$APRC \xrightarrow{O_2} DCRB + CARB + CO + X$	10^{4}**	0
61	$APRC \xrightarrow{O_2} CARB + CARB + CO + CO$	10^{4}**	0
62	$PHEN + NO_3 \rightarrow PHO + HNO_3$	5000	0
63	$PHO + NO_2 \rightarrow NPHN$	4000	0
64	$PHO + HO_2 \rightarrow PHEN$	5.00×10^{4}	0
65	$OPEN + O_3 \rightarrow DCRB + X + APRC$	40	0
66	$OH + PHEN \xrightarrow{O_2} HO_2 + APRC + PAR + CARB$	3.00×10^{4}	0
67	$DCRB \xrightarrow{O_2} 1/2\ (HO_2 + ACO_3 + CO)$ $1/2\ (MEO_2 + HO_2 + 2CO)$	$(\approx 0.04\ K_1)$*	0
68	$PHEN + OH \rightarrow PHO$	10^{4}	0
69	$CRO_2 + NO \xrightarrow{O_2} NO_2 + HO_2 + DCRB$	1.20×10^{4}	0
70	$DCRB + OH \rightarrow ACO_3 + CO$	7000	0
71	$HONO \rightarrow OH + NO$	$(\approx 0.3\ K_1)$*	0
72	$OH + NO \rightarrow HONO$	9770	0
73	$O_3 \rightarrow O^1D$	$(\approx 4 \times 10^{-4}\ K_1)$*	0
74	$O^1D \xrightarrow{+(M)} O$	4.44×10^{10}	0
75	$O^1D + H_2O \rightarrow OH + OH$	3.4×10^{5}	0

* Sunlight-dependent; units of min^{-1}.

† Units of $ppm^{-2}min^{-1}$.

§ Heterogeneous; pseudo third order. Equal to $591 \times N_2O_5 + H_2O$.

** Units of min^{-1}.

TABLE 2. CARBON-BOND MECHANISM-3M.

	Reaction	Rate Constant at 298 K (ppm^{-1} min^{-1})	Activation Energy (°K)
1	$NO_2 \rightarrow NO + O$	1.0*	0
2	$O + (O_2) + (M) \rightarrow O_3$	4.40×10^{6}**	0
3	$NO + O_3 \rightarrow NO_2 + O_2$	26.6	1450
4	$NO_2 + O_3 \rightarrow NO_3 + O_2$	0.048	2450
5	$NO_2 + O \rightarrow NO + O_2$	1.3×10^{4}	0
6	$OH + O_3 \rightarrow HO_2 + O_2$	100	1000
7	$HO_2 + O_3 \rightarrow OH + 2O_2$	2.40	1525
8	$OH + NO_2 \rightarrow HNO_3$	1.60×10^{4}	0
9	$OH + CO \xrightarrow{O_2} HO_2 + CO_2$	440	0
10	$NO + NO + (O_2) \rightarrow NO_2 + NO_2$	1.50×10^{-4}	0
11	$NO + NO_3 \rightarrow NO_2 + NO_2$	2.80×10^{4}	0
12	$NO_2 + NO_3 + H_2O \rightarrow 2HNO_3$	2.600×10^{-5}	-1.06×10^{4}
13	$NO + HO_2 \rightarrow NO_2 + OH$	1.20×10^{4}	0
14	$HO_2 + HO_2 \rightarrow H_2O_2 + O_2$	1.50×10^{4}	0
15	$X + PAR \rightarrow$	10^{5}	0
16	$OH + PAR \xrightarrow{O_2} RO_2 + X + H_2O$	1200	560
17	$O + OLE \xrightarrow{O_2} RO_2 + ACO_3 + XX$	2700	325
18	$O + OLE \rightarrow HCHO + PAR$	2700	325
19	$OH + OLE \xrightarrow{O_2} RAO_2 + X$	3.70×10^{4}	-540

Continued

TABLE 2 (continued)

	Reaction	Rate Constant at 298 K ($ppm^{-1}\ min^{-1}$)	Activation Energy (°K)
20	O_3 + OLE → HCHO + CRIG + X	0.008	1900
21	O_3 + OLE → HCHO + MCRG + X	0.008	1900
22	O + ETH $\xrightarrow{O_2}$ MEO_2 + HO_2 + CO	600	800
23	O + ETH → HCHO + PAR	600	800
24	OH + ETH $\xrightarrow{O_2}$ RBO_2	1.20×10^4	-382
25	O_3 + ETH → HCHO + CRIG	0.0024	2560
26	NO + ACO_3 $\xrightarrow{O_2}$ NO_2 + MEO_2	1.04×10^4	0
27	NO + RBO_2 $\xrightarrow{O_2}$ NO_2 + HCHO + HO_2 + HCHO	1.20×10^4	0
28	NO + RAO_2 $\xrightarrow{O_2}$ NO_2 + CARB + HO_2 + HCHO	1.20×10^4	0
29	NO + MEO_2 $\xrightarrow{O_2}$ NO_2 + CARB + RO_2 + XX	5.00×10^3	0
30	NO + MEO_2 $\xrightarrow{O_2}$ NO_2 + CARB + HO_2	6.00×10^3	0
31	NO + MEO_2 → NRAT + PAR	1.20×10^3	0
32	O_3 + RBO_2 → HCHO + HCHO + HO_2 + O_2	5.0	0
33	O_3 + RAO_2 → CARB + HCHO + HO_2 + O_2	20	0
34	OH + CARB → CRO_2 + X	200	0
35	OH + HCHO $\xrightarrow{O_2}$ HO_2 + CO	1.50×10^4	0
36	OH + CARB $\xrightarrow{O_2}$ ACO_3 + X	2.00×10^4	0
37	HCHO → CO + H_2	0.39	0
38a	HCHO + $\xrightarrow{O_2}$ CO + HO_2 + HO_2	1	0
38b	XCO + PAR → CO	10^5	

Continued

TABLE 2 (continued)

	Reaction	Rate Constant at 298 K (ppm^{-1} min^{-1})	Activation Energy (°K)
39	$NO_2 + ACO_3 \rightarrow PAN$	7000	0
40	$PAN \rightarrow ACO_3 + NO_2$	0.022	1.35×10^4
41	$HO_2 + ACO_3 \rightarrow$	1.50×10^4	0
42	$HO_2 + MEO_2 \rightarrow$	9000	0
43	$NO + CRIG \rightarrow NO_2 + HCHO$	1.20×10^4	0
44	$NO_2 + CRIG \rightarrow NO_3 + HCHO$	8000	0
45	$HCHO + CRIG \rightarrow$	2000	0
46	$NO + MCRG \rightarrow NO_2 + CARB + PAR$	1.20×10^4	0
47	$NO_2 + MCRG \rightarrow NO_3 + CARB + PAR$	8000	0
48	$HCHO + MCRG \rightarrow$	2000	0
49	$CRIG \rightarrow CO + H_2O$	670**	0
50	$CRIG \rightarrow$	240**	0
51	$CRIG \xrightarrow{O_2} HO_2 + HO_2 + CO$	90**	0
52	$MCRG \rightarrow$	150**	0
53	$MCRG \xrightarrow{O_2} RO_2 + OH + CO + X$	340**	0
54	$MCRG \xrightarrow{O_2} RO_2 + HO_2 + X$	425**	0
55	$MCRG \xrightarrow{O_2} CARB + HO_2 + XCO + HO_2$	85**	0
56	$OH + ARO \xrightarrow{O_2} RARO + H_2O$	6000	600
57	$OH + ARO \xrightarrow{O_2} HO_2 + OPEN$	1.45×10^4	400
58	$NO + RARO \xrightarrow{O_2} NO_2 + PHEN + HO_2$	4000	0

Continued

TABLE 2 (continued)

	Reaction	Rate Constant at 298 K (ppm^{-1} min^{-1})	Activation Energy (°K)
59	$OPEN + NO \xrightarrow{O_2} NO_2 + DCRB + X + APRC$	6000	0
60	$APRC \xrightarrow{O_2} DCRB + HCHO + CO + X$	10^{4**}	0
61	$APRC \xrightarrow{O_2} HCHO + HCHO + CO + CO$	10^{4**}	0
62	$PHEN + NO_3 \rightarrow PHO + HNO_3$	5000	0
63	$PHO + NO_2 \rightarrow NPHN$	4000	0
64	$PHO + HO_2 \rightarrow PHEN$	5.00×10^4	0
65	$OPEN + O_3 \rightarrow DCRB + X + APRC$	40	0
66	$OH + PHEN \xrightarrow{O_2} HO_2 + APRC + PAR + CARB$	3.00×10^4	0
67	$DCRB \xrightarrow{O_2} HO_2 + ACO_3 + CO$	$(0.02 \times K_1)^{**}$	0
68	$PHEN + OH \rightarrow PHO$	10^4	0
69	$CRO_2 + NO \xrightarrow{O_2} NO_2 + CARB + ACO_3 + X$	1.20×10^4	0
70	$DCRB + OH \rightarrow ACO_3 + CO$	25000.	0
71	$HONO \rightarrow OH + NO$	$(3.1^{*}$ or $0.18^{**} \times K_1)$	0
72	$OH + NO \rightarrow HONO$	9770	0
73	$O_3 \rightarrow O^1D$	1.15	0
74	$O^1D \xrightarrow{+(M)} O$	4.44×10^{10}	0
75	$O^1D + H_2O \rightarrow OH + OH$	3.4×10^5	0
76	$O_3 \rightarrow O$	$(1.0)^{*}$	
77	$NR \rightarrow$	0.0	
78	$OH \rightarrow HO_2$	88	0

Continued

TABLE 2 (concluded)

	Reaction	Rate Constant at 298 K (ppm^{-1} min^{-1})	Activation Energy (°K)
79	CARB → MEO_2 + HO_2 + CO	1	0
80	NO + MEO_2 → NO_2 + HCHO + HO_2	1.20×10^4	0
81	HO_2 + RO_2 →	9.00×10^3	0
82	CARB + CRIG →	2.00×10^3	0
83	CARB + MCRG →	2.00×10^3	0
84	OH + METH → HCHO + HO_2	1.60×10^3	0
85	XX + PAR → X	1.00×10^5	0

* Sunlight-dependent; rate constant is correction factor for OZIPM input, units of min^{-1}.

† Units of $ppm^{-2}min^{-1}$.

** Units of min^{-1}.

85111/ 8

CARB in the CBM-3 assumed that a fixed percentage (55 percent) of the CARB reacted as formaldehyde. When substantial amounts of methanol are added to an urban atmosphere, the fraction of carbonyls that is formaldehyde may change from this fixed 55 percent. The formaldehyde ratio can also change with the time of day. Hence, the explicit treatment of formaldehyde is an improvement in accuracy over the original CBM-3 and is more appropriate for assessing the impacts of methanol substitution on oxidant formation. Finally, the separate treatment of formaldehyde chemistry is useful for assessing the changes in the formaldehyde concentrations themselves because formaldehyde is a toxic substance.

Additional improvements in the CBM-3M chemistry are associated with the radical species MEO_2, RO_2, and ACO_3. First, all organic peroxyl radicals containing more than one carbon are lumped into a new species and MEO_2 is used exclusively for the methylperoxy radical. In the CBM-3 (Table 1), MEO_2 represents all organic peroxyl radicals, whereas in CBM-3M (Table 2), the acylperoxy radical, ACO_3, reacts to form MEO_2, which yields 100 percent formaldehyde from PAN decomposition in the presence of NO (reaction 40 followed by reaction 26). In the original CBM-3, the MEO_2 formation implied only 55 percent formaldehyde (reactions 40 and 26). Although 100 percent formaldehyde represents an overestimation of formaldehyde production because other PAN-like compounds can lead to carbonyls other than formaldehyde, most atmospheric measurements show that PAN itself is by far the main peroxyacetylnitrate seen in urban atmospheres. Hence, the 55 percent formaldehyde value in the original CBM-3 is an underestimate.

The main parameter adjustments in the modified CBM-3M are found in reactions 29, 30, and 31 of Table 2. The ratios of these three pathways control the recirculation of RO_2 and the formation of organic nitrates. The former represents the unimolecular decomposition and isomerization reactions of alkoxy radicals. The organic nitrate formation pathway was revised somewhat from that of the CBM-3 because the methylperoxy radicals, which are treated explicitly as MEO_2 in CBM-3M, form very few nitrates. The final values chosen for reactions 29, 30, and 31 in the CBM-3M were based more on their agreement with the original CBM-3 than on fundamental principles since such a fundamental approach was beyond the scope of this project. The overall reactivity of the CBM-3 and CBM-3M was tested by comparing two EKMA runs that used the two different mechanisms and identical inputs from data taken on 24 June 1980 in Philadelphia. Table 3 lists hourly ozone predictions for both EKMA runs and shows that results obtained with the two mechanisms agree within 8 percent. The pathway ratios of reactions 29, 30, and 31 were adjusted within the range of fundamental uncertainty to match the overall reactivity of the CBM-3.

TABLE 3. HOURLY OZONE PREDICTIONS FOR CBM-3 and CBM-3M EKMA SIMULATIONS

Hour	Ozone (ppm)	
	CBM-3	CBM-3M
0800	9×10^{-3}	9×10^{-3}
0900	1.63×10^{-2}	1.70×10^{-2}
1000	3.21×10^{-2}	3.40×10^{-2}
1100	4.84×10^{-2}	5.15×10^{-2}
1200	6.88×10^{-2}	7.32×10^{-2}
1300	9.53×10^{-2}	1.00×10^{-1}
1400	1.24×10^{-1}	1.28×10^{-1}
1500	1.45×10^{-1}	1.47×10^{-1}
1600	1.55×10^{-1}	1.577×10^{-1}
1700	1.65×10^{-1}	1.68×10^{-1}
1800	1.71×10^{-1}	1.74×10^{-1}

DESCRIPTION OF THE URBAN AIRSHED MODEL

The Urban Airshed Model (UAM) simulates the major physical and chemical processes associated with ozone formation in the polluted troposphere. These processes include gas-phase chemistry, advective transport, and turbulent diffusion. The UAM model domain is divided into a large array of grid cells (Figure 1). The horizontal cells are uniform 5 x 5 km squares. Typically, four or five layers of cells represent the vertical domain. The depth of the cells is determined by the height of the mixed layer and the height of the top of the modeling domain. The mixed layer typically ranges from as low as 50 m in the morning hours to 1000 m or more in the afternoon. Emissions are injected into individual cells depending on the location of the sources, their height release, and the buoyant rise of individual stack gas plumes.

The UAM is first operated for some base-case situation to identify a point in the gridded array at which an important feature occurs in both space and time. For this project, the important feature was the time and place of the maximum ozone concentration occurring within the entire UAM modeling region. Other important features might have been the monitoring station site showing the highest one-hour maximum ozone concentration or the grid point in space and time at which the highest formaldehyde concentration was simulated to occur.

DESCRIPTION OF THE SYSTEMS APPLICATIONS TRAJECTORY MODEL AND THE BOX MODEL USED IN THE PHILADELPHIA STUDY

Two models were used in conjunction with the UAM to assess the effects of methanol use in Philadelphia; the Systems Applications trajectory model (Myers et al., 1979) was used to trace and process UAM inputs. These inputs were then used in a single cell box model, which served as the primary trajectory model for this study. Using the grid point in space and time determined by the UAM, the Systems Applications' cell trajectory model is first run backwards through the UAM wind field in the mixed layer. Because in this study wind shear was present within the mixed layer for the days simulated by the UAM, the winds in the two layers that make up the mixed layer were vector-averaged to define the trajectory path. This path was then traced backwards in time until the boundary of the modeling region was reached or until the UAM midnight starting time if the boundary was not reached by midnight. Two days in 1979, 13 and 19 July, formed the meteorological base cases. The trajectory for the 13 July case started within the gridded region at the UAM midnight starting time; the trajectory for the 19 July case started from the eastern boundary at 0700 hours.

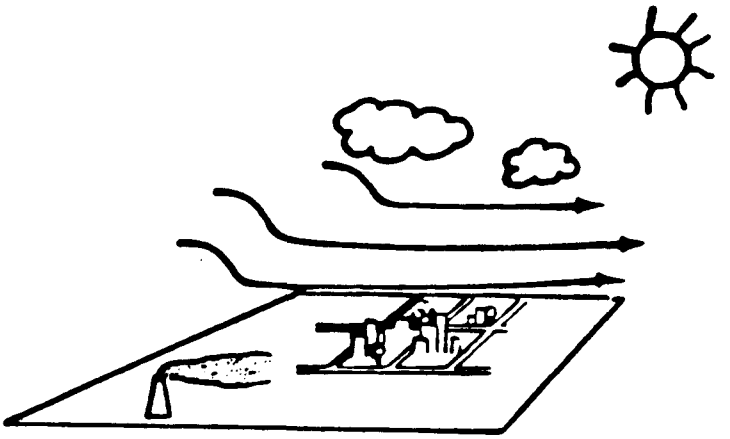

(a) The Area To be Modeled

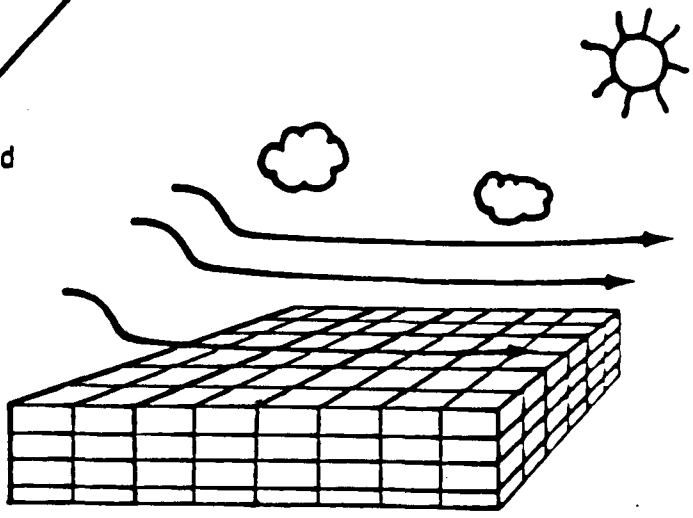

(b) Specification of the Grid

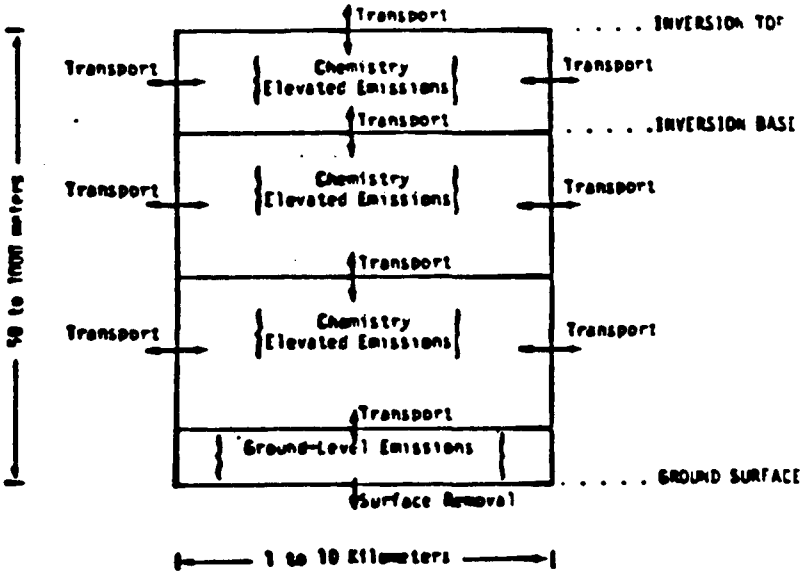

(c) Atmospheric Processes Treated in a Column of Grid Cells

FIGURE 1. Schematic illustration of the grid used and treatment of atmospheric processes in the SAI Airshed Model.

As the intermediate trajectory model runs forward in time, it traces the gridded emissions inventory following a path one grid cell in width. The same vertical cell structure and chemical algorithms are used for both the trajectory model and the UAM. Hence, there are four cells that mix vertically, react chemically, and entrain fresh emissions using the same input files and computer code as the UAM itself. The only differences between the UAM and this intermediate trajectory model, besides the vast difference in the number of total cells simulated, are the lack of vertical winds and horizontal dispersion in the intermediate trajectory model. Hence, the lack of agreement between results of the UAM and those of the intermediate trajectory model for the final important point defining the termination of the trajectory path becomes a measure of (1) the sensitivity or importance of the vertical winds and (2) horizontal dispersion. Unfortunately, the presence of wind shear adds a confusing factor to this measure of sensitivity because the "proper" weighting of the vector-averaging used to define the trajectory path is uncertain and wind shear adds a large amount of horizontal dispersion. A simple weighting scheme of equal contribution of each layer was used for this study.

The primary trajectory model used in this study is a box (i.e., single-cell) model developed under previous EPA contracts designed to test various components of the Empirical Kinetic Modeling Approach (EKMA). The first of these projects was reported in Whitten et al. (1981). A more recent model application that assessed methanol substitution in the Los Angeles area is described by Whitten and Hogo (1983). Although much of the computer code used to run this moving box model is identical to the code used in EKMA, the model is considerably different from the standard EKMA model; therefore, the name "EKMA" should not be used to describe the box model used in this study. The standard EKMA trajectory model is a stand-alone model that uses inputs generated by prescribed guidelines and that is dominated by initial conditions at the 0800 starting time. The inputs, chemical mechanism, and starting time of the box model used in this study are all identical to those of the UAM.

Although inputs used by the box model are the same as those used by the UAM, the box model uses only a subset of the UAM inputs. These simplified input requirements make it easier to run sensitivity tests with the box model than with UAM and trajectory models. To discover the effect of changing certain parameters on UAM or trajectory model results, inputs to the entire grid system must be changed, which can be very expensive. However, such inputs as emissions, initial conditions, and temperature need only be changed along the trajectory path if the box model is used. Before the box model can be run, however, the UAM and trajectory models must be used at least once to establish appropriate wind fields and a trajectory path. Thereafter, the box model can be run numerous times at a minimal cost. Finally, the UAM can be run to confirm interesting cases discovered from exploratory tests using the box model.

SECTION 3

DESCRIPTION OF MODEL INPUTS

URBAN AIRSHED MODEL GENERAL INPUT PREPARATION PROCEDURES

The Urban Airshed Model (UAM) is capable of providing the most accurate air quality predictions obtainable, given the current state of knowledge of atmospheric processes and available air pollution data. Almost any aerometric measurements pertaining to a physical or chemical atmospheric process can be input to the UAM. However, in many instances it is not possible to establish a model input directly from measured data. For example, it is not practical to measure the wind speed and direction in every grid cell; therefore, available wind data can be used in conjunction with a mathematical interpolation routine to generate suitable inputs. In some instances, if sufficient data are not available for a specific parameter, it may be necessary to assume that the value of the parameter in one area is equal to that measured in another area. Interpolation between data points can also be used.

In general, data input preparation procedures should be adapted to the region of interest through algorithms that make the best possible use of available data. Such algorithms are especially important when the data are insufficient or otherwise inappropriate to characterize a specific input. For example, in a Los Angeles study by Reynolds et al. (1973), the available data were not adequate to develop complete temperature profiles of the area. Therefore, instead of employing an algorithm that used only the limited data available, a specific algorithm was developed that used both available data and the results of previous studies, which indicated that mixing depth contours should be parallel to the coastline. Straightforward mathematical interpolation of the data would have yielded different, and less accurate, mixing depths.

Emission, meteorological, and air quality inputs provide further illustrations of UAM input preparation procedures. Emission inputs are prepared from available information pertaining to mobile, stationary, and natural sources of organic compounds, NO_x, CO, SO_2, and particulates.

Gridded mobile emission inputs are most conveniently obtained from a transportation model that calculates traffic volumes and then relates them to motor vehicle emission factors. If a transportation model is not available for use in the area of interest, then the Vehicle-Miles-Traveled (VMT) in each grid cell can be estimated from existing traffic-count data and used in place of the traffic volume information. Distributed area source emission inputs (both natural and anthropogenic) can be estimated from land-use data. Emission rates and plume rise data for large point sources are usually available from local or state air pollution control agencies.

The organic compounds emitted from each type of source are apportioned among reactive groups in the UAM through the use of splitting factors. These factors can be derived from local measurements, or they can be estimated from data for other similar urban areas.

Preparation of UAM meteorological inputs entails estimation of three-dimensional wind fields from available surface and upper-level wind observations. Theoretical wind shear relationships can also be used in some situations to calculate wind flows aloft. Mixing depth inputs are generated from vertical temperature soundings and ground-level temperature observations. Atmospheric stability can be characterized through the use of insolation or vertical temperature sounding data.

URBAN AIRSHED MODEL INPUTS

Primary inputs to the UAM include point and area source emissions for seven species (NO, NO_2, and five carbon-bond types), initial and boundary concentrations both at the surface and aloft for eight species (seven emitted plus O_3), and a variety of meteorological data. These include a three-dimensional wind field, mixing depths, solar radiation (expressed as the equivalent NO_2 photolysis rate), surface temperature, and exposure class (an indicator of thermal instability). Inputs to the UAM are given in Table 4.

Air quality inputs are needed to establish UAM initial and boundary conditions. At the start of the simulation, the pollutant concentrations of all species must be specified for each grid call. These inputs are established through the use of existing air quality data and suitable interpolation techniques. During the simulation, the upwind "background" concentration of each pollutant must also be specified along the boundary. These values are obtained either from actual air quality observations or from estimates of natural background pollutant levels.

TABLE 4. INPUTS TO THE URBAN AIRSHED MODEL

(a) Meteorological Inputs

Category	Required Input Data
Wind speed and direction	One hour-average surface observations
	Pibal, radiosonde, or tower observations (as available)
Temperature	Hourly surface measurements
	Radiosonde, acoustic sounder, or tower observations for hourly estimates of mixing depths, vertical temperature gradient, and atmospheric stability
Water concentration	Relative humidity observations
Atmospheric pressure	Atmospheric pressure observations
Insolation	Hourly surface observations

(b) Air Quality Inputs

Category	Required Input Data
Initial conditions	One-hour-average ground-level pollutant concentrations
	Vertical pollutant distribution sounding
Boundary conditions	Ground-level pollutant concentrations at points on the upwind boundary of the modeling region
	Pollutant concentrations aloft at the top and upwind sides of the modeling region.

Continued

TABLE 4 (Continued)

(c) Emissions and Surface Uptake Inputs

Category	Required Input Data
Motor vehicle emissions	Gridded hourly emissions of each pollutant
Distributed area source emissions (including small point sources)	Gridded hourly emissions of each pollutant
Large point source emissions	Source locations
	Hourly emissions rate for each pollutant
	Stack height
	Heat flux calculated from flow rate and exit temperature data
Surface uptake process	Gridded estimates of surface roughness
	Gridded surface uptake vegetation factors

(d) Miscellaneous Inputs

Category	Required Input Data
Grid specification	Number of grid cells in the x, y, and z directions
	Horizontal grid spacing
	Location (UTM coordinates) of grid origin

Continued

TABLE 4 (Concluded)

Category	Required Input Data
Program control parameters	Start and end times for the simulation
	Initial integration time step size
	Interval over which predictions will be time-averaged (e.g., 60 minutes for one-hour-average preditions)
Chemical mechanism parameters	Reaction rate constants Activation energies

In general, the quantity of data needed by the UAM depends on the application. The number of measurements needed is related to

(1) The sensitivity of the model to variations in the parameters of interest. If the model is relatively insensitive to variations in a parameter, the data used to construct inputs for that parameter are not as important as when the model is sensitive to the particular parameter.

(2) The degree of uncertainty in the predicted results that is acceptable for the application. Model verification generally requires much more data than does rough estimation of the impact of a control strategy.

(3) The characteristics of the region, e.g., for studies that require resolution of the primary features of the wind field, fewer measurements would be required in flat terrain than in hilly or mountainous areas.

The UAM inputs used for the Philadelphia methanol study utilized data for two days--13 and 19 July 1979--previously modeled to evaluate the model as an air quality planning tool in large metropolitan areas (Haney, 1985). Although the Philadelphia-methanol UAM inputs are based on the 1979 UAM application, projections were made to the year 2000. We first present a summary of the 1979 inputs, followed by a description of the changes made to these inputs for the year 2000 Philadelphia UAM application.

INPUTS USED IN THE 1979 URBAN AIRSHED MODEL SIMULATIONS

In this section, we summarize the inputs used for each of the two modeling days.

Emissions

The emission inventory used in the 1979 UAM simulations was developed by Engineering Science (EPA, 1982). The emission region has an area of 12,500 km^2 and comprises five counties in New Jersey, five counties in Pennsylvania, and one county in Delaware. The grid system used for the emission inventory consists of 502 cells, five km on a side. Surrounding each side of the modeling region is a row of cells representing the boundary cells and containing the boundary conditions (concentrations) used in the UAM simulations. Initial conditions for all species were specified using all available monitoring data in the Philadelphia region. Initial conditions in surface grid cells without monitors were

obtained by employing a Poisson interpolation. Following the computation of the surface field, a vertical interpolation method was employed in which the background concentration at the top of the modeling region (TOPCONC) was used in levels 3 and 4, and the level 2 value was obtained by a linear interpolation between the surface (level 1) value and the level-3 value. Using this method, all grid cells in all levels were initialized with appropriate concentrations for all species. For further discussion of interpolation techniques, refer to The User's Manual for the SAI Airshed Model, (Ames et al., 1978). The monitored surface conditions for 13 and 19 July are shown in Tables 5 and 6. The Carbon-Bond fractions in Tables 5 and 6 were calculated by the EPA using the Philadelphia emissions inventory (EPA, 1982) and the Carbon-Bond system described in Killus and Whitten (1981).

Boundary Conditions

The physical boundaries and the trajectory path used in the 13 July simulation are presented in Figure 2. Because of the stagnation characteristics of this episode, much of the large airshed region was "blocked off" and not included in the simulation; however, no cells containing major emission sources were excluded by this procedure. Background values for all species for 13 July were designated for all boundaries except the southeast boundary (Table 7). Because an urban plume from Philadelphia was transported to the east late on 12 July and then recirculated back by a southeasterly flow on 13 July, there is a different set of concentrations for the southeast boundary grid cells below the mixing height (Table 8); these concentrations were made to duplicate the inflow of aged air parcels from the previous day's emissions.

Because of wind flow through the airshed on 19 July and the need to limit simulation costs, unnecessary grid cells were eliminated for this simulation. The physical boundaries and the trajectory path used for the July 19 simulation are shown in Figure 3. Background values were designated for all boundaries except the east and northeast boundaries. Estimates of boundary conditions for the east and northeast boundaries below the mixing height are presented in Table 9. Observed NO and NO_2 for 0500-0600 EST were used as input boundary values for 0000-0600. Since hydrocarbons were not measured at the Van Hiseville monitor, estimates of the influx of total reactive hydrocarbons across the northeast and east boundaries below the mixing height were specified by multiplying the hourly NO_x concentrations at the Van Hiseville monitor by the Philadelphia surface layer emission inventory hydrocarbon/NO_x ratio of 6. The total reactive hydrocarbon value was then speciated into carbon-bond components using the carbon-bond fractions of the emission inventory.

TABLE 5. MONITORED SURFACE CONDITIONS FOR 13 JULY 1979 (CONCENTRATIONS IN PPM).

Station	Easting (m)	Northing (m)	NO	NO_2	CO	O_3	RHC
AMS Lab.	491600	4428500	0.005	0.075	1.5	0.035	1.05
Ancora	511800	4392400	--	--	--	0.051	--
Brigantine	546000	4377506	--	--	--	0.037	--
Bristol	511000	4440000	--	--	--	0.000	--
Camden	491700	4419000	0.022	0.105	2.4	0.004	--
Chester	469000	4410000	--	0.030	00	0.058	2.10
Claymont	461500	4406400	--	0.045	--	--	--
Conshohocken	474500	4435600	--	--	--	0.000	--
Defense Support	483800	4418300	--	--	--	0.020	--
Downington	436000	4426000	0.002	0.012	0.2	0.073	0.00
Franklin Inst.	485200	4422800	0.010	0.065	--	0.035	--
Island Rd. Airp. Cir.	480300	4414800	--	--	--	0.010	--
Lumberton	518000	4423000	0.006	0.031	1.2	0.010	0.20
Norristown Armory	473500	4440000	--	0.075	--	0.000	0.39
Northeast Airp.	499000	4436000	0.035	0.060	--	0.000	--
Roxy Water Pump	479500	4433100	--	--	--	0.045	--
SE Sewage Plant	487200	4417300	--	--	--	0.010	--
South Broad	486100	4421600	0.020	0.080	3.5	0.035	0.30
Summit Bridge	441000	4376000	0.000	0.003	0.2	0.046	0.05
SW Corner Broad/Butler	487000	4428000	--	--	--	0.035	--
Trenton	520000	4452000	--	--	--	0.009	--
Van Hiseville	559000	4439500	0.001	0.006	0.2	0.005	--
Vineland	498200	4371200	--	0.024	--	0.054	--

RHC Component	Carbon-Bond Fraction (% as Carbon)
PAR	74.0
OLE	2.8
ETH	4.1
ARO	13.2
CARB	5.9

TABLE 6. MONITORED SURFACE CONDITIONS FOR 19 JULY 1979 (CONCENTRATIONS IN PPM).

Station	Easting (m)	Northing (m)	NO	NO_2	CO	O_3	RHC
AMS Lab.	491600	4428500	0.000	0.025	0.5	0.015	0.35
Ancora	511800	4392400	--	--	--	0.015	--
Brigantine	546000	4337506	--	--	--	0.017	--
Bristol	511000	4440000	--	0.039	--	0.012	--
Camden	491700	4419000	0.011	0.051	2.5	0.004	--
Chester	469000	4410000	--	0.024	--	0.026	0.95
Claymont	461500	4406400	--	0.045	--	0.020	--
Conshohocken	474500	4435600	--	--	--	0.000	--
Defense Support	483800	4418300	--	--	--	0.000	--
Downington	436000	4426000	0.006	0.015	0.2	0.024	0.05
Franklin Inst.	485200	4422800	0.030	0.050	0.5	0.010	--
Island Rd. Airp. Cir.	480300	4414800	--	--	--	0.015	--
Lumberton	518000	4423000	0.000	0.028	0.0	0.008	0.40
Norristown Armory	473500	4440000	--	--	--	0.030	0.29
Northeast Airp.	499000	4436000	0.000	0.015	--	--	--
Roxy Water Pump	479500	4433100	--	--	--	0.010	--
SE Sewage Plant	487200	4417300	--	--	--	0.005	--
South Broad	486100	4421600	0.020	0.045	1.5	0.010	0.25
Summit Bridge	441000	4376000	0.000	0.009	0.2	0.009	0.10
SW Corner Broad/Butler	487000	4418000	--	--	--	--	--
Trenton	520000	4452000	--	--	--	0.002	--
Van Hiseville	559000	4439500	0.000	0.006	0.2	0.021	--
Vineland	498200	4371200	--	0.025	--	0.010	--

RHC Component	Carbon-Bond Fraction (% as Carbon)
PAR	74.0
OLE	2.8
ETH	4.1
ARO	13.2
CARB	5.9

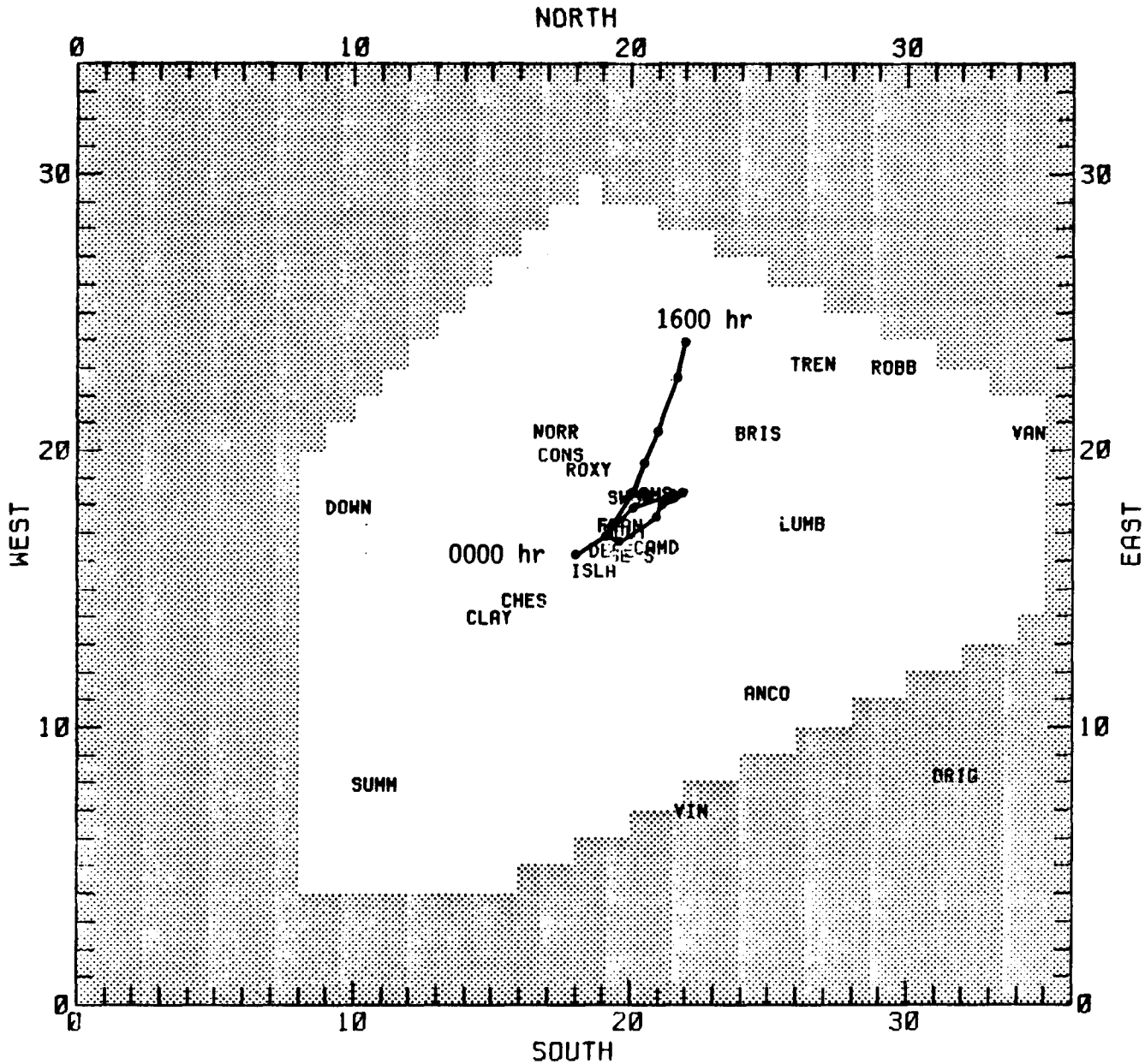

FIGURE 2. Trajectory path for July 13 regional ozone maximum.

TABLE 7. BACKGROUND CONCENTRATION VALUES FOR 13 JULY AT THE TOP OF THE MODELING REGION (TOPCONC), AS INITIAL CONCENTRATIONS ABOVE THE MIXING HEIGHT, AND FOR ALL LEVELS OF ALL BOUNDARIES EXCEPT THE LEVELS BELOW THE MIXING HEIGHT ON THE SOUTHEAST BOUNDARY.

Species	Concentration (ppm)
NO	0.001
NO_2	0.002
O_3	0.08
CO	0.2
ETH	0.001
OLE	0.0004
PAR	0.040
CARB	0.010
ARO	0.0008
PAN	0.000025
BZA	0.00001

TABLE 8. SOUTHEAST BOUNDARY CONDITIONS FOR CELLS BELOW THE MIXING HEIGHT FOR THE SIMULATION OF 13 JULY 1979 (CONCENTRATIONS IN PPM)

Time interval	NO	NO_2	O_3	PAR	OLE	ETH	ARO	CARB	PAN
0000-0100	0.001	0.009	0.053	0.1041	0.00105	0.0026	0.0021	0.0261	0.0040
0100-0200	0.001	0.009	0.041	0.1041	0.00105	0.0026	0.0021	0.0261	0.0040
0200-0300	0.001	0.009	0.037	0.1041	0.00105	0.0026	0.0021	0.0261	0.0040
0300-0400	0.001	0.009	0.036	0.1041	0.00105	0.0026	0.0021	0.0261	0.0040
0400-0500	0.001	0.009	0.028	0.1041	0.00105	0.0026	0.0021	0.0261	0.0040
0500-0600	0.001	0.009	0.010	0.1041	0.00105	0.0026	0.0021	0.0261	0.0040
0600-0700	0.001	0.009	0.021	0.1041	0.00105	0.0026	0.0021	0.0261	0.0040
0700-0800	0.001	0.007	0.035	0.0983	0.00065	0.0022	0.0017	0.0259	0.0044
0800-0900	0.001	0.004	0.072	0.0904	0.00040	0.0018	0.0012	0.0244	0.0054
0900-1000	0.001	0.002	0.102	0.0825	0.00040	0.0015	0.0008	0.0218	0.0062
1000-1100	0.001	0.002	0.111	0.0758	0.00040	0.0012	0.0008	0.0188	0.0062
1100-1200	0.001	0.002	0.121	0.0698	0.00040	0.0010	0.0008	0.0157	0.0058
1200-1300	0.001	0.002	0.139	0.0644	0.00040	0.0010	0.0008	0.0129	0.0052
1300-1400	0.001	0.002	0.113	0.0596	0.00040	0.0010	0.0008	0.0107	0.0047
1400-1500	0.001	0.002	0.105	0.0546	0.00040	0.0010	0.0008	0.0100	0.0040
1500-1600	0.001	0.002	0.093	0.0525	0.00040	0.0010	0.0008	0.0100	0.0037
1600-1700	0.001	0.002	0.069	0.0506	0.00040	0.0010	0.0008	0.0100	0.0032
1700-1800	0.001	0.002	0.068	0.0506	0.00040	0.0010	0.0008	0.0100	0.0032

TABLE 8 (Concluded)

Time interval	NO	NO_2	O_3	PAR	OLE	ETH	ARO	CARB	PAN
1800-1900	0.001	0.002	0.058	0.0506	0.0004	0.001	0.0008	0.010	0.0032
1900-2000	0.001	0.002	0.065	0.0506	0.0004	0.001	0.0008	0.010	0.0032
2000-2100	0.001	0.002	0.059	0.0506	0.0004	0.001	0.0008	0.010	0.0032
2100-2200	0.001	0.002	0.056	0.0506	0.0004	0.001	0.0008	0.010	0.0032
2200-2300	0.001	0.002	0.051	0.0506	0.0004	0.001	0.0008	0.010	0.0032
2300-2400	0.001	0.002	0.050	0.0506	0.0004	0.001	0.0008	0.010	0.0032

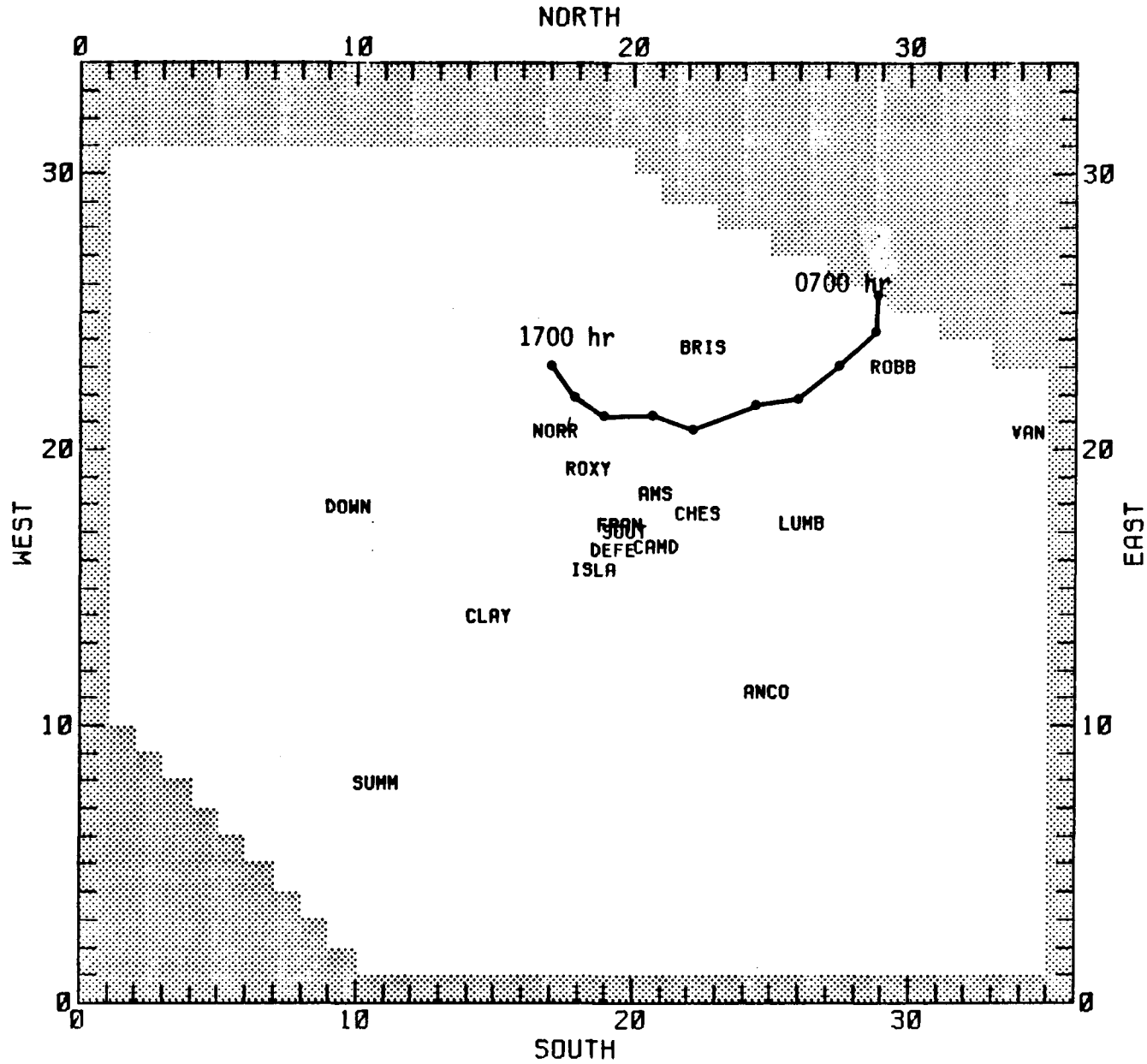

FIGURE 3. Trajectory path for July 19 regional ozone maximum.

HEIGHT ESTIMATED FROM DATA COLLECTED AT THE VAN HISEVILLE, NEW JERSEY MONITOR
(CONCENTRATIONS IN PPM)

Hour (EST)	NO	NO_2	O_3	PAR	OLE	ETH	ARO	CARB	PAN
0000-0100	0.044	0.036	0.018	0.3552	0.00672	0.00985	0.01056	0.02832	0.0002
0100-0200	0.044	0.036	0.009	0.3552	0.00672	0.00985	0.01056	0.02832	0.0001
0200-0300	0.044	0.036	0.000	0.3552	0.00672	0.00985	0.01056	0.02832	0.0000
0300-0400	0.044	0.036	0.000	0.3552	0.00672	0.00985	0.01056	0.02832	0.0000
0400-0500	0.044	0.036	0.000	0.3552	0.00672	0.00985	0.01056	0.02832	0.0000
0500-0600	0.044	0.036	0.000	0.3552	0.00672	0.00985	0.01056	0.02832	0.0000
0600-0700	0.047	0.041	0.000	0.39072	0.00739	0.010825	0.01162	0.03115	0.0000
0700-0800	0.043	0.0494	0.004	0.40996	0.007755	0.01135	0.01218	0.03269	0.0004
0800-0900	0.026	0.0478	0.015	0.32782	0.0062	0.00908	0.00975	0.02614	0.0008
0900-1000	0.009	0.0273	0.051	0.16132	0.00305	0.00447	0.0048	0.01286	0.0013
1000-1100	0.001	0.0099	0.083	0.04839	0.000915	0.00134	0.00143	0.00386	0.0019
1100-1200	0.000	0.0058	0.078	0.02575	0.000487	0.000716	0.000767	0.00205	0.0018
1200-1300	0.000	0.0054	0.075	0.02397	0.0004535	0.000665	0.000717	0.00191	0.0014
1300-1400	0.000	0.0072	0.072	0.03196	0.000605	0.000885	0.00095	0.00255	0.0012
1400-1500	0.000	0.0047	0.072	0.02087	0.0003945	0.000578	0.00062	0.00166	0.0007
1500-1600	0.000	0.0035	0.062	0.01554	0.000294	0.0004305	0.000462	0.00124	0.0005
1600-1700	0.000	0.0043	0.059	0.01909	0.000361	0.000529	0.000568	0.00152	0.0003
1700-1800	0.000	0.0053	0.052	0.0235	0.000445	0.000652	0.0007	0.001876	0.0003
1800-1900	0.000	0.0072	0.044	0.03197	0.000605	0.000885	0.00095	0.00255	0.0002
1900-2000	0.000	0.0071	0.036	0.03152	0.0005965	0.000875	0.000937	0.00251	0.0001
2000-2100	0.000	0.0041	0.020	0.0182	0.0003445	0.000505	0.000542	0.00145	0.0001
2100-2200	0.002	0.0030	0.010	0.0222	0.00042	0.000615	0.00066	0.00177	0.0000
2200-2300	0.005	0.0060	0.000	0.04884	0.000925	0.001355	0.00145	0.00389	0.0000
2300-2400	0.008	0.0030	0.001	0.04884	0.000925	0.001355	0.00145	0.00389	0.0000

Philadelphia Inventory Split

Species	Carbon-Bond Fraction (% as Carbon)
PAR	74.
OLE	2.8
ETH	4.1
ARO	13.2
CARB	5.9

Mixing Height Profiles

Mixing height profiles for 13 July were estimated using temperature soundings from JFK and Dulles airports since no soundings were available for Philadelphia on this day. Mixing heights for 13 July are shown in Table 10 and Figure 4. Mixing height profiles for 19 July were developed using available radiosonde observations and sodar data for the Philadelphia area. Mixing heights for 19 July are shown in Table 11 and Figure 5.

Wind Fields

Three-dimensional wind fields for 13 July and 19 July were generated from station measurements and aloft winds obtained from radiosonde data. Wind direction on the morning of 13 July was very light and predominantly from the north. Around 1000 EST, however, a shift occurred and winds with higher speeds came from the southeast for the rest of the day. Winds on the morning of 19 July were predominantly from the north. Throughout the day a 180° shift occurred: at noon the wind direction was predominantly from the east; during the evening it came from the south-southeast. The gridded, smoothed surface vectors for selected hours are presented in Figure 6 for 13 July and in Figure 7 for 19 July.

Background Concentrations

Except for the ozone concentration, the background concentrations above the mixing height are the same for both days. On the basis of examination of upwind monitoring data at the time of mixing, the value specified for ozone for 19 July is 0.06 ppm, compared to 0.08 ppm for 13 July. Background concentrations for July 19 are listed in Table 12. The gridded area source and elevated point source emission inventory was prepared for EPA in 1981 by Engineering Science, Inc. (EPA, 1982). Total daily emission values for total NO_x and total hydrocarbon are presented in Table 13.

MODIFICATIONS TO 1979 UAM INPUTS FOR PHILADELPHIA APPLICATION

For the year 2000 base case projections, the changes made to the 1979 UAM inputs involved mobile source emissions, major point, minor point and area source emissions, and initial and boundary conditions. When modifying the year 2000 base case for methanol substitution, changes made to mobile source emissions and fueling operation emissions were limited to

TABLE 10. URBAN AND RURAL MIXING HEIGHT VALUES USED IN THE DIFFBREAK FILE FOR 13 JULY 1979.

Time (EST)	Urban (m)	Rural (m)
0000	250	100
0030	250	100
0100	250	100
0130	250	100
0200	250	100
0230	250	100
0300	250	100
0330	250	100
0400	250	100
0430	250	100
0500	250	100
0530	250	100
0600	250	100
0630	270	135
0700	295	150
0730	375	250
0800	450	350
0830	680	620
0900	925	925
0930	1160	1160
1000	1200	1200
1030	1330	1330
1100	1480	1480
1130	1480	1480
1200	1480	1480
1230	1500	1500
1300	1530	1530
1330	1530	1530
1400	1530	1530
1430	1475	1475
1500	1420	1420
1530	1365	1365
1600	1310	1310
1630	1220	1220
1700	1130	1130
1730	1035	1035
1800	950	950
1830	855	730
1900	770	525
1930	675	320
2000	590	100
2030	500	100
2100	410	100
2130	370	100
2200	330	100
2230	290	100
2300	250	100
2330	250	100
2400	250	100

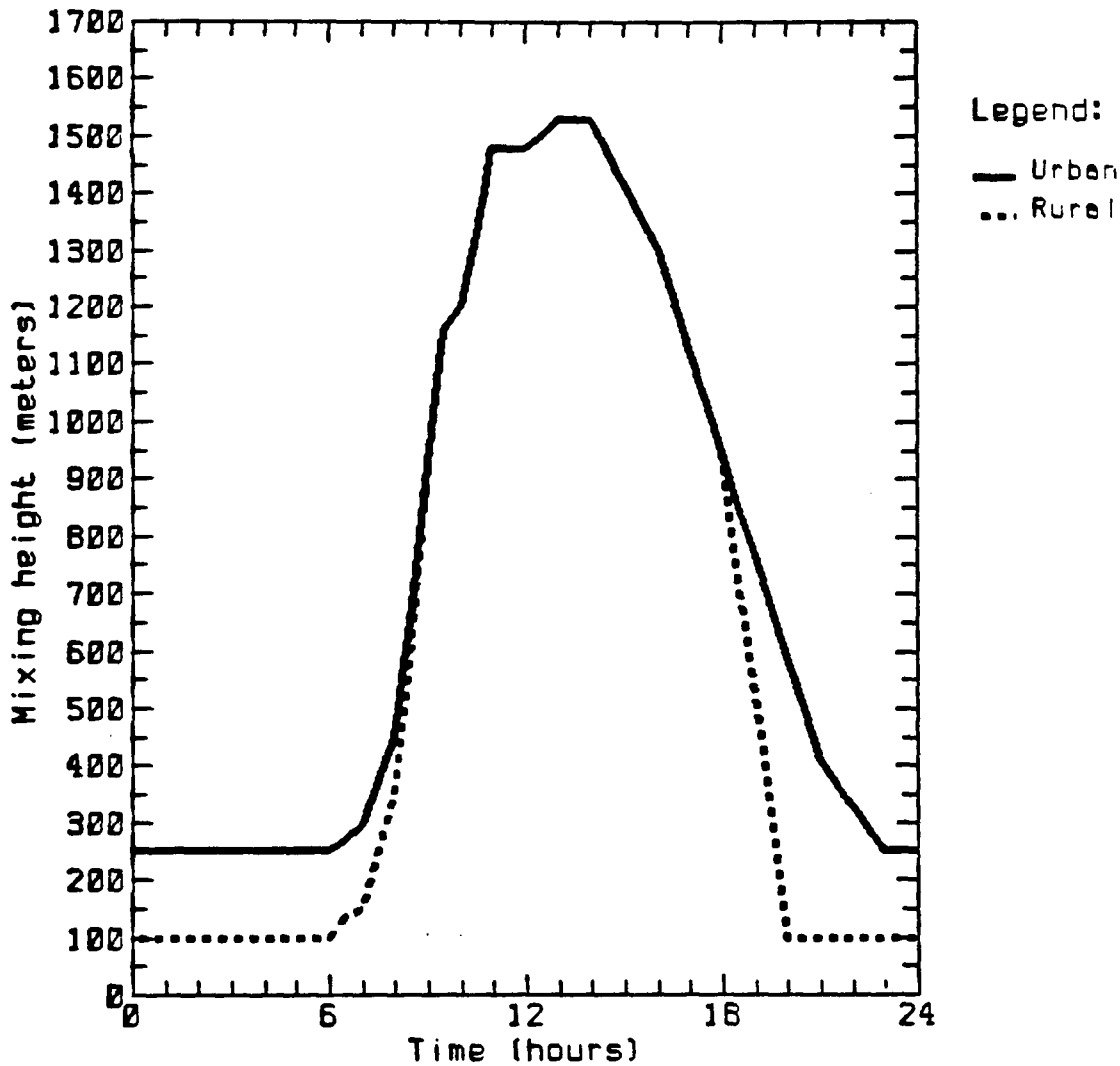

FIGURE 4. Mixing height profiles for urban and rural cells for the 13 July 1979 simulation.

TABLE 11. URBAN AND RURAL MIXING HEIGHT VALUES USED IN THE DIFFBREAK FILE FOR 19 JULY 1979.

Time (EST)	Urban (m)	Rural (m)
0000	190	100
0030	190	100
0100	190	100
0130	190	100
0200	190	100
0230	190	100
0300	190	100
0330	190	100
0400	190	100
0430	190	100
0500	190	100
0530	190	100
0600	190	100
0630	190	100
0700	190	100
0730	240	260
0800	350	440
0830	460	490
0900	600	540
0930	740	560
1000	890	580
1030	1060	630
1100	1240	880
1130	1420	1320
1200	1530	1430
1230	1530	1430
1300	1480	1380
1330	1410	1310
1400	1340	1240
1430	1270	1170
1500	1200	1100
1530	1120	1020
1600	1020	920
1630	940	840
1700	850	750
1730	750	480
1800	660	160
1830	570	100
1900	480	100
1930	410	100
2000	340	100
2030	300	100
2100	250	100
2130	250	100
2200	250	100
2230	250	100
2300	250	100
2330	250	100
2400	250	100

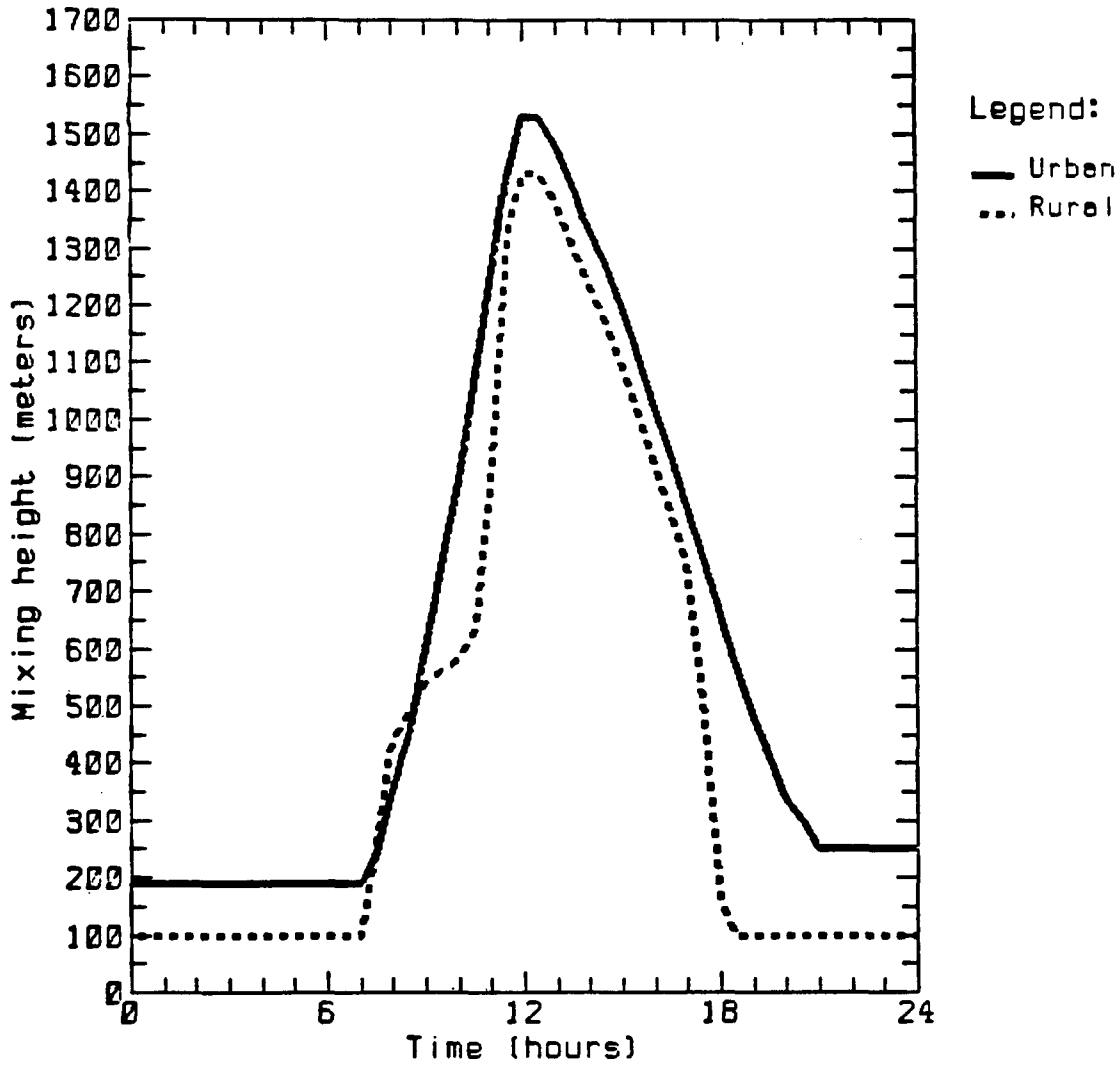

FIGURE 5. Mixing height profiles for urban and rural cells for the 19 July 1979 simulation.

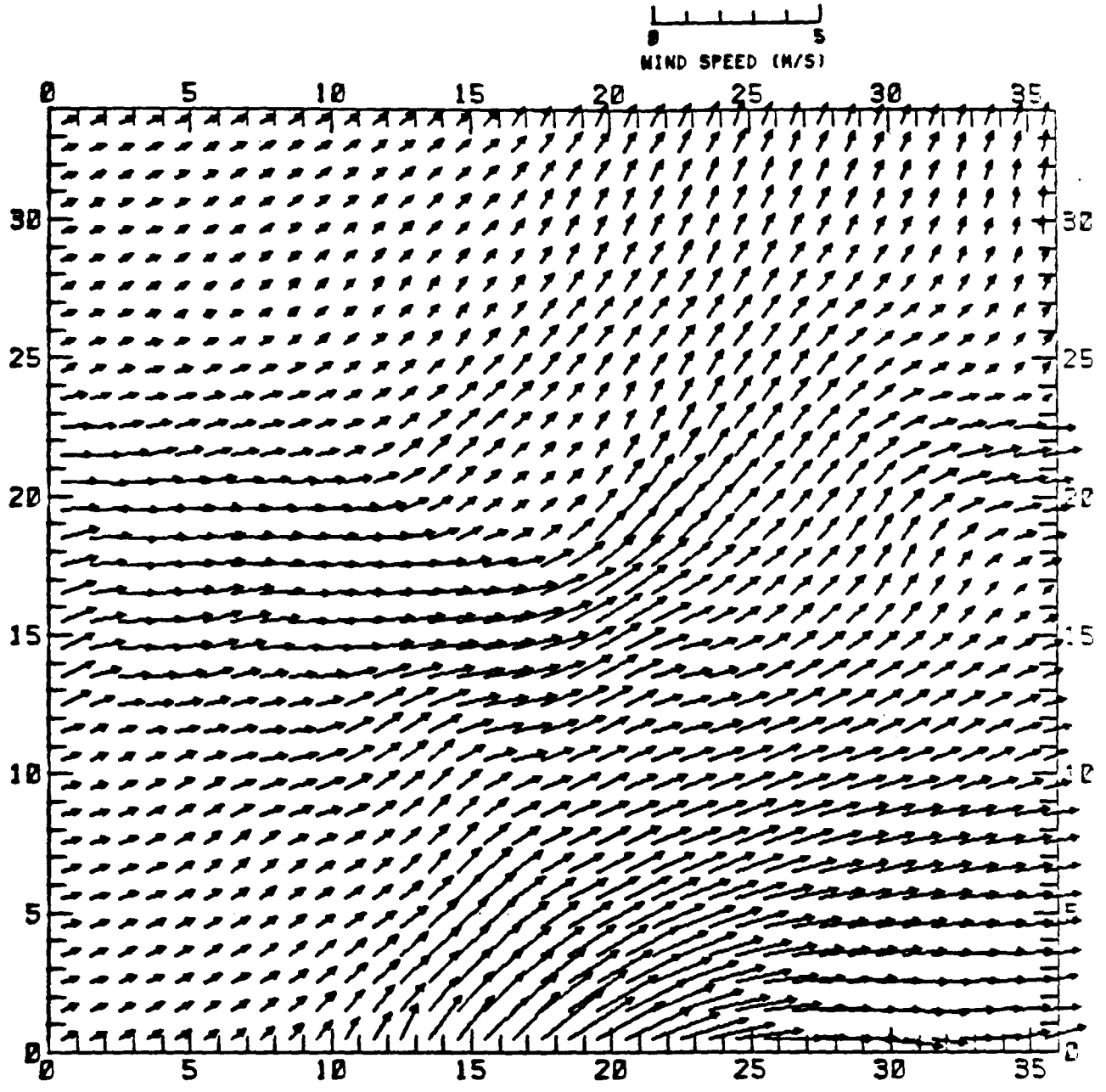

(a) 0 - 100 EST

FIGURE 6. Airshed model surface winds for 13 July 1979.

B3033r

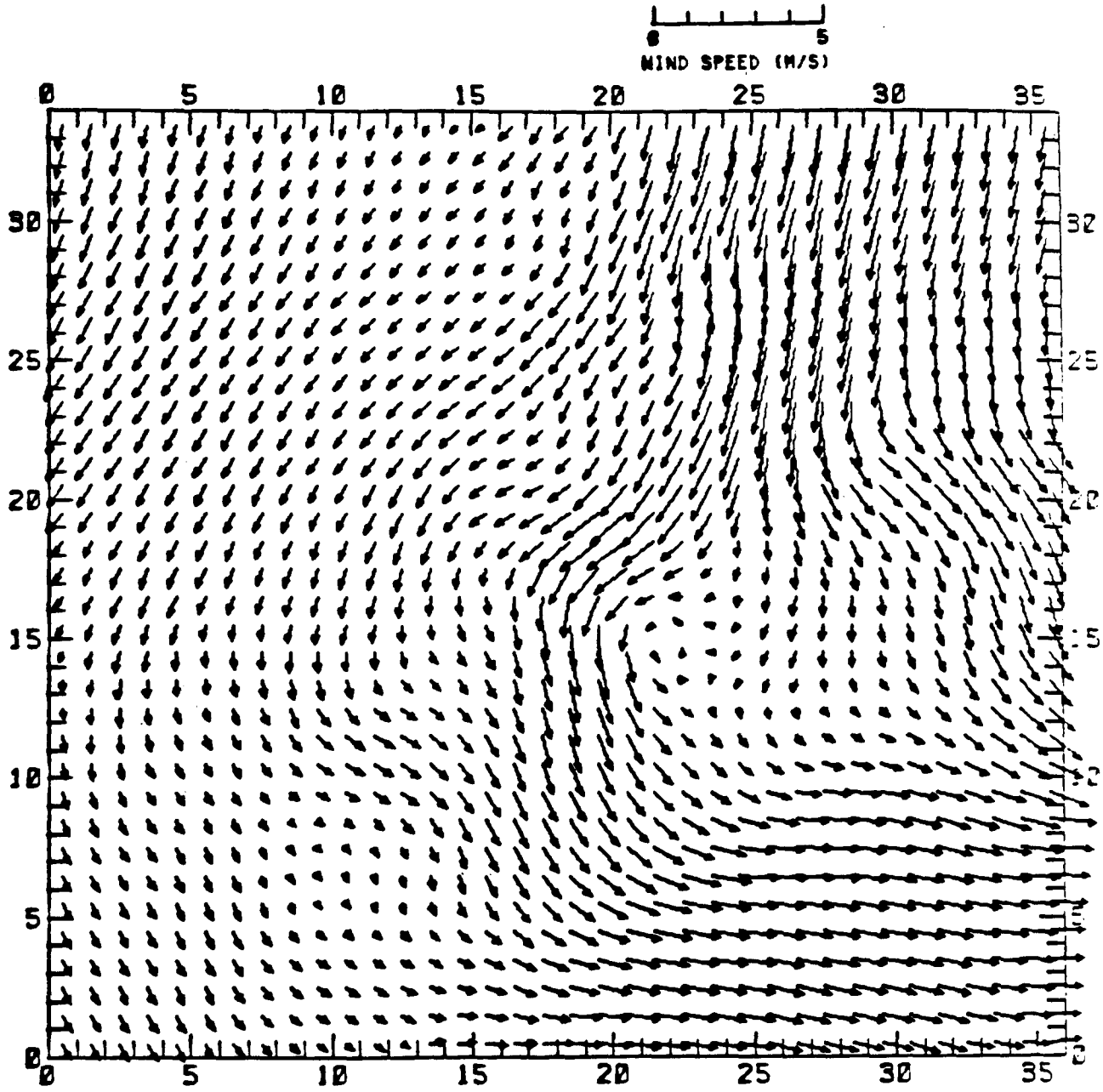

(b) 600 - 700 EST

FIGURE 6 (continued)

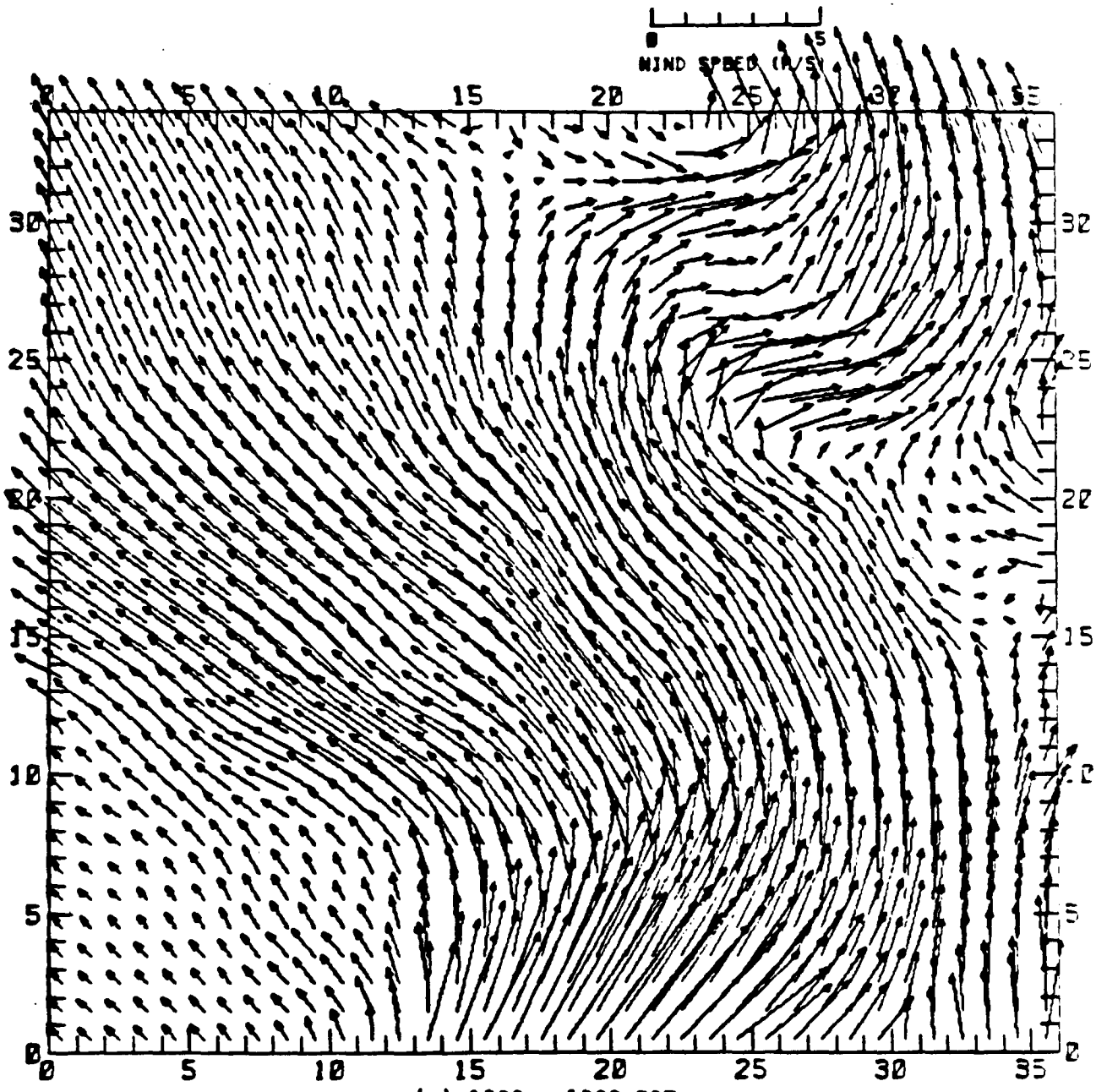

FIGURE 6 (continued)

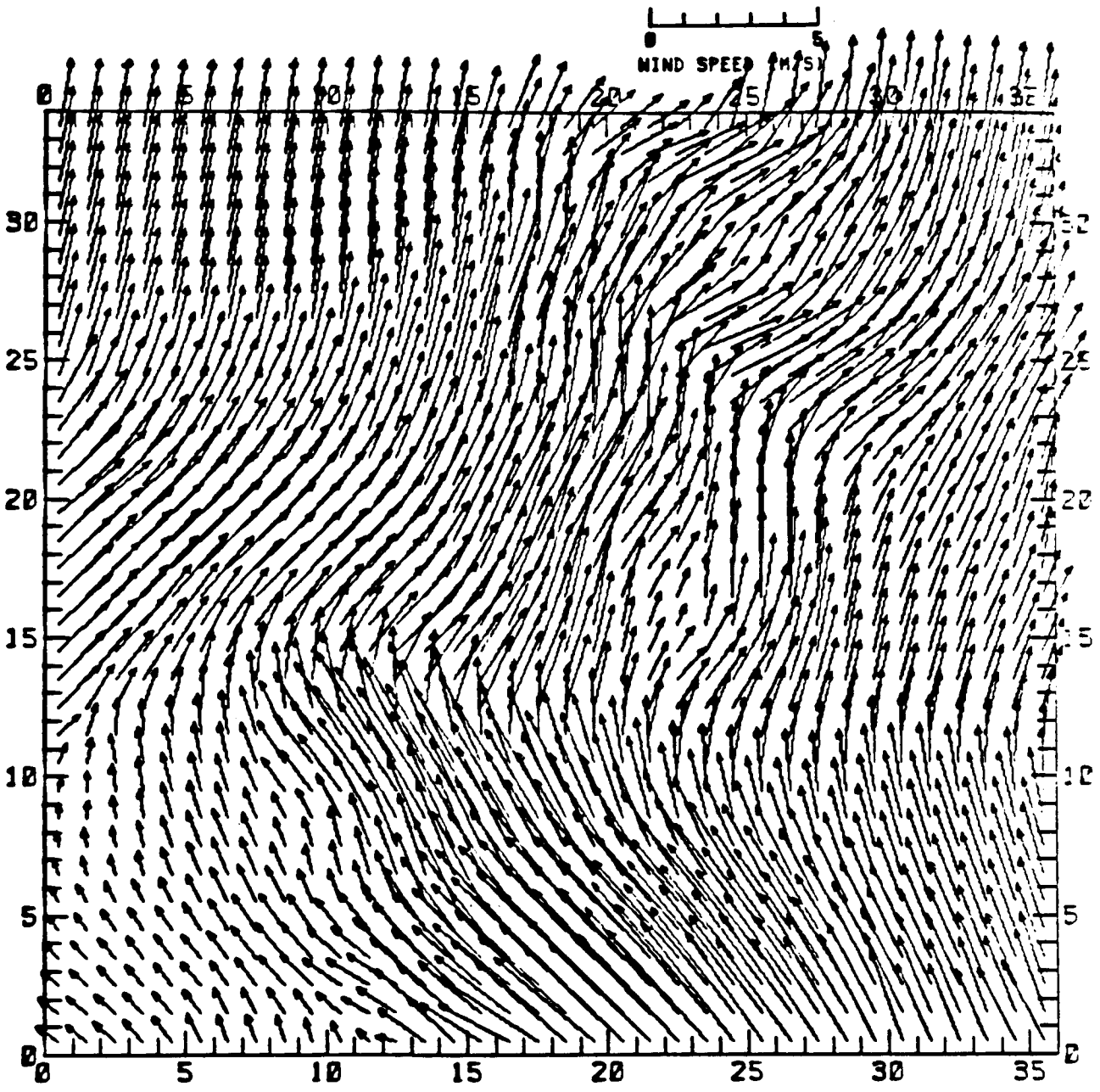

(d) 1800 - 1900 EST

FIGURE 6 (concluded)

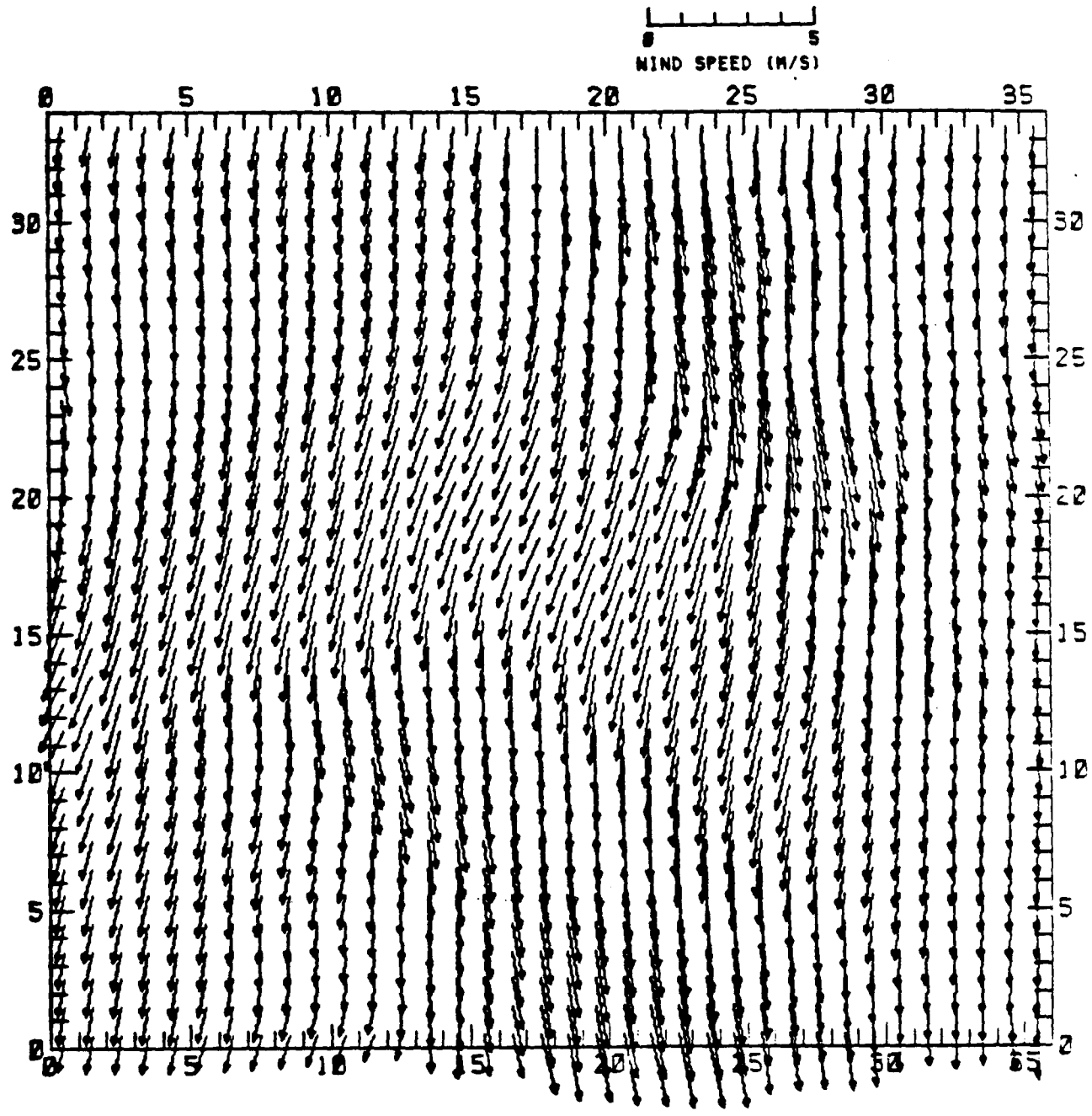

(a) 400 - 500 EST

FIGURE 7. Airshed model surface winds for 19 July 1979.

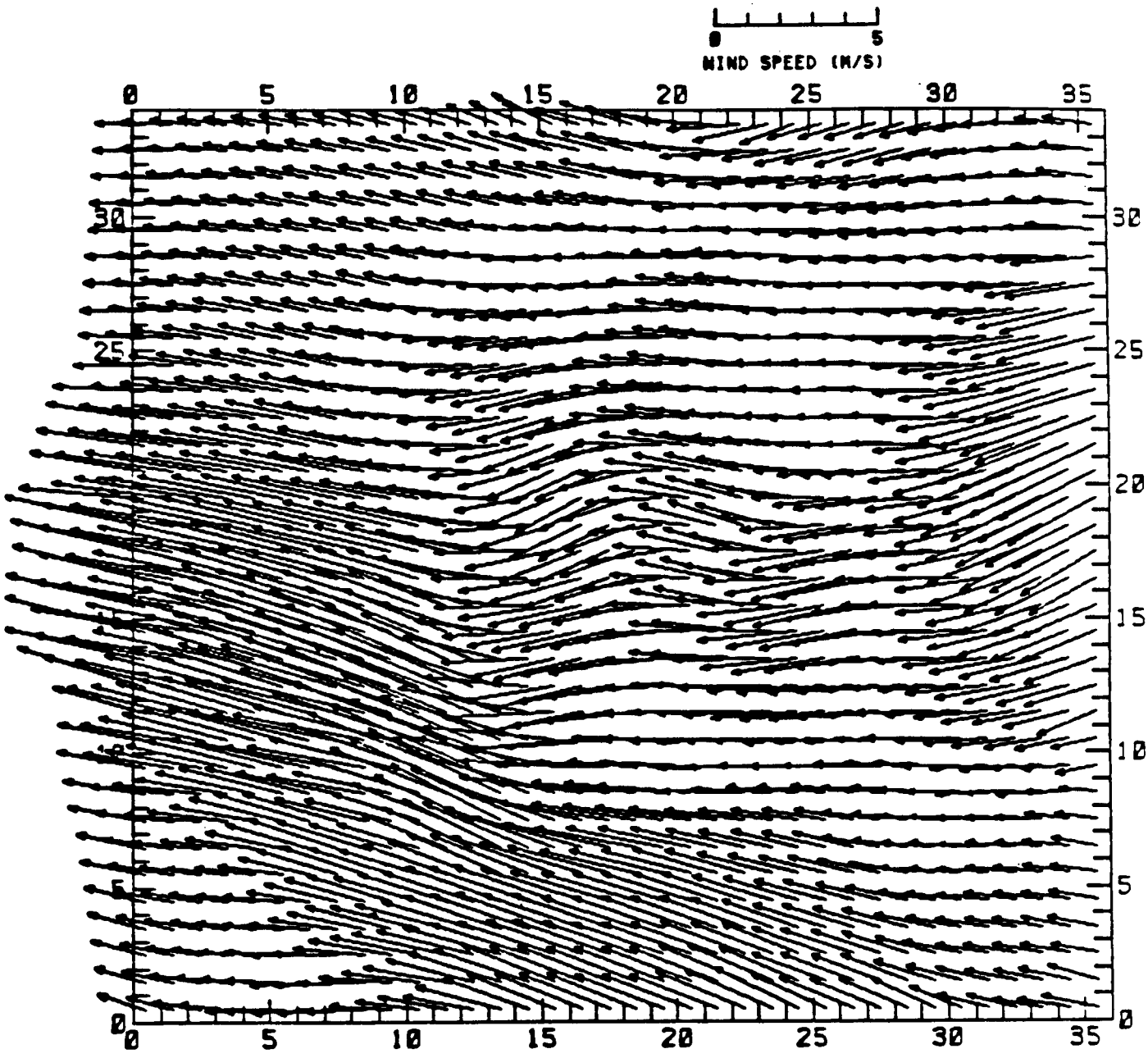

(b) 1200 - 1300 EST

FIGURE 7 (continued).

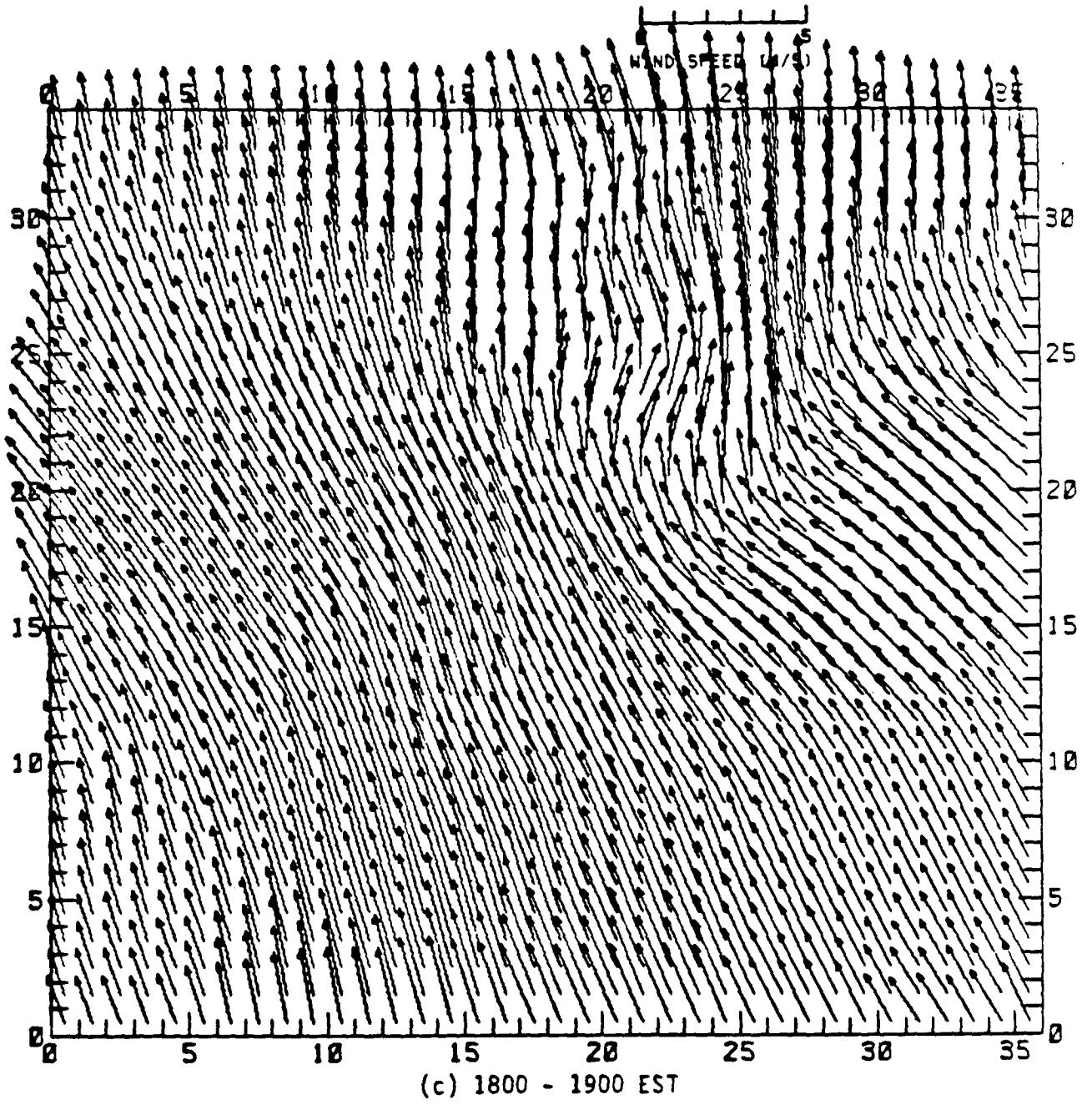

(c) 1800 - 1900 EST

FIGURE 7 (concluded).

TABLE 12. BACKGROUND CONCENTRATIONS VALUES USED AT THE TOP OF THE MODELING REGION (TOPCONC), AS INITIAL CONCENTRATIONS ABOVE THE MIXING HEIGHT, AND FOR ALL LEVELS OF ALL BOUNDARIES EXCEPT THE LEVELS BELOW THE MIXING HEIGHT ON THE NORTHEAST AND EAST BOUNDARIES

Species	Concentration (ppm)
NO	0.001
NO_2	0.002
O_3	0.06*
CO	0.2
ETH	0.001
OLE	0.0004
PAR	0.040
CARB	0.010
ARO	0.0008
PAN	0.000025
BZA	0.00001

* A value of 0.05 ppm was used below the mixing height for all boundaries except the Northeast and East boundaries.

TABLE 13. TOTAL DAILY EMISSIONS BY SOURCE TYPE (g•mole) IN THE 1979 PHILADELPHIA INVENTORY

Source	NO	NO_2	ETH	OLE	PAR	CARB	ARO
Elevated Point	5,738,955	257,086	12,144	7,792	901,823	570,765	139,960
Minor Point	2,041,679	114,837	385,284	183,632	15,846,729	818,880	510,799
Area Source	2,705,097	207,808	295,258	194,471	26,841,639	1,669,555	491,833
Mobile Source	6,646,688	738,496	827,355	664,553	11,635,952	1,337,697	495,926
TOTAL	17,132,419	1,318,227	1,520,041	1,050,448	55,226,197	4,396,897	1,638,518

Total HC = 63,832,101 Total NO_x = 18,450,646

Philadelphia Hydrocarbon Splits

Species	Carbon-Bond Fraction (% as Carbon)
PAR	74.0
OLE	2.8
ETH	4.1
ARO	13.2
CARB	5.9

area sources. For selected scenarios, methanol was also substituted for a portion of initial and aloft concentrations.

This section discusses in further detail the modifications made to the 1979 UAM inputs. The simulations chosen for this study are also discussed. The 1979 inventory contains hourly mobile source emissions for each of the 502 grids in the modeling region as well as daily mobile source emissions for each county. It would have been a massive undertaking in terms of resources and time to revise the hourly emissions on a grid-to-grid basis. Instead, rough percentage reductions in the 1979 mobile source inventory were made for the year 2000 projections. This was done for each of the 11 counties in the Philadelphia AQCR.

Exhaust HC, evaporative HC, and NO_x emission factors (g/mile) for the year 2000 for each of the 11 counties were determined using MOBILE3 and were then multiplied by the appropriate year-2000 daily VMT to obtain kg/day emissions for each county for the year-2000 base case. The MOBILE3 input parameters specific to each county (e.g., average speed) as well as the year-2000 projected daily VMT for each county are contained in the Delaware Region's Year-2000 transportation plan (DVRPC, 1982). The exhaust HC emissions predicted by MOBILE3 were multiplied by 1.016 to account for aldehydes and ketones. The value of 1.016 is based on VOC data for 1981 and 1982 vehicles (Sigsby et al., 1984).

County adjustment factors, which are ratios of the year 2000 to the year 1979 kg/day emissions, were then estimated. These adjustment factors are listed in Table 14. The adjustment factors given for each county were then used for each grid within that county. The adjustment factors were multiplied by the appropriate mass-per-grid-cell values contained in the 1979 mobile source inventory to obtain revised year 2000 mass-per-grid-cell values for exhaust HC, evaporative HC and NO_x.

County adjustment factors for the methanol replacement scenarios differ from those calculated for the base case because different assumptions were made regarding the mass of exhaust and evaporative emissions from methanol-fueled vehicles. NO_x emissions from methanol-fueled vehicles were assumed to be the same as those of the base case.

The specific box model scenarios are listed in Table 15. The UAM runs are more limited in scope, i.e., not all scenarios were simulated:

TABLE 14. COUNTY ADJUSTMENT FACTORS

County	1979 Base Case (kg/day)	2000 Base Case 1A	Complete 2A	Methanol 2B	Replacement 2C	Revised 2000 Base Case 1B
Burlington						
Exh. HC	14127	0.31	0.31	0.78	1.55	0.34
Evap. HC	9108	0.45	0.14	0.35	0.70	0.14
NO_x	33068	0.39	0.39	0.39	0.39	0.39
Camden						
Exh. HC	16039	0.36	0.36	0.90	1.80	0.32
Evap. HC	9188	0.48	0.14	0.35	0.70	0.14
NO_x	31855	0.43	0.43	0.43	0.43	0.43
Gloucester						
Exh. HC	6899	0.31	0.31	0.78	1.55	0.38
Evap. HC	4829	0.46	0.14	0.35	0.70	0.14
NO_x	18247	0.38	0.38	0.38	0.38	0.38
Mercer						
Exh. HC	10453	0.34	0.34	0.85	1.70	0.33
Evap. HC	6007	0.50	0.15	0.37	0.75	0.15
NO_x	21208	0.44	0.44	0.44	0.44	0.44
Bucks						
Exh. HC	20646	0.25	0.25	0.62	1.25	0.25
Evap. HC	9569	0.47	0.14	0.35	0.70	0.14
NO_x	33553	0.41	0.41	0.41	0.41	0.41
Chester						
Exh. HC	14372	0.24	0.24	0.60	1.20	0.26
Evap. HC	7057	0.46	0.15	0.37	0.75	0.15
NO_x	25443	0.40	0.40	0.40	0.40	0.40
Delaware						
Exh. HC	21265	0.29	0.29	0.72	1.45	0.24
Evap. HC	8421	0.52	0.16	0.40	0.80	0.16
NO_x	27610	0.50	0.50	0.50	0.50	0.50
Montgomery						
Exh. HC	33108	0.28	0.28	0.70	1.40	0.25
Evap. HC	14059	0.51	0.16	0.40	0.80	0.16
NO_x	48105	0.46	0.46	0.46	0.46	0.46
Philadelphia						
Exh. HC	51702	0.28	0.28	0.70	1.40	0.18
Evap. HC	17096	0.48	0.14	0.35	0.70	0.14
NO_x	55725	0.49	0.49	0.49	0.49	0.49
Salem						
Exh. HC	4078	0.33	0.33	0.82	1.65	0.44
Evap. HC	3218	0.47	0.14	0.35	0.70	0.14
NO_x	11482	0.42	0.42	0.42	0.42	0.42
New Castle						
Exh. HC	23149	0.25	0.25	0.62	1.25	0.23
Evap. HC	9636	0.47	0.14	0.35	0.70	0.14
NO_x	34250	0.41	0.41	0.41	0.41	0.41

TABLE 15a. BOX MODEL SCENARIOS FOR 13 JULY 2000

1. Base Case
   - 1A. Year 2000 base case
   - 1B. Revised mobile source year 2000 base case (see text for explanation)

2. Complete methanol replacement scenario for mobile sources
   - 2A. Same exhaust HC as base case (1A), evap at standards
   - 2B. 2.5 times base case exhaust HC (1A), evap 2.5 times standards
   - 2C. 5.0 times base case exhaust HC (1A), evap 5 times standards
   - 2D. 2B with surface deposition
   - 2E. 2B with 20 % methanol for aloft and initial conditions

3. Partial methanol replacement scenario for mobile sources
   - 3A. 80% 1A, 20% 2A
   - 3B. 80% 1A, 20% 2B
   - 3C. 80% 1A, 20% 2C

4. Formaldehyde sensitivity analysis for 2B
   - 4A. 5% of methanol exhaust emissions
   - 4B. 20% of methanol exhaust emissions

5. Formaldehyde sensitivity analysis for 2C
   - 5A. 5% of methanol exhaust emissions
   - 5B. 20% of methanol exhaust emissions

6. Ozone isopleth diagrams based on 2B

7. Removal of all mobile source emissions
   - 7A. From base case 1A
   - 7B. Base NO_x, zero VOC from mobile sources

8. Stationary source sensitivity analysis for 2B
   - 8A. Elimination of mobile-related stationary source methanol contribution
   - 8B. Upper limit assumption for mobile-related stationary source methanol contribution; substitution of methanol (no formaldehyde) for 50% of <u>all</u> VOC emissions
   - 8C. 8B with 50% methanol in initial conditions
   - 8D. 8B with 50% methanol aloft and in initial conditions

9. Carbon percent replacement scenarios (all mobile source HC replaced with methanol or formaldehyde on a C% basis)
   - 9A. 100% of base case (1B) carbon replaced with methanol (no formaldehyde)
   - 9B. 150% of base case (1B) carbon replaced with methanol (no formaldehyde)
   - 9C. 200% of base case (1B) carbon replaced with methanol (no formaldehyde)
   - 9D. 10% of base case (1B) carbon replaced with formaldehyde (no methanol)
   - 9E. 20% of base case (1B) carbon replaced with formaldehyde (no methanol)

TABLE 15a (Concluded)

10. 50% reduction of total base case (1B) HC

11. 30% mobile source emissions of the total base case 1A emissions
    11A. Revised year 2000 base case
    11B. Revised complete methanol substitution scenario based on 2B with initial methanol conditions

12. 50% mobile source emissions of the total base case 1A emissions
    12A. Revised year-2000 base case emissions
    12B. Revised complete methanol substitution scenario based on 2B with initial methanol conditions

TABLE 15b. METHANOL, FORMALDEHYDE, METHYL NITRATE, AND HYDROCARBON FOR BOX MODEL SCENARIOS AS PERCENT CARBON OF BASE-CASE 1B MOBILE SOURCES.**

Scenario	Methanol*	Formaldehyde*	Methyl Nitrate*	Hydrocarbons*
1. Base Case				
1B	0	0	0	100
1A	0	0	0	151
2. Complete methanol replacement scenario				
2A	63	7.33	0.36	0
2B	158	18.2	0.90	0
2C	315	36.6	1.80	0
2D	158	18.2	0.90	0
2E	158	18.2	0.90	0
3. Partial methanol replacement scenario				
3A	12.6	1.46	0.07	121
3B	31.5	3.65	0.18	121
3C	63	7.30	0.36	121
4. Formaldehyde sensitivity analysis (2B)				
4A	167	9.10	0.90	0
4B	140	36.6	0.90	0
5. Formaldehye sensitivity analysis (2C)				
5A	333	183	1.80	0
5B	280	73.3	1.80	0
8. Mobile-related stationary-source sensitivity analysis (2B)				
8A	151	17.6	0.04	0
8B	104	12.1	0.59	0
8C	104	12.1	0.59	
8D	104	12.1	0.59	

Continued

TABLE 15b (Concluded)

Scenario	Methanol*	Formaldehyde*	Methyl Nitrate*	Hydrocarbons*
9. Carbon percent replacement scenarios				
9A	100	0	0	0
9B	150	0	0	0
9C	200	0	0	0
9D	0	10	0	0
9E	0	20	0	0
10. 50% reduction of base case 1B mobile source HC	0	0	0	50
11. 30% of total 1B emissions***				
11A	0	0	0	151
11B	158	18.2	0.9	0
12. 50% of total emissions***				
12A	0	0	0	151
12B	158	18.2	0.9	0

* For 1B base case mobile sources only.
** See Table 15a for complete scenario descriptions.
*** Mobile source contribution was increased to 30% by lowering the total emissions.

Scenarios
Simulated by the UAM

13 July 2000	19 July 2000
1A	1A
2B	
3B	
5A	

The year 2000 base case 1A is based on the MOBILE3 projections. Base case 1B assumed that gasoline- and diesel-fueled vehicles in the year 2000 will meet their projected exhaust and evaporative emission standards.

The second scenario assumes complete replacement of gasoline- and diesel-fueled vehicles with methanol-fueled vehicles. Scenarios 2A, 2B, and 2C differ with respect to the quantity of exhaust and evaporative HC emissions assumed to be emitted by methanol-fueled vehicles. Scenario 2A assumes that methanol-fueled vehicles will meet current exhaust and evaporative emission standards. For example, the mass of exhaust HC emissions (composed of methanol, formaldehyde, and methyl nitrite) from a light-duty methanol-fueled vehicle total 0.42 g/mile (0.41 x 1.016). Scenarios 2B and 2C assume that both exhaust and evaporative emissions, on a mass basis, will equal 2.5 and 5 times the standards, respectively. It was anticipated that these scenarios would bracket the range of emissions possible from in-use methanol-fueled vehicles.

Scenario 3 is a partial methanol replacement scenario in which 20 percent of the gasoline- and diesel-fueled vehicles are replaced with methanol-fueled vehicles. For this scenario, the mobile source inventory is composed of 80 percent of the base case inventory (Scenario 1A), and 20 percent of the complete replacement inventory (Scenario 2) on a mass basis. Three emissions inventories were examined for Scenario 3 since three emissions inventories were available for the complete replacement scenario on the basis of the three in-use methanol emission rates assumed.

The remaining scenarios were chosen to examine the sensitivity of the model predictions to formaldehyde, stationary source, and mobile source emissions in general. For Scenario 10, methanol or formaldehyde replacement of mobile source VOC was made on a per carbon basis. This procedure differs from that of the other scenarios, in which methanol substitution was done on a mass basis. Scenario 10 was included to provide a more direct comparison of the results of this study with results obtained in the previous modeling study of methanol substitution in the Los Angeles basin.

The hydrocarbon splits for motor vehicles contained in the 1979 inventory are based on data from 1979 and earlier model-year light-duty vehicles. For the year 2000 inventory, revised HC speciation data for motor vehicles were incorporated, based on emissions from in-use 1982 light-duty vehicles (Sigsby et al., 1984). It was believed that the composition of emissions from in-use 1982 vehicles would more closely approximate the composition of vehicle emissions in the year 2000 than that contained in the 1979 inventory. The hydrocarbon splits for motor vehicles in the 1979 inventory can be compared to the hydrocarbon splits for motor vehicles in the year 2000 inventory in Table 16. The hydrocarbon reactivity was somewhat reduced in the year 2000 as evidenced by the increase in paraffins and the decrease in olefins, carbonyls, and ethylenes, in spite of an increase in the fairly reactive aromatics.

For the complete methanol replacement scenarios, the exhaust HC emissions were replaced by methanol, formaldehyde, and methyl nitrite. The composition of the exhaust emissions on a mass basis is 89 percent methanol, 10 percent formaldehyde and one percent methyl nitrite. The composition of the evaporative HC emissions was assumed to be 100 percent methanol. Figure 8 illustrates the steps taken to prepare the mobile-source emission inputs for a 20 percent methanol, 80 percent base case UAM run.

At every grid in the modeling region, the total reactive hydrocarbon is first split into two parts: one representing emissions from gasoline-fueled vehicles, the other representing emissions from methanol-fueled vehicles. In Figure 8 (Scenario 3), 80 percent of the mass of RHC is treated as emissions from gasoline-fueled vehicles and 20 percent is treated as emissions from methanol-fueled vehicles. The next step is the same for both gasoline and methanol type emissions. The emissions are divided into exhaust and evaporative fractions on the basis of the county in which the grid cell is located. The proportions determined from the total emissions by county for the year 1979 are listed in Table 14. Multiplying by the projection factor in Table 14 for the appropriate scenario yields the mass of RHC in each of the categories. The final step involves splitting the mass into species for modeling. The factors used for gasoline exhaust and evaporative emissions are shown in Table 16. The evaporative emissions for the methanol case were treated as 100 percent methanol. Methanol exhaust emissions were split into 89 percent methanol, 10 percent formaldehyde and 1 percent methyl nitrite. The fractions of methanol and formaldehyde for Scenario 5 were modified to test the effects of 94/5 percent and 79/20 percent splits.

To project HC and NO_x emissions for stationary and off-road mobile sources, estimates of future HC emissions contained in a recent State Implementation Plan revision for the region were reviewed (DVRPC, 1983).

TABLE 16. MOBILE SOURCE INVENTORY SPLITS FOR 1979 AND 2000

	Exhaust	
	Carbon-Bond Fraction	(% as Carbon)
Species	1979	2000
PAR	61.4	67.0
OLE	7.0	3.8
ETH	7.1	2.6
ARO	15.7	22.1
CARB	8.8	4.5

	Evaporative	
	Carbon-Bond Fraction	(% as Carbon)
Species	1979	2000
PAR	92.8	68.7
OLE	1.7	3.4
ETH	0	0.49
ARO	0.6	22.1
CARB	4.8	5.2

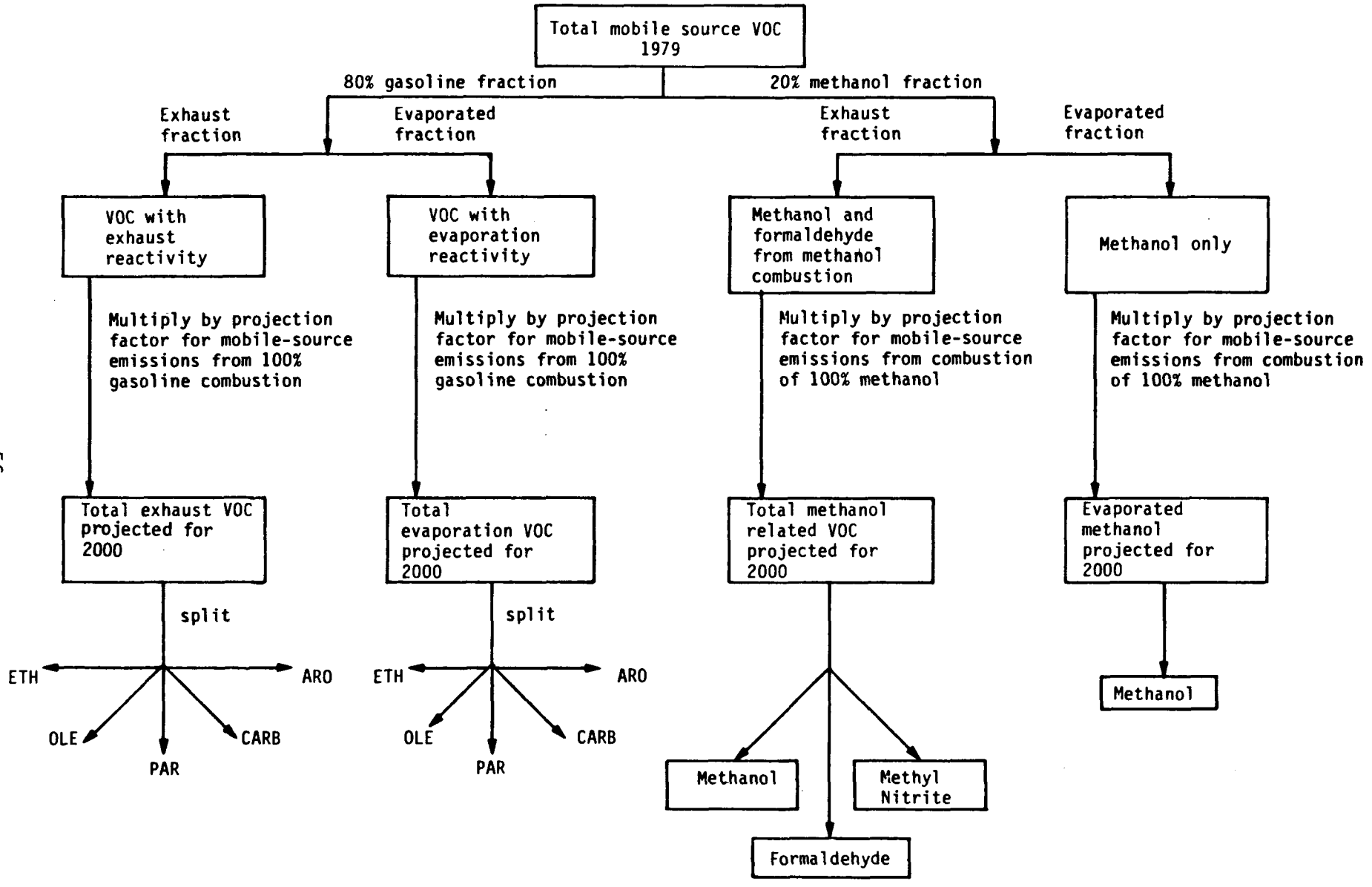

FIGURE 8. Schematic of preparation of mobile emission and evaporation inputs for 20 percent methanol/80 percent gasoline simulation.

85117

Stationary sources include major and minor point sources, and area sources. Area sources are defined as small local sources such as dry cleaners, automotive repair shops, and residential emissions. Mobil sources include both on-road motor vehicles and mobile-related stationary sources. Area sources are the major contributors to reactive hydrocarbon emissions for both the 1979 and 2000 Philadelphia emissions inventory. Attainment of the ozone standard was projected for 1987, with a 36 percent reduction in HC emissions from all sources other than motor vehicles. Accordingly, it was assumed that a 36 percent reduction from 1979 HC emissions would be maintained through the year 2000 by point and area sources. Furthermore, the implementation plan revision estimated a 4 percent increase in NO_x emissions by 1987 from all sources other than motor vehicles. This figure is consistent with a 4.1 percent increase in 1987 population estimated for the Philadelphia region (ESI, 1982). Since population in the year 2000 is expected to have increased 10.7 percent over the 1979 population (ESI, 1982), the point and area source NO_x emissions in the year 2000 were increased by 10.7 percent.

Evaporation from fueling operations (i.e., gas stations) for the year 2000 was estimated by calculating the ratio of hydrocarbon evaporation to total hydrocarbon emissions for the 1979 inventory and then multiplying that same ratio by the total hydrocarbon emissions from area sources estimated for the year 2000; it was determined that 8.5 percent of the total HC from area sources would be due to fueling operations. For the complete methanol replacement scenarios, this percentage (8.5 percent) was assumed to be methanol. This value accounts for roughly 4 percent of the total HC inventory. For the partial replacement scenarios, 1.7 percent (0.20 x 8.5 percent) of evaporative emissions due to fueling operations were assumed to be methanol.

Total daily emissions (tons per day) by source type for the year 2000 base case (1A) are compared to those of the 1979 inventory in Table 17. For mobile sources only, the percentage of the HC inventory is reduced from 31 percent in 1979 to 16 percent in the year 2000. The hydrocarbon splits for 1979 and 2000 are also shown for comparison. Percentages of total inventory due to mobile sources with complete methanol replacement are 4.8, 12.3, and 24.4, respectively, for Scenarios 2A, 2B, and 2C.

Initial Conditions

The maximum initial ozone concentration for the year 2000 was set at 0.08 ppm and is an estimate of that value in the year 2000. In most cases the 1979 initial ozone concentrations were equal to 0.08 ppm.

TABLE 17. 1979 AND YEAR 2000 PHILADELPHIA EMISSION INVENTORIES

Source File	Emissions (tons per day, summer weekday) 1979 RHC*		1979 NO_x†		2000 RHC*		2000 NO_x†	
Major Point	41.5	(3%)§	304.0	(34)	26.6	(4%)	336.6	(39)
Minor Point	386.1	(26)	109.3	(12)	235.5	(31)	121.0	(14)
Area	526.4	(37)	147.7	(16)	336.8	(45)	163.5	(19)
Mobile-Related Stationary	45.8	(3)	0	(0)	29.3	(4)	0	(0)
On-Road Motor Vehicles**	442.9	(31)	343.9	(38)	117.4	(16)	243.0	(28)
TOTAL	1424.7	(100)	904.9	(100)	745.6	(100)	864.1	(100)

* Emissions expressed as methane.
† Emissions expressed as nitrogen dioxide.
§ Percentages of the total inventory
** Emissions based on MOBILE3.

Species	Philadelphia Inventory Splits: Carbon-Bond Fraction (% as Carbon) 1979	2000
PAR	74.0	79.0
OLE	2.8	1.1
ETH	4.1	9.7
ARO	13.2	8.5
CARB	5.9	1.7

85117r2 5

Initial and boundary hydrocarbon conditions for the year 2000 were calculated by subtracting an estimated middle hydrocarbon background value (Table 18) from the total 1979 initial conditions. The resulting difference represents the portion of hydrocarbons that can be controlled by changing the volume or composition of emissions in Philadelphia. In comparison, the hydrocarbon background is considered uncontrollable because it remains unaffected by changes in the emissions. An example of an uncontrollable background source is the influx of hydrocarbons emissions from natural vegetation. The controlled portion of hydrocarbon concentration is multiplied by 0.52, which is a projection factor of the reduction in Philadelphia's contribution to initial hydrocarbon concentrations in the year 2000. This calculation estimates the change in initial and boundary hydrocarbon concentrations in the year 2000 due only to controllable sources. It is assumed that areas outside of Philadelphia might also control VOC emissions to the same degree as those within the Philadelphia airshed (i.e., by 48 percent). The initial and boundary conditions in the year 2000 are given in Tables 19, 20, 21.

Inputs Used in the Systems Applications' Trajectory and Box Model Simulations

The meteorological and emissions files used in the Systems Applications' trajectory model are the same as those used by the UAM. By running the Systems Applications trajectory model in a backward mode, a path to the maximum ozone observed can be determined for the day of interest. The trajectory paths for 13 and 19 July 1979 are shown in Figures 9a and b, respectively. For a more detailed explanation of the use and application of the Systems Applications trajectory model (see Myers et al., 1979).

Using the results of the Systems Applications trajectory model, emissions and meteorological conditions are constructed for a Level II type box model with Carbon-Bond chemistry (Ozone Isopleth Plotting Package) (OZIPM/CBM). OZIPM is a computer routine used in box modeling that can handle different chemical mechanisms. The trajectory model prints out the emissions and mixing heights along the trajectory path at hourly intervals. These mixing heights can be used as direct inputs to the OZIPM computer code. The emission rates from the trajectory model are in units of moles/hr for each of the Carbon-Bond species and are converted to ppmC/hr for volatile organic compounds (VOC) by the following equation:

$$\text{Emissions Rate (ppmC/hr)} = [24450/(Z_0 * 4000^2)][\text{Emissions Rate (moles/hr)}] \quad ,$$

where Z_0 is the initial mixing height.

TABLE 18. BACKGROUND OF REACTIVE HYDROCARBONS. (Source: Killus and Whitten, 1984).

Carbon Fraction		Concentration	Species	
Low	0.91	0.03 ppmC	PAR	0.03 ppmC
	0.09	0.003 ppm	CARB	
		0.1 ppm	CO	OH to RO_2 reactivity = 125 min^{-1}
Mid	0.61	0.035 ppmC	PAR	0.043 ppmC
	0.083	0.0008 ppm	ARO	(+ 0.015 ppm CARB)
	0.034	0.001 ppm	ETH	
	0.014	0.0004 ppm	OLE	
	0.26	0.015 ppm	CARB	OH to RO_2 reactivity
	0.0005	0.00003 ppm	DCRB	
		0.2 ppm	CO	= 387 min^{-1}
High	0.57	0.1 ppmC	PAR	0.144 ppmC
	0.07	0.002 ppm	ARO	(+ 0.03 ppm CARB)
	0.12	0.01 ppm	ETH	
	0.07	0.006 ppm	OLE	
	0.17	0.03 ppm	CARB	
	0.0005	0.00008 ppm	DCRB	OH to RO_2 reactivity
		0.5 ppm	CO	1153 min^{-1}

Note: All estimates include 0.015 ppmC PAR as surrogate for background methane.

TABLE 19. LOWER BACKGROUND CONCENTRATION VALUES FOR THE YEAR 2000 FOR ALL LEVELS OF ALL BOUNDARIES EXCEPT THE LEVELS BELOW THE MIXING HEIGHT ON THE NORTHEAST AND EAST BOUNDARIES

Species	Concentration (ppm)
NO	0.001
NO_2	0.002
CO	0.2
ETH	0.001
OLE	0.0004
PAR	0.050
CARB	0.015
ARO	0.0008
PAN	0.000025
BZA	0.00001

85117r2 5

TABLE 20. LOWER INITIAL CONDITIONS FOR THE YEAR 2000 (ppm)

	PAR	OLE	ETH	ARO	CARB
AMS Lab.	0.1602	0.0012	0.0093	0.0030	0.0150
Ancora	--	--	--	--	--
Brigantine	--	--	--	--	--
Bristol	--	--	--	--	--
Camden	--	--	--	--	--
Chester	0.4071	0.0029	0.0244	0.0074	0.0150
Claymont	--	--	--	--	--
Conshohocken	--	--	--	--	--
Defense Support	--	--	--	--	--
Downington	0.037	0.0004	0.0017	0.0008	0.0150
Franklin Inst.	--	--	--	--	--
Island Rd. Airport Cir.	--	--	--	--	--
Lumberton	0.1811	0.0013	0.0106	0.0033	0.0150
Norristown Armory	0.1359	0.0010	0.0078	0.0025	0.0150
Northeast Airport	--	--	--	--	--
Roxy Water Pump	--	--	--	--	--
SE Sewage Plant	--	--	--	--	--
South Broad	0.1195	0.0009	0.0068	0.0022	0.0150
Summit Bridge	0.0579	0.0005	0.0030	0.0011	0.0150
SW Corner Broad/Butler	--	--	--	--	--
Trenton	--	--	--	--	--
Van Hiseville	--	--	--	--	--
Vineland	--	--	--	--	--

TABLE 21. BOUNDARY CONDITIONS FOR THE YEAR 2000 USED FOR THE NORTHEAST AND EAST BOUNDARIES BELOW THE MIXING HEIGHT ESTIMATED FROM DATA COLLECTED AT THE VAN HISEVILLE, NEW JERSEY MONITOR (ppm)

Hour (EST)	NO	NO_2	PAR	OLE	ETH	ARO	CARB	PAN
0000-0100	0.044	0.036	0.1627	0.0004	0.001	0.0008	0.015	0.0002
0100-0200	0.044	0.036	0.1627	0.0004	0.001	0.0008	0.015	0.0001
0200-0300	0.044	0.036	0.1627	0.0004	0.001	0.0008	0.015	0.0000
0300-0400	0.044	0.036	0.1627	0.0004	0.001	0.0008	0.015	0.0000
0400-0500	0.044	0.036	0.1627	0.0004	0.001	0.0008	0.015	0.0000
0500-0600	0.044	0.036	0.1627	0.0004	0.001	0.0008	0.015	0.0000
0600-0700	0.047	0.041	0.1773	0.0004	0.001	0.0008	0.015	0.0000
0700-0800	0.043	0.0494	0.1852	0.0004	0.001	0.0008	0.015	0.0004
0800-0900	0.026	0.0478	0.1515	0.0004	0.001	0.0008	0.015	0.0008
0900-1000	0.009	0.0273	0.0831	0.0004	0.001	0.0008	0.015	0.0013
1000-1100	0.001	0.0099	0.0367	0.0004	0.001	0.0008	0.015	0.0019
1100-1200	0.000	0.0058	0.0350	0.0004	0.001	0.0008	0.015	0.0018
1200-1300	0.000	0.0054	0.0350	0.0004	0.001	0.0008	0.015	0.0014
1300-1400	0.000	0.0072	0.0350	0.0004	0.001	0.0008	0.015	0.0012
1400-1500	0.000	0.0047	0.0350	0.0004	0.001	0.0008	0.015	0.0007
1500-1600	0.000	0.0035	0.0350	0.0004	0.001	0.0008	0.015	0.0005
1600-1700	0.000	0.0043	0.0350	0.0004	0.001	0.0008	0.015	0.0003
1700-1800	0.000	0.0053	0.0350	0.0004	0.001	0.0008	0.015	0.0003
1800-1900	0.000	0.0072	0.0350	0.0004	0.001	0.0008	0.015	0.0002
1900-2000	0.000	0.0071	0.0350	0.0004	0.001	0.0008	0.015	0.0001
2000-2100	0.000	0.0041	0.0350	0.0004	0.001	0.0008	0.015	0.0001
2100-2200	0.002	0.0030	0.0350	0.0004	0.001	0.0008	0.015	0.0000
2200-2300	0.005	0.0060	0.0350	0.0004	0.001	0.0008	0.015	0.0000
2300-2400	0.008	0.0030	0.0350	0.0004	0.001	0.0008	0.015	0.0000

85117r2 5

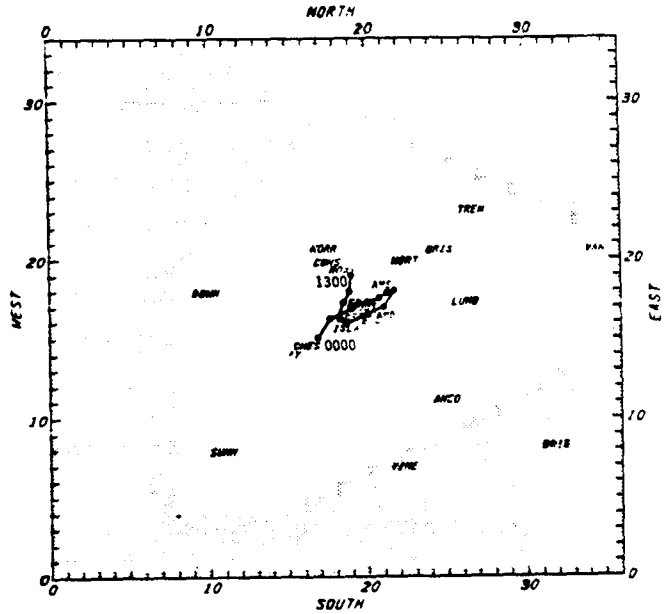

FIGURE 9a. Averaged trajectory path for 13 July 1979.

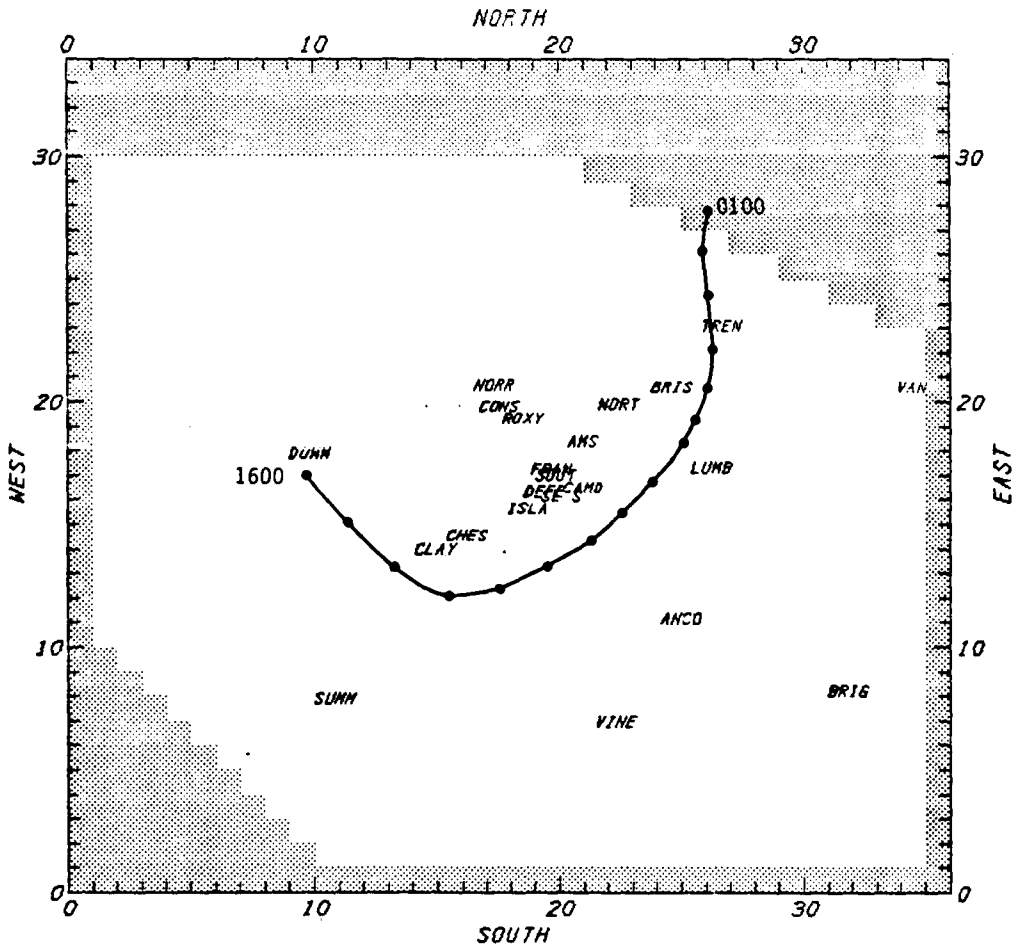

FIGURE 9b. Trajectory path for 19 July 1979.

Initial NO_x and VOC precursors for OZIPM are determined from the initial conditions using the average of the layers below the mixing height in the trajectory model. NO_x and VOC precursors aloft are determined from the amount of precursors that entered the mixed layer from aloft in the trajectory model simulations. Tables 22 and 23 describe the initial conditions and emission rates used for the 13 and 19 July base case (1A). OZIPM was run for 13 July using both the lower initial conditions and those from 1979. Emission rates were changed according to the list of scenarios. July 19 was run with 1979 initial conditions for the base case, which was also the only scenario simulated for that day with OZIPM. For a more detailed explanation of the use and application of OZIPM see EPA (1978).

TABLE 22. INITIAL CONDITIONS AND EMISSION RATES USED FOR OZIPM CALCULATIONS FOR THE BASE CASE (1A)--JULY 13.

(a) Initial Conditions*

Species	Surface	Aloft
O_3	0.0363 ppm	0.0782 ppm
VOC	0.0891 ppmC	0.0539 ppmC
NO_x	0.0332 ppm	0.0004 ppm

Hydrocarbon Reactivity: Carbon Fraction

	Surface	Aloft
OLE =	0.0263	0.0062
PAR =	0.6931	0.5650
ARO =	0.1259	0.0711
ETH =	0.0400	0.0285
METH =	0.0000	0.0000
HCHO =	0.0381	0.1002
DCRB =	0.0003	0.0023
CARB =	0.0763	0.2266

TABLE 22. CONCLUDED.

(b) Emission Rates and Mixing Heights

Time (CDT)	Species VOC (mole/hr)	NO_x (mole/hr)	Mixing Heights at Beginning of Each Hour (m)
0000-1000	1994	2056	250.0
0100-0200	1577	4316	250.0
0200-0300	1217	3005	250.0
0300-0400	2864	2763	250.0
0400-0500	7505	4972	250.0
0500-0600	11671	6387	250.0
0600-0700	42260	10699	250.0
0700-0800	77379	15940	295.0
0800-0900	72265	22218	450.0
0900-1000	51171	14038	925.0
1000-1100	43113	10257	1200.0
1100-1200	34344	6974	1480.0
1200-1300	26227	5399	1480.0
1300-1400	12866	3187	1530.0
1400-1500	12199	2494	1530.0
1500-1600	3876	856	1420.0
1600-1700	1445	370	1310.0
1700-1800	1380	271	1130.0
1800-1900	167	41	950.0
1900-2000			525.0

* Lower initial conditions for 2000.

TABLE 23. INITIAL AND BOUNDARY CONDITIONS FOR OZIPM CALCULATIONS FOR THE BASE CASE (1A)--JULY 19.

(a) Initial Conditions*

Species	Surface	Aloft
O_3	0.0034	0.0659
VOC	0.5414	0.0518
NO_x	0.0871	0.0015

Hydrocarbon Reactivity: Carbon Fraction

	Surface	Aloft
OLE =	0.0270	0.0085
PAR =	0.7139	0.6331
ARO =	0.1308	0.0695
ETH =	0.0398	0.0314
METH =	0.0000	0.0000
HCHO =	0.0292	0.0839
DCRB =	0.0009	0.0039
CARB =	0.0584	0.1696

85117r2 5

TABLE 23. CONCLUDED.

(b) Emission Rates and Mixing Heights

Time (CDT)	Species VOC (mole/day)	Species NO_x (mole/day)	Mixing Heights at Beginning of Each Hour (m)
0000-1000	4313	892	80.0
0100-0200	12323	1887	431.6
0200-0300	22721	3441	600.0
0300-0400	17367	1445	856.7
0400-0500	8115	1762	1240.0
0500-0600	9304	2217	1530.0
0600-0700	9843	2614	1480.0
0700-0800	6266	1763	1332.6
0800-0900	3640	1108	1117.8

SECTION 4

DISCUSSION OF MODEL RESULTS

Study results indicate that atmospheric sensitivity to VOC and NO_x precursors in Philadelphia in the year 2000 appears to be strongly governed by the ratio of VOC/NO_x, and only to a small degree by total precursor concentrations. This finding is most clearly illustrated by the isopleth diagram produced specifically by OZIPM shown in Figure 10. An isopleth diagram is a series of lines connecting the points at which a given variable has a specified constant value. This isopleth diagram shows the maximum one-hour ozone concentrations resulting from NO_x and VOC emissions relative to the base-case emissions (the 1,1 point on the diagram). VOC and NO_x are measured here as a percentage of the base-case emissions. For example, at 0.75 along the relative VOC scale and 0.60 along the relative NO_x scale, VOC emissions are 75 percent and NO_x emissions are 60 percent of the base-case emissions. Therefore, the base-case point on the isopleth diagram has the coordinates (1,1), since VOC and NO_x are equal to the equivalent emission inventory value at that point.

The isopleth diagram shown in Figure 10 also explains the unexpected ozone insensitivity when mobile source emissions are eliminated. Since the percent reduction in overall emissions is slightly greater for NO_x than for VOC when mobile source emissions are eliminated, the overall VOC/NO_x ratio increases somewhat. As the total emissions from the (1,1) base case point of Figure 10 decrease and the VOC/NO_x ratio is increased to the zero mobile equivalent point, the predicted ozone closely follows the isolines, indicating little change in ozone. Removing mobile sources and mobile-source-related stationary emissions reduces the area-wide VOC in the year 2000 by about 20 percent, as shown in Table 17. Hence, the point marked "No Mobile Source Point" in Figure 10 shows about the same ozone maximum as the (1,1) base case point.

The lack of ozone reduction from zero mobile-related emissions is related to the slanting parallel lines of Figure 10. Essentially, the slanted lines result from the initial "loss" of emitted NO to form NO_2 via the NO-to-NO_2 conversions related to VOC photooxidation. Once the initial NO has reacted to NO_2, further NO-to-NO_2 conversions start the production

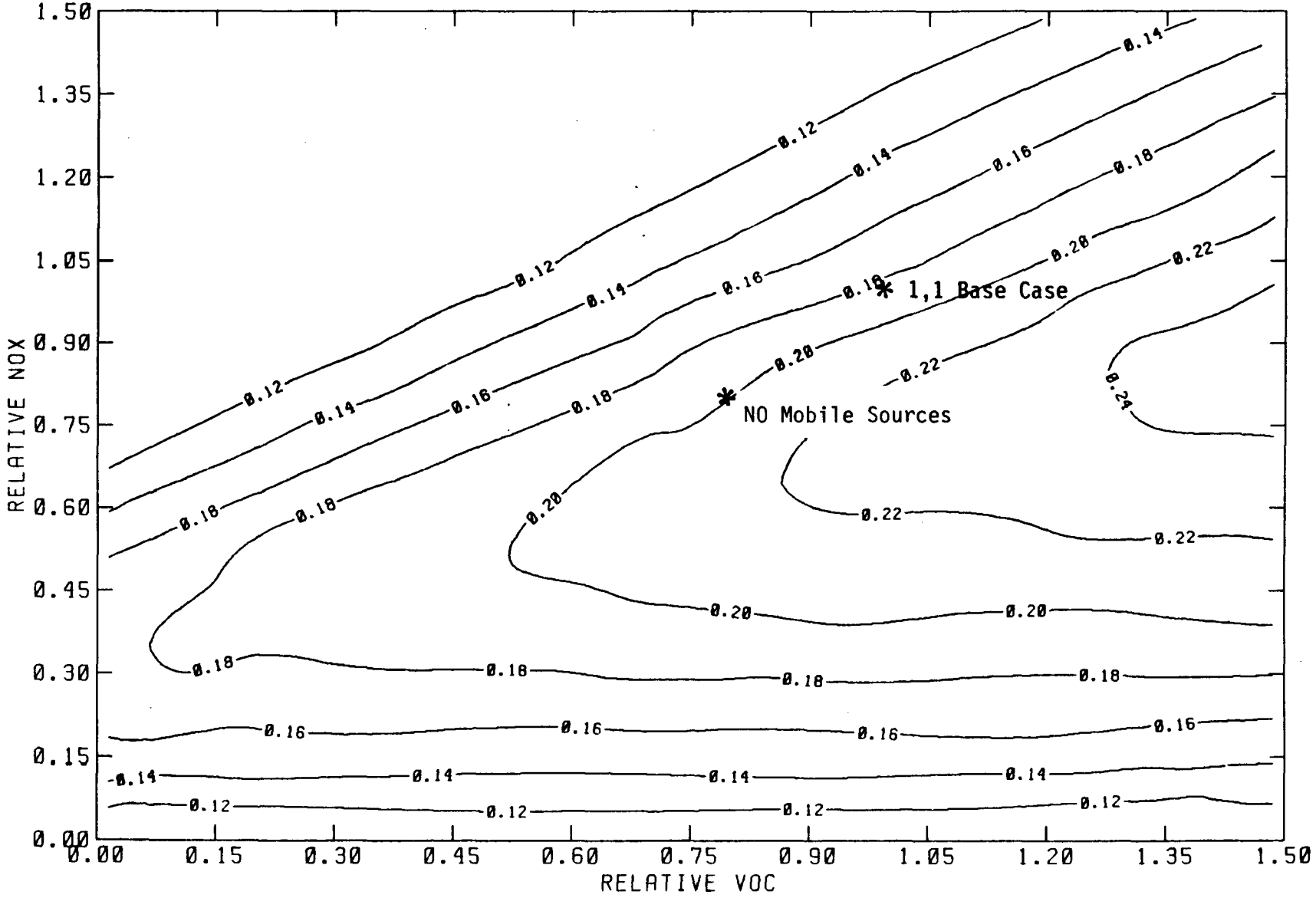

FIGURE 10. Overall emission sensitivity for the 13 July 2000 base case with low initial conditions.

of ozone. In the initial conversion of NO to NO_2, the amount of VOC that is photooxidized is directly related to the amount of NO; however, once the NO has reacted, the amount of ozone formed is essentially independent of the amount of NO_x present, but closely related to the amount of VOC, which continues to photooxidize and convert NO to NO_2. Hence, there is a threshold at which the chemistry changes from NO to NO_2 reaction and to ozone formation; this threshold appears on the isopleths as a slanted straight line with a slope related to the amount of VOC expended to convert the emitted NO. The ozone formed thereafter essentially depends only on the VOC, which continues to photooxidize. Hence, a series of isolines, all parallel to the threshold line, are formed.

The validity of this explanation was also presented by Whitten (1983), who demonstrated that converting NO_x emissions from NO to NO_2 virtually removes the "slant," causing the threshold to be nearly vertical. Hence, an important sidelight of the present study is the reemphasis of the importance of the high ratio of NO in NO_x emissions. If NO_x emissions were composed mostly of NO_2 instead of NO, the atmospheric models would predict much higher urban ozone levels, independent of NO_x emissions, until very low NO_x levels were reached. Virtually all ozone isopleth diagrams have isolines nearly parallel to the VOC axis for low levels of NO_x. However, the 0.12 ppm ozone isoline is typically far below both present and near-future NO_x emissions levels.

METHANOL FUEL SUBSTITUTION

The effect of emission control devices on mobile sources has been predicted to account for a factor of 3 reduction in mobile source VOC emissions for Philadelphia between 1979 and 2000. The overall contribution to VOC emissions from mobile sources drops from 34 percent in 1979 to only 20 percent in 2000, in addition to which total VOC emissions are expected to be nearly half of the 1979 value by the year 2000 (Table 17).

The substitution of methanol and some formaldehyde in exchange for gasoline-fueled auto exhaust has been shown by Pefley, Pullman, and Whitten (1984) to reduce the reactivity of the atmosphere towards ozone formation. However, the ozone isopleth diagram 13 July 2000 (Figure 11), shows virtually no change in ozone levels for Philadelphia as a result of methanol substitution. Tables 24 and 25 also show that in many of the scenarios studied there was no significant change in ozone levels from the base case simulations. For the 19 July 2000 cases shown in Table 25, the base case was already too low in ozone to justify any further consideration. Hence, the present study focused on the 13 July 2000 cases, which were clearly above the air quality standard of 0.12 ppm ozone.

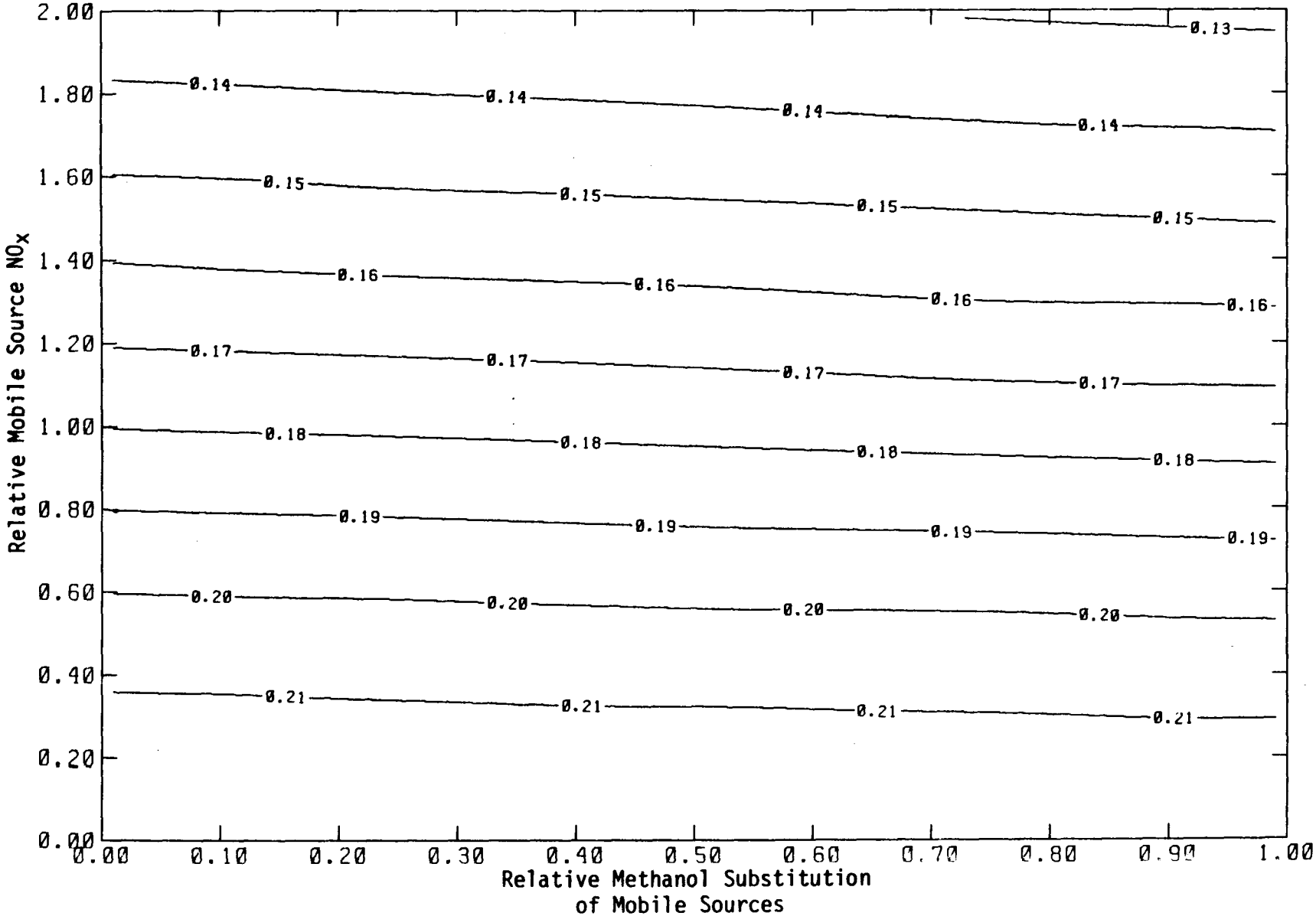

FIGURE 11. Methanol and NO_x sensitivity for mobile source emissions relative to 13 July 2000 (low initial) base case.

TABLE 24a. METHANOL IMPACT MODELING FOR 13 JULY 2000

Scenario	Description	UAM	UAM*	TRAJ	TRAJ*	BOX	BOX*
1A	Base case	192	185	211	194	223	204
1B				202		219	192
2A	Full methanol						183
2B	(x 2.5)	192	186	210	192	219	198
2C	(x 5.0)						216
2D	2B with surface deposition				189		
2E	2B with 20 percent IC,‡ aloft					203	177
	Partial methanol (20 percent)						
3A							198
3B		192	185	211	194	223	201
3C							205
	Based on 2B;		185		188	214	190
4A	formaldehyde, 5 percent					228	206
4B	20 percent						
	Based on 2C;						206
5A	formaldehyde, 5 percent						233
5B	20 percent						

* Lower initial and boundary conditions; all results in ppb instantaneous ozone at 1600 hours at regional maximum site. Lower initial and boundary conditions were calculated as previously discussed.

‡ IC = initial conditions.

TABLE 24b. BOX MODEL SENSITIVITY TESTS FOR 13 JULY 2000

Scenario	Description	Ozone (ppb)
7A	Zero mobile sources,	201*
7B	Base NO_x, zero VOC from mobile	156
8A	Stationary methanol at zero (based on 2B)	192
8B	Overall substitution 50 percent methanol	156
8C	Same with 50 percent methanol in IC‡	134
8D	Same with 50 percent methanol aloft and IC	113
9A	Mobile carbon replacement by methanol (no formaldehyde)	179
9B	carbon (x 1.5) methanol	183
9C	(x 2.0) methanol	187
9D	carbon, 0.1 formaldehyde (no methanol)	184
9E	0.2 formaldehyde (no methanol)	196
10A	50 percent VOC overall, no methanol; base NO_x, IC, aloft	124

* Lower initial and boundary conditions; all results in ppb ozone at 1600 hours at regional maximum site.

‡ IC = initial conditions.

TABLE 25. METHANOL IMPACT MODELING FOR 19 JULY 2000*

Scenario		UAM	TRAJ	BOX
Base case	1A	137	130	124
Full methanol for mobile source	2B			126
No mobile source	7A		114	107

* All results in ppb ozone at 1600 hours at regional maximum site; high carryover conditions.

85117r 8

The general lack of effect from methanol substitution can be partly explained by the relatively low (16 percent) contribution from mobile sources and the high sensitivity of the models to the small amount of formaldehyde emissions that are found in methanol exhaust. The lack of sensitivity to mobile source substitution by methanol fuel may be explained in part by the extreme slant shown in the isopleth curves of Figure 10. Although most of the slant probably results from NO titration, as discussed, the remainder is due to ozone and ozone precursor/carryover either from Philadelphia or from neighboring cities. Figure 10 shows that zero VOC emissions in conjunction with a small amount of NO_x emissions can produce simulated ozone levels in excess of 0.12 ppm. The necessary VOC precursors in such cases come from assumed initial and aloft concentrations.

The sensitivity results for cases 8C and 8D shown in Table 24b indicate that initial VOC is only slightly more important than aloft VOC even though the assumed concentrations aloft are much lower than the initial concentrations. This nearly equal sensitivity can be explained by two factors. First, the aloft precursors enter the simulation only as the mixing height rises and have not dissipated when they enter the simulation, whereas the initial precursors are partially dissipated through chemical reactions and wind. Second, the ratio between the initial and highest mixing height values accounts for a reduction due to dilution by a factor of 6.1 for the initial precursors, which nearly equals the contributions of the two carryover sources.

If the total concentration of the carryover sources of VOC in initial and aloft conditions is lowered by 20 percent, and if methanol replaces that missing 20 percent, reactivity is greatly reduced. The sensitivity results in Table 24 for Scenario 2E show greater decreases in ozone than when methanol is substituted in the primary mobile-related emissions for Philadelphia (Scenario 2A). Assessment of the contribution of Philadelphia emissions to carryover and the contribution from sources upwind of Philadelphia is beyond the scope of the present study; such an assessment would require multiple-day regional modeling. However, the box model is an effective tool for assessing the atmospheric sensitivity to such changes. Scenarios 8B, 8C, and 8D were designed to show the gross sensitivity to methanol substitution. The results shown in Table 24b indicate that a 50 percent substitution of methanol for half of all VOC emissions reduces peak ozone from the base case (1A) value of 201 ppb to 156 ppb. Further, a 50 percent substitution for half of all the initial VOC reduces peak ozone to 134 ppb; when aloft VOC is then added to the 50 percent methanol substitution, the final peak predicted ozone is only 113 ppb.

These simulations assumed no reduction in NO_x emissions; however, a reduction in formaldehyde levels equivalent to 50 percent resulted from substitution of methanol since all VOC species were reduced by 50 percent and methanol was added to keep the total VOC constant.

Since the lack of effect on ozone production of methanol substitution can be partly explained by the low contribution of mobile sources (16 percent from vehicles; 4 percent from mobile-related sources) to total emissions, two additional scenarios were set up. Scenarios 11 and 12 increased the contribution of mobile sources to 30 percent and 50 percent, respectively. In both cases, mobile source emissions were kept the same but stationary source emissions were decreased until the mobile source contributions equaled 30 and 50 percent, resulting in a decrease in total emissions of about 33 percent and 60 percent, respectively.

Decreasing the overall emissions by reducing stationary source emissions to the point at which mobile sources contribute 30 percent of the total emissions (Scenario 11A) significantly decreases the amount of ozone produced by the base case 1A from 201 ppb to 136 ppb at 1600 hr. Substituting methanol for the 30 percent mobile source contribution (Scenario 11B), further decreases the amount of ozone produced, bringing it close to the EPA standard of 120 ppb (Table 26).

Simply decreasing the overall emissions by reducing stationary source emissions to the point at which the mobile sources contribute 50 percent of the total emissions (Scenario 12A) decreases the amount of ozone predicted by the base case 1A from 201 ppb to 90 ppb, which is already far below the EPA standard. Full substitution of methanol for the 50 percent mobile source contribution (Scenario 12B) reduces ozone even further (Table 26).

Methanol was incorporated into the initial and aloft conditions for Scenarios 11 and 12 since it is reasonable to assume that complete methanol substitution for the mobile source contribution to emissions would lead to the presence of methanol in VOC carryover. Ozone production for Scenario 11B (with methanol substitution for initial and aloft conditions) reaches the EPA standard ozone level. With either initial or aloft methanol removed, more ozone is produced, bringing the level above the EPA standard (Table 26). Scenario 2E also showed the sensitivity of ozone production to the substitution of methanol for initial and aloft conditions.

For Scenarios 11 and 12, the box model was run an additional three hours because, though 1600 hours is the regional maximum simulated by the UAM, the box model shows a positive slope for ozone at that time. Ozone concentration does not begin to level off until about 1800 hour and

TABLE 26. BOX MODEL METHANOL-IMPACT OZONE RESULTS (ppb) FOR 13 JULY 2000 WITH 30 PERCENT AND 50 PERCENT MOBILE SOURCE EMISSIONS

Scenario*	30% Mobile Emissions				50% Mobile Emissions	
	No Initial or Aloft Methanol	Initial and Aloft Methanol	Initial Methanol Only	Aloft Methanol Only	No Initial and Aloft Methanol	Initial and Aloft Methanol
Base Case:						
Instantaneous ozone at 1600 hr†	136	--	--	--	90	--
Average hourly maximum ozone	151	--	--	--	94	--
Full Methanol:						
Instantaneous ozone at 1600 hr†	129	120	123	126	--	75
Average houly maximum ozone	142	131	134	138	--	76

* All scenarios with lower initial and boundary conditions calculated as previously discussed.

† Ozone at 1600 hr, the regional maximum site simulated by the UAM.

results in a higher average maximum ozone value. This difference in the UAM and box model results can be attributed to wind shear between the layers below the mixing height in the UAM, starting in the late morning of the modeling day and ending in the aftrnoon of the same day; wind shear can not be accounted for in the single-layer box model. Since wind shear introduces a horizontal dilution factor, limiting precursor concentrations and diluting the ozone, the box model, which is not subject to this dilution factor, predicts a higher ozone peak occurring later than that of the UAM. For further discussion of wind shear see Volume III of Whitten et al. (1985).

The concentrations of ozone and selected products predicted in Scenarios 11 and 12 are given in Tables 27 and 28 for two different VOC/NO_x ratios--1:1 and 1:0.2--which are relative ratios based on the base case values. For Scenario 11 (30 percent mobile), methanol substitution is beneficial in decreasing ozone under low VOC/NO_x conditions, but at higher values a nominal increase in ozone is predicted (Tables 26 and 27). A similar trend is predicted for Scenario 12 (50 percent mobile). As reported previously, a decrease in ozone production should result from methanol substitution at a VOC/NO_x ratio of 1:1. Although Table 28 shows somewhat lower ozone for methanol substitution at 1600 hours for the high VOC/NO_x 50 percent case (Scenario 12), the overall maximum ozone comparison for all hours shows that the methanol substitution simulation predicts 178 ppb, which is slightly more than the 173 ppb ozone predicted without methanol substitution. It appears that for higher VOC/NO_x conditions, the base-case Scenario (12A) was slightly more reactive earlier in the simulation, but the methanol-substituted Scenario (12B) produced ozone for a slightly longer period. The relative differences in these maximum concentrations are small, however, compared to the reductions predicted in the 1:1 ratio simulations (EPA VOC/NO_x ratios projected for the year 2000 give greater weight to the 1:1 results). The effect of the VOC/NO_x ratio on ozone reduction from methanol substitution shown in these simulations is consistant with the smog chamber results of Pefley, Pullman, and Whitten (1984).

The predicted product concentrations for the high and low VOC/NO_x conditions used in Scenario 11 (30 percent mobile emissions) indicate that full methanol substitution should reduce the production of PAN, nitrophenols, and organic nitrates, all of which are potentially harmful to humans. In addition, the results given in Table 28 show that these reductions are far less dependent on VOC/NO_x ratio than is ozone production. That is, although the beneficial effect of methanol substitution on ozone production is minimized by raising the VOC/NO_x ratio through NO_x control, the predicted decreases in the concentrations of these nitrogen-containing species occur for all cases; this is because the VOCs replaced by methanol would have produced products that react with NO_2 to form PAN,

TABLE 27. PRODUCT CONCENTRATIONS PREDICTED FOR SCENARIO 11*

Species§	No Methanol Substitution		Full Methanol Substitution†	
	VOC/NO_x = 1:1	VOC/NO_x = 1:0.2	VOC/NO_x = 1:1	VOC/NO_x = 1:0.2
Ozone	136	169	120	176
PAN	6.57	9.10	4.20	7.86
Nitrophenols	0.43	0.61	0.21	0.34
Formaldehyde	10.9	8.64	10.8	9.56
Nitric Acid	37.0	9.3	36.6	10.7
Organic Nitrates	1.66	2.03	1.16	1.70

* VOC/NO_x ratios are relative to absolute base-case values.

† Methanol substitution for initial conditions and aloft.

§ ppb at 1600.

TABLE 28. PRODUCT CONCENTRATIONS PREDICTED FOR SCENARIO 12*

Species§	No Methanol Substitution		Full Methanol Substitution‡	
	VOC/NO_x = 1:1	VOC/NO_x = 1:0.2	VOC/NO_x = 1:1	VOC/NO_x = 1:0.2
Ozone	90	167	75	173
PAN	2.56	7.71	1.30	5.79
Nitrophenols	0.19	0.43	0.06	0.16
Formaldehyde	7.9	6.7	6.8	7.37
Nitric Acid	29.1	11.0	27.1	13.2
Organic Nitrates	0.81	1.58	0.49	1.92

* VOC/NO_x ratios ar relative to absolute base-case values.

‡ Methanol substitution for initial conditions and aloft.

§ ppb at 1600.

nitrophenols, and organic nitrates. Since methanol forms no such long-chain organic products upon reaction, the production rates are lowered, not by lack of NO_2, but by the decrease in organic products with which NO_2 reacts. This is emphasized in the 1:0.2 simulation; these results indicate that some of the NO_2 that cannot react with the missing VOC products was oxidized through inorganic pathways to form additional nitric acid and ozone (Table 27).

Also of particular importance to an understanding of the chemistry is the fact that a formaldehyde molecule is formed for every methanol molecule reacted. This is not quite the case for other VOCs. However, Table 27 indicates only a slight increase in hourly formaldehyde values between the base case and the substitution simulations of Scenario 11. That is, formaldehyde concentrations in the full methanol substitution simulation do not exceed those of the base case by more than about 10 percent, on the average, with maximum differences in hourly values of no more than 20 percent.

For Scenario 12, in which mobile sources represent 50 percent of emissions, the effects of methanol substitution are more definite. Table 28 shows the predicted product yields for these simulations. Since the percentage of methanol is larger in these cases, the predicted decreases in PAN, organic nitrates, and nitrophenols are larger than those from the 30 percent mobile exhaust simulations. Again, however, the relative reductions in these species show far less relationship to the VOC/NO_x conditions than do the predicted ozone maximum concentrations. Rather, as noted, these changes relate more to the amount of methanol present.

SENSITIVITY OF THE MODEL SIMULATIONS TO FORMALDEHYDE

The sensitivity of the model simulations to formaldehyde is shown by comparing Scenarios 4A and 4B with Scenario 2B in Table 24a. In these three scenarios, 100 percent methanol was used; however, in Scenario 4A formaldehyde exhaust emissions were reduced from 10 percent (Scenario 2B) to 5 percent. In Scenario 4B, the formaldehyde exhaust was assumed to be as high as 20 percent.

The maximum ozone values produced from the 5, 10, and 20 percent formaldehyde exhaust levels were 190, 196, and 206 ppb, respectively, for the box model simulations using low initial conditions, and 214, 219, and 228 ppb ozone for the cases assuming higher initial conditions. The amount of overall formaldehyde emissions for these three cases was only 3.6, 4.2, and 5.4 percent, respectively, of the entire VOC emissions. The base case (1A) formaldehyde emissions were 3.3 percent.

Comparison of Scenarios 5A and 5B with 2C provides another indication of formaldehyde sensitivity. These scenarios are similar to 4A, 2B, and 4B, except that the 5A, 2C, 5B series substitutes 2.5 times as much methanol and formaldehyde for gasoline-related emissions. Thus the 5, 10, and 20 percent formaldehyde exhaust assumptions for the 5A, 2C, 5B series lead to overall percentages of formaldehyde emissions of 4.2, 5.4, and 7.8 percent, respectively. This series of formaldehyde levels produces ozone maxima of 206, 216, and 233 ppb, respectively, in the box model simulations shown in Table 24a.

A more dramatic demonstration of the model's sensitivity to formaldehyde is shown in the results of Scenarios 9D and 9E in Table 24b. For these tests, 10 and 20 percent of all mobile-related emissions were replaced by formaldehyde as carbon, i.e., no methanol or gasoline-related emissions were present. Two or more base case points can be compared with the 9D and 9E Scenarios. With no mobile VOC emissions (case 7B), the maximum ozone is only 156 ppb. Adding only 10 percent of the mobile VOC as formaldehyde (case 9D) raises the simulated ozone peak to 190 ppb. Doubling the formaldehyde addition (case 9E) further increases peak ozone only to 207 ppb. Hence the model shows a very high sensitivity to the first addition of formaldehyde, raising the ozone peak to 190 ppb (from 156 ppb), which is nearly the peak predicted for 150 percent replacement by pure methanol (case 9B). This implies a formaldehyde-to-methanol reactivity ratio of 15 to 1. The overall percentages for formaldehyde in cases 9D and 9E are 6 and 8.3 percent of the total VOC emissions. For case 7B (no mobile source VOC emissions), formaldehyde was only 3.7 percent of the emissions. Hence the model shows a very high sensitivity when formaldehyde is increased from 3.7 to 6 percent.

FORMALDEHYDE CONCENTRATION LEVELS

The UAM is an appropriate model for assessing the spatial and temporal impact of changes in formaldehyde emissions resulting from substitution of methanol fuel. Table 29 shows the contrast in maximum hourly formaldehyde levels between the 2000 base case and 100 percent methanol mobile source substitution. Figure 12* shows the year 2000 base case formaldehyde levels from the beginning of the simulation at midnight until noon, when the mixing heights have increased to such an extent that the formaldehyde levels are no longer important because of dilution. Figure 13 presents contour lines of the change in formaldehyde due to 100 percent substitution of mobile sources with methanol (case 2B minus base case). Figures 14 and 15 present the overall maximum values seen in Figures 12 and 13. The area of maximum formaldehyde impact is in a region of heavy

---

* For the convenience of the reader, Figures 12 through 16 are placed at the end of the report.

TABLE 29. MAXIMUM HOURLY FORMALDEHYDE (ppb) LEVELS COMPARING YEAR 2000 BASE CASE (1A) TO 100 PERCENT METHANOL SUBSTITUTION OF MOBILE SOURCES (2B)

Hour	1A*	2B*
0000-0100	27.3	27.3
0100-0200	25.7	25.8
0200-0300	24.0	24.1
0300-0400	24.1	24.2
0400-0500	24.2	25.2
0500-0600	25.2	27.1
0600-0700	24.6	27.1
0700-0800	22.5	25.9
0800-0900	18.2	20.6
0900-1000	14.1	15.3
1000-1100	13.1	13.7
1100-1200	13.2	13.3

* Lower initial and boundary conditions.

traffic emissions. The area of maximum ozone in the 2000 base case simulations is shown in Figure 16. The maximum ozone occurs in grid cell 22,24 between 1600 and 1700 hours for all UAM simulations on 13 July 2000.

SECTION 5

CONCLUSIONS

The principal findings regarding methanol fuel substitution for Philadelphia in the year 2000 were derived from the results of three models: the UAM, the Systems Applications trajectory model, and a box model. Model results indicate that when methanol fuel is used for mobile sources,

(1) There are minor increases in formaldehyde levels in the vicinity of major traffic emissions;

(2) There is virtually no change in maximum ozone levels;

(3) Methanol displacement of carryover pollutants or initial boundary condition pollutants can combine with local methanol emissions to produce synergistic reductions in ozone maxima;

(4) Formaldehyde emissions can be very important as the reactivity (via methanol substitution) or the total amount of overall VOC levels is reduced; and

(5) The Philadelphia area is strongly sensitive to NO_x emissions.

Regarding the last finding, this sensitivity is exhibited both in the reactivity of NO_x emissions and in the total amount of NO_x emissions. The reactivity of NO_x increases as the ratio of NO_2 to NO_x increases. For this study, the total NO_x level is such that if it is decreased, the amount of ozone will increase. Thus, minor control of NO_x (a small decrease), or a change in the NO_x emissions that increases the NO_2-to-NO_x ratio, will result in increased ozone levels.

The results of the present study can be compared with results of a previous study by Whitten and Hogo (1983), which simulated methanol substitution in the Los Angeles area. Minor increases in formaldehyde levels were seen in both studies and both showed enhanced ozone reduction when methanol replaced VOC in carryover and boundary pollutant concentrations. However, the previous study shows substantial ozone reductions when methanol is substituted as a transportation fuel. The present study

shows no ozone benefit from such a substitution unless carryover pollutants are also assumed to be displaced by methanol. The difference in the results of this study and those of the previous study in the Los Angeles area can be explained by the small percentage of mobile source VOC (20 percent) predicted for the year 2000 in Philadelphia. Sensitivity studies performed with the box model suggest that an overall 50 percent substitution of methanol for VOC may produce large reductions in ozone if (1) formaldehyde emissions are minimized, (2) NO_x is left at predicted 2000 levels, and (3) methanol is present to displace VOC in carryover pollutants. However, the use of a regional multiday model would be required to study the intercity and carryover effects of such widespread methanol use.

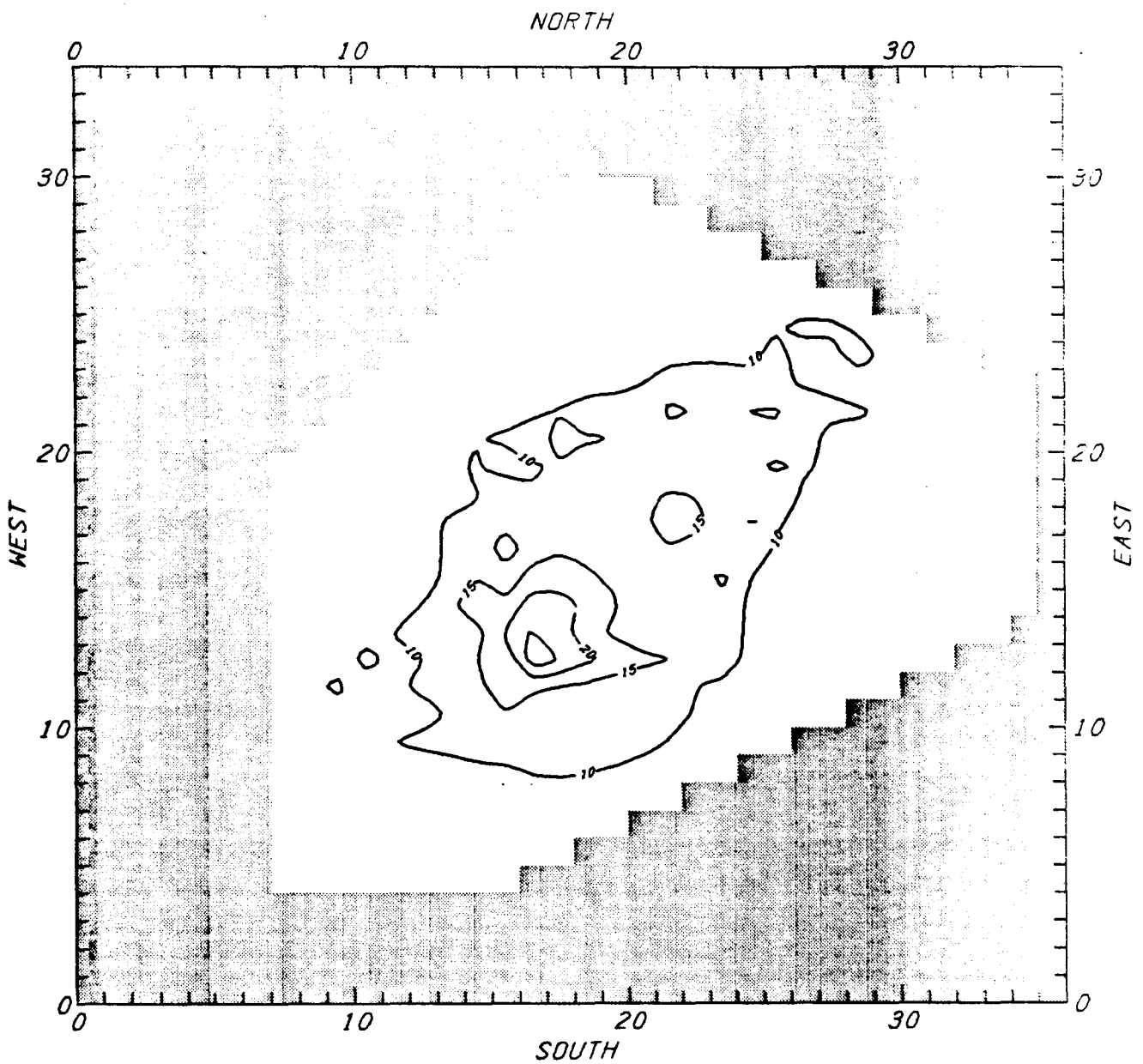

FORMALDEHYDE CONC (JULY 13) IN PPB - YEAR 2000 BASE CASE (LOWER IC)

(a) BETWEEN THE HOURS OF 0 AND 1

FIGURE 12

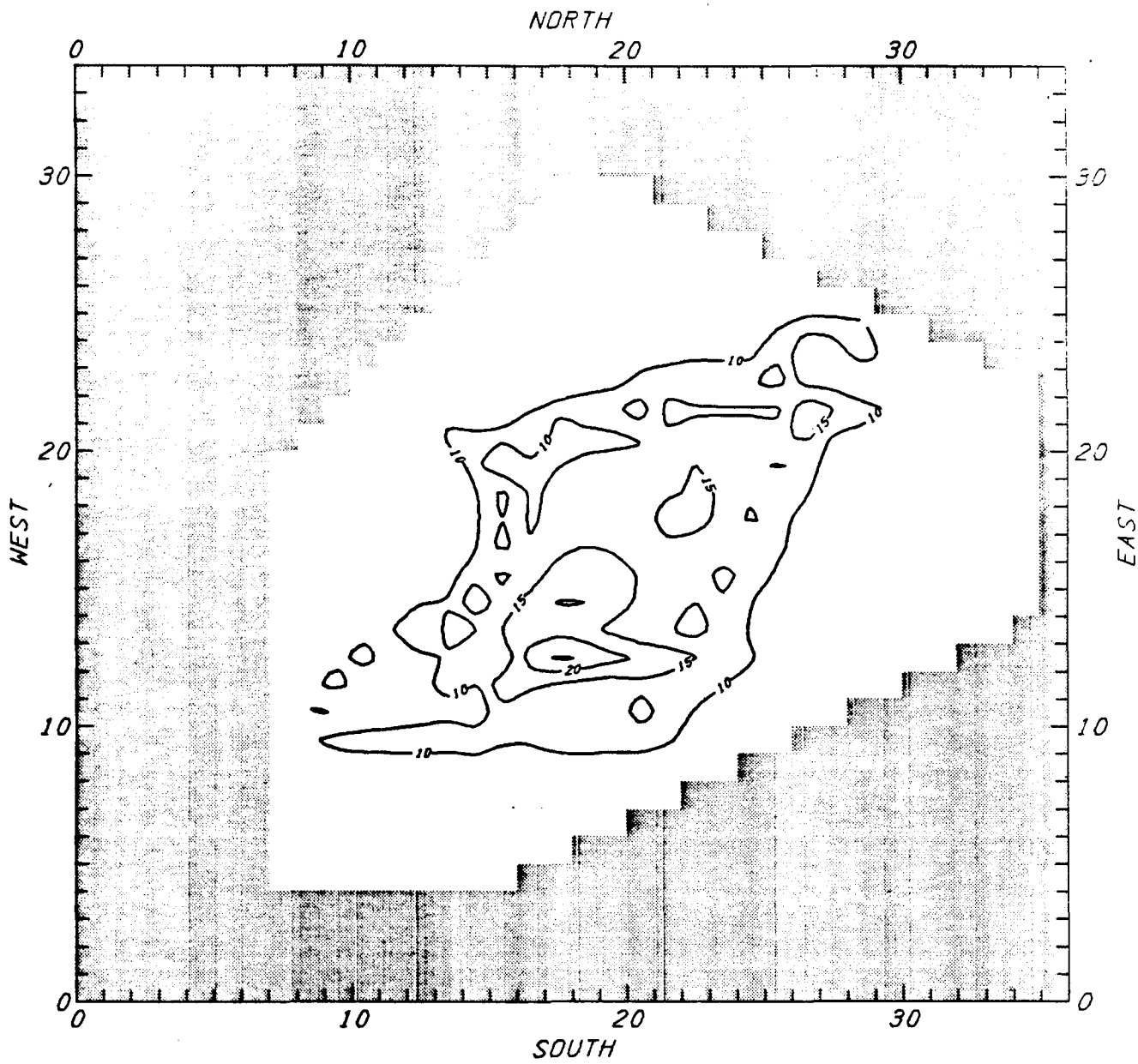

FORMALDEHYDE CONC (JULY 13) IN PPB - YEAR 2000 BASE CASE (LOWER IC)
(b) BETWEEN THE HOURS OF 1 AND 2

FIGURE 12 (continued)

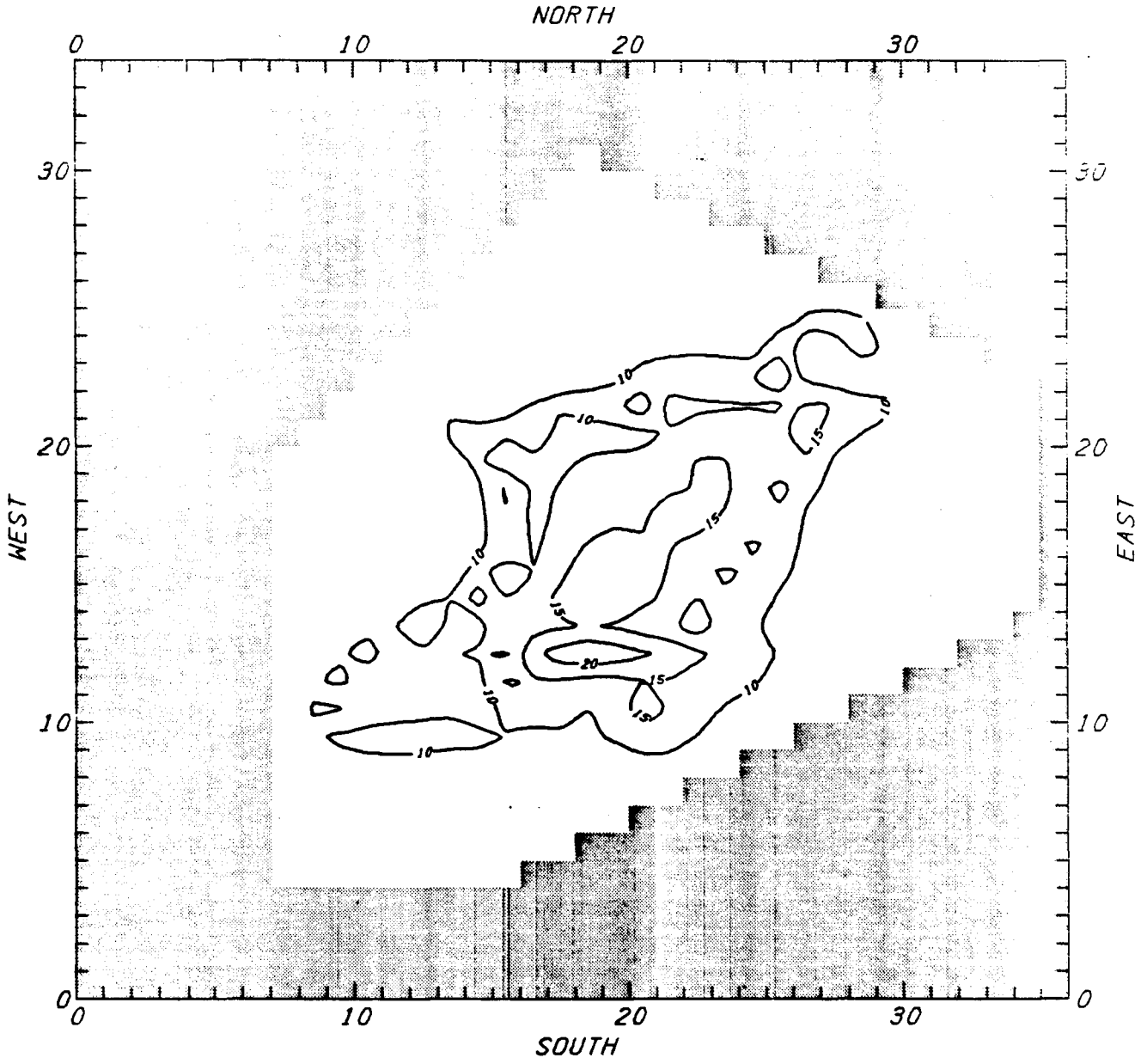

FORMALDEHYDE CONC (JULY 13) IN PPB - YEAR 2000 BASE CASE (LOWER IC)

(c) BETWEEN THE HOURS OF 2 AND 3

FIGURE 12 (continued)

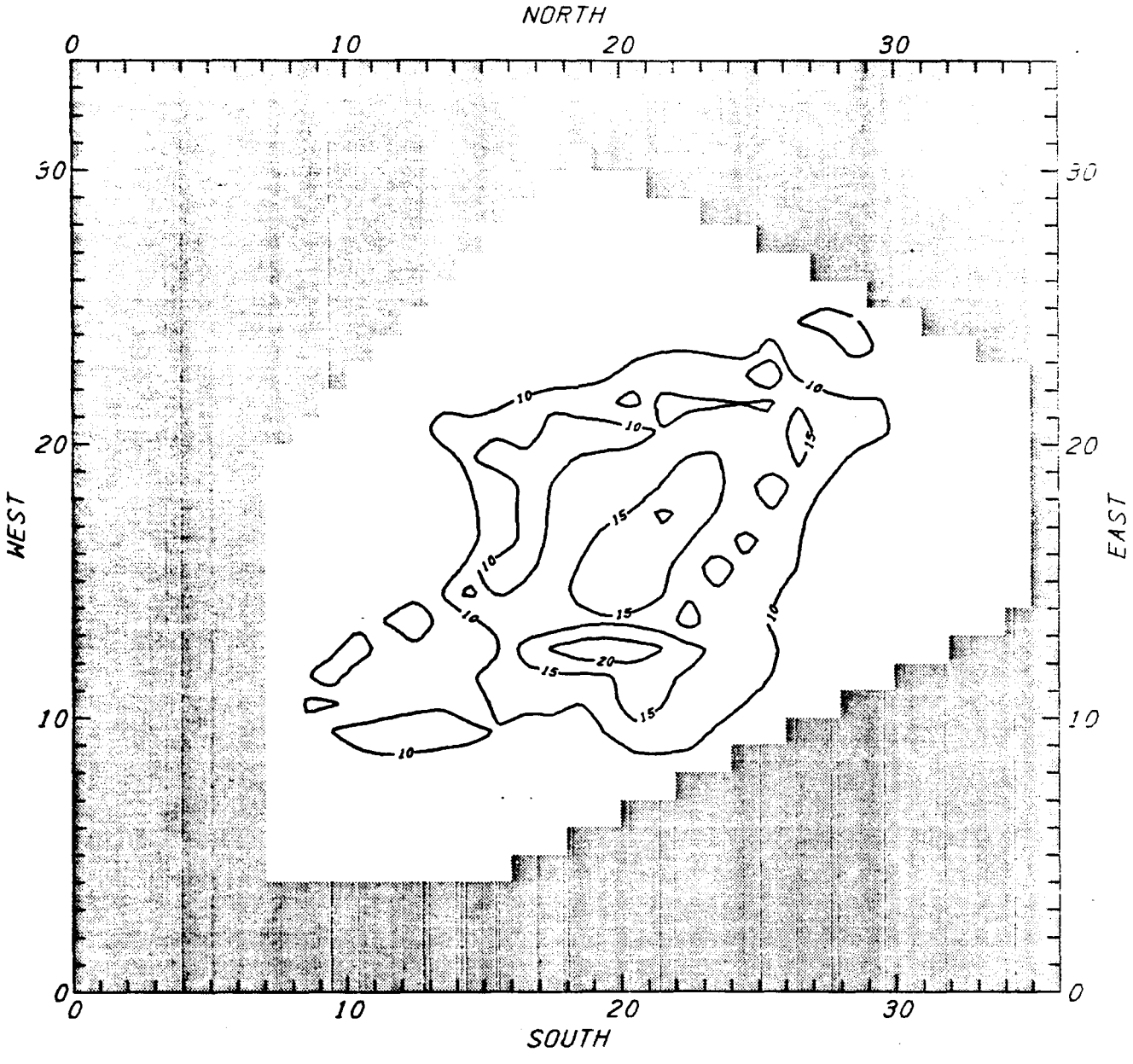

FORMALDEHYDE CONC (JULY 13) IN PPB - YEAR 2000 BASE CASE (LOWER IC)
(d) BETWEEN THE HOURS OF 3 AND 4

FIGURE 12 (continued)

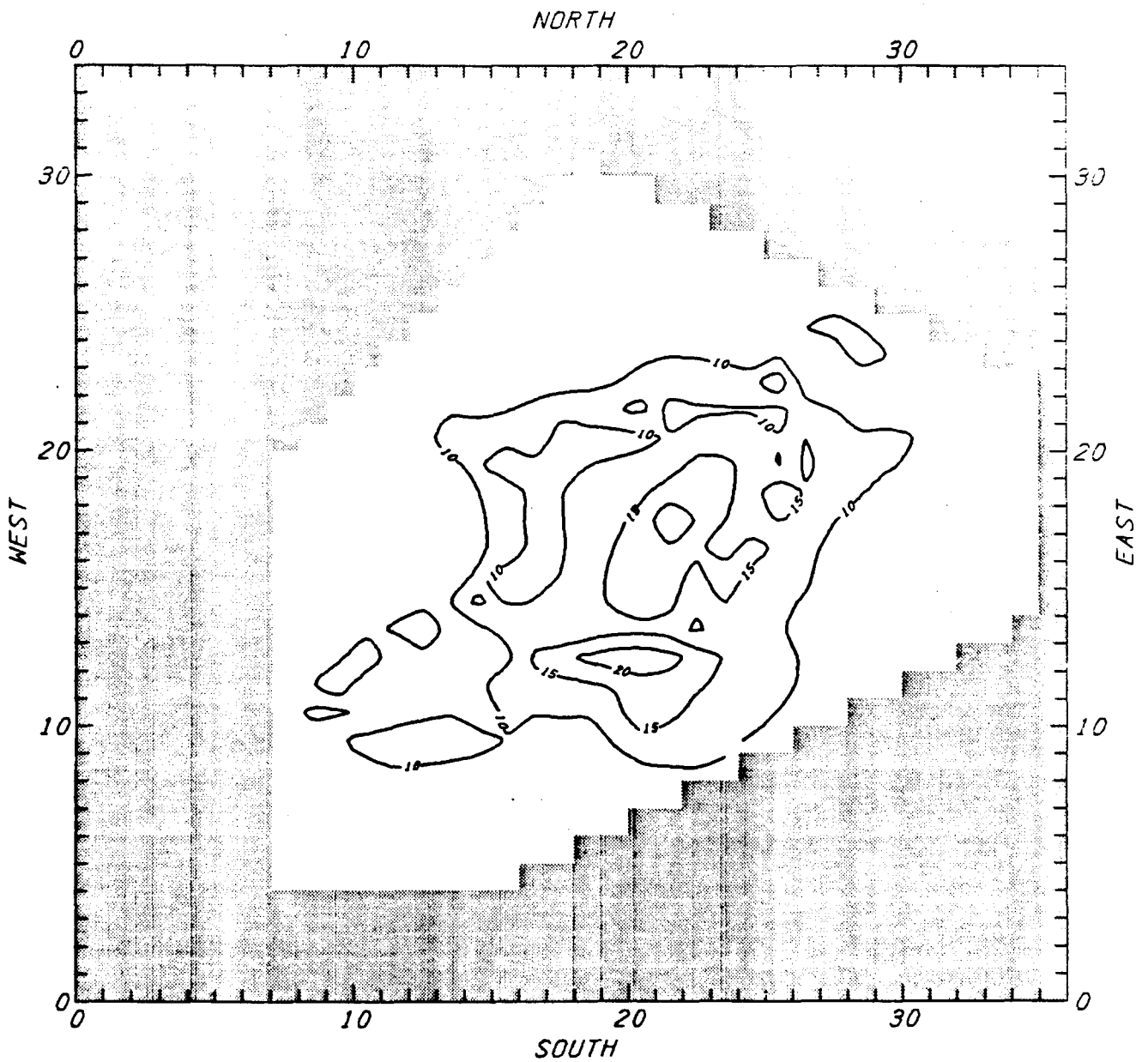

FORMALDEHYDE CONC (JULY 13) IN PPB - YEAR 2000 BASE CASE (LOWER I-C)

(e) BETWEEN THE HOURS OF 4 AND 5

FIGURE 12 (continued)

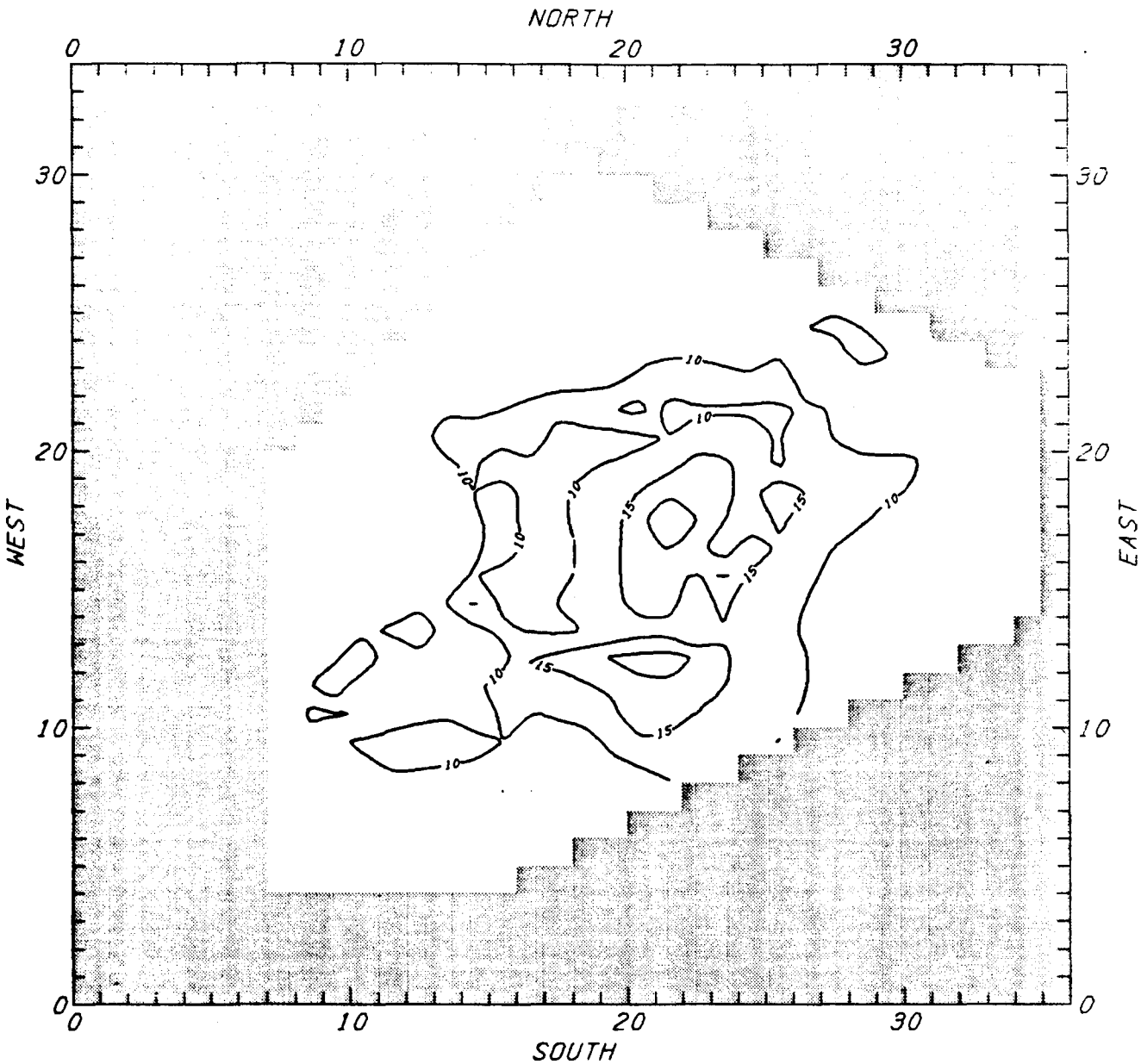

FORMALDEHYDE CONC (JULY 13) IN PPB - YEAR 2000 BASE CASE (LOWER IC)

(f) BETWEEN THE HOURS OF 5 AND 6

FIGURE 12 (continued)

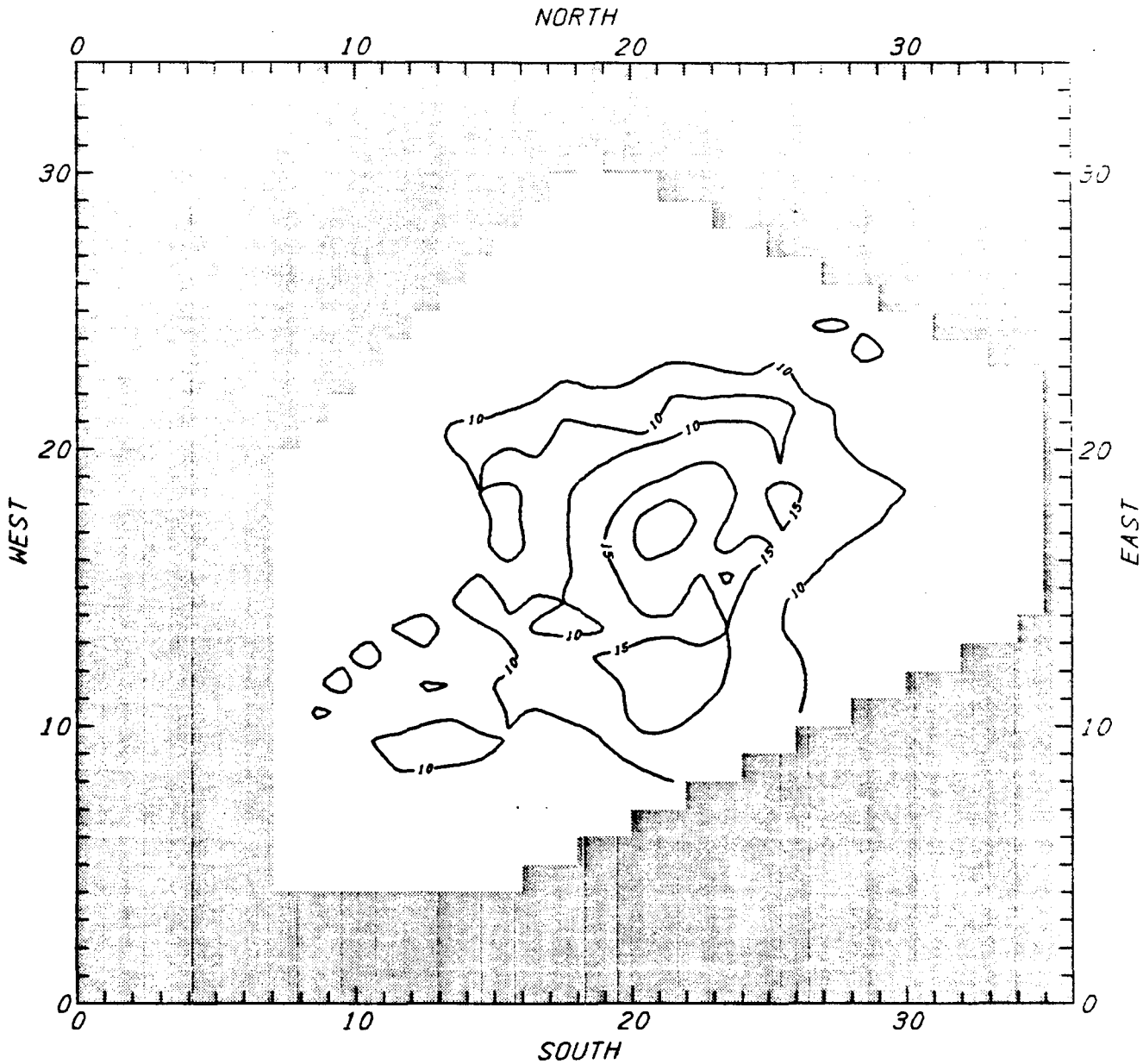

FORMALDEHYDE CONC (JULY 13) IN PPB - YEAR 2000 BASE CASE (LOWER IC)

(q) BETWEEN THE HOURS OF 6 AND 7

FIGURE 12 (continued)

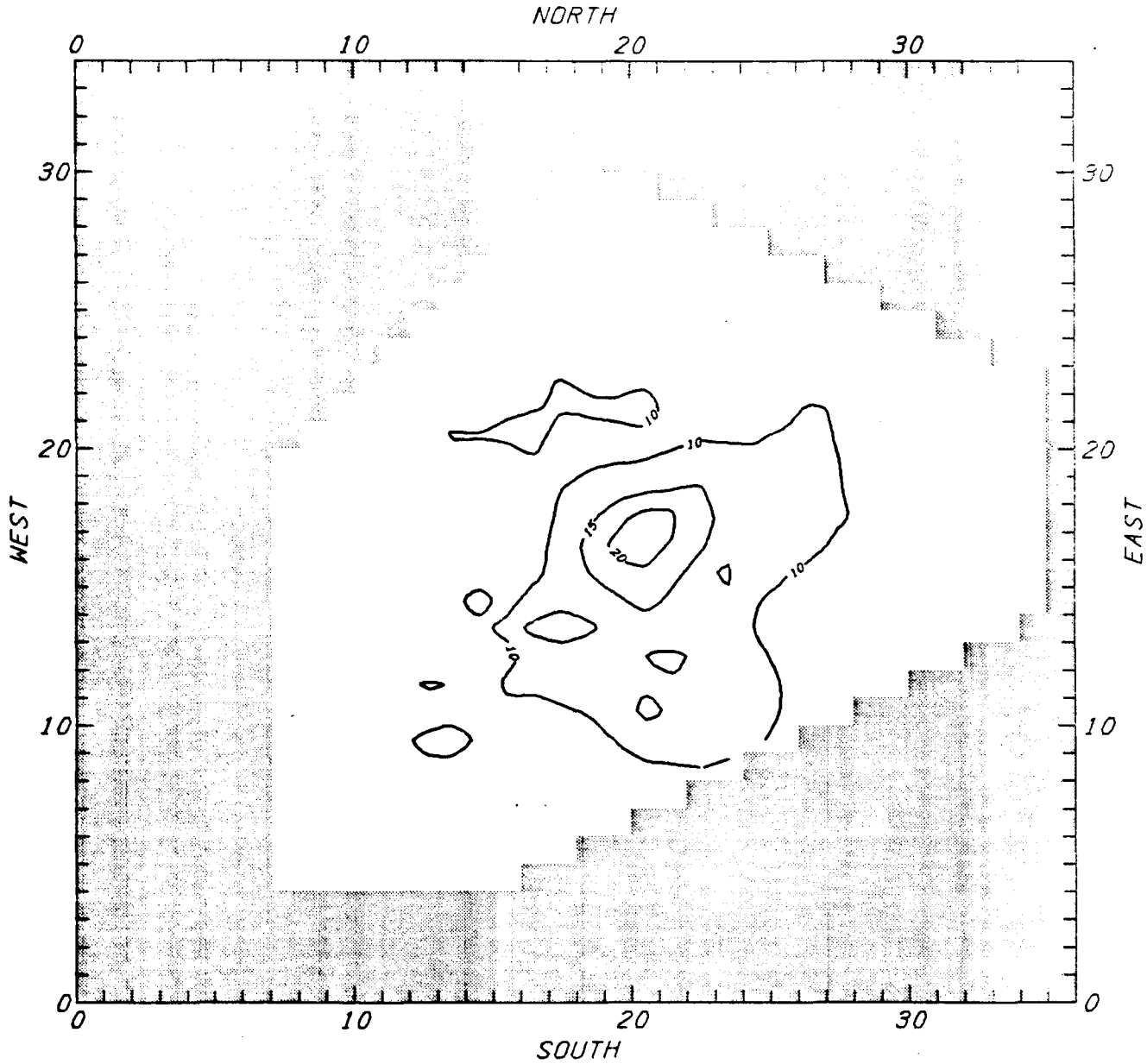

FORMALDEHYDE CONC (JULY 13) IN PPB - YEAR 2000 BASE CASE (LOWER IC)

(h) BETWEEN THE HOURS OF 7 AND 8

FIGURE 12 (continued)

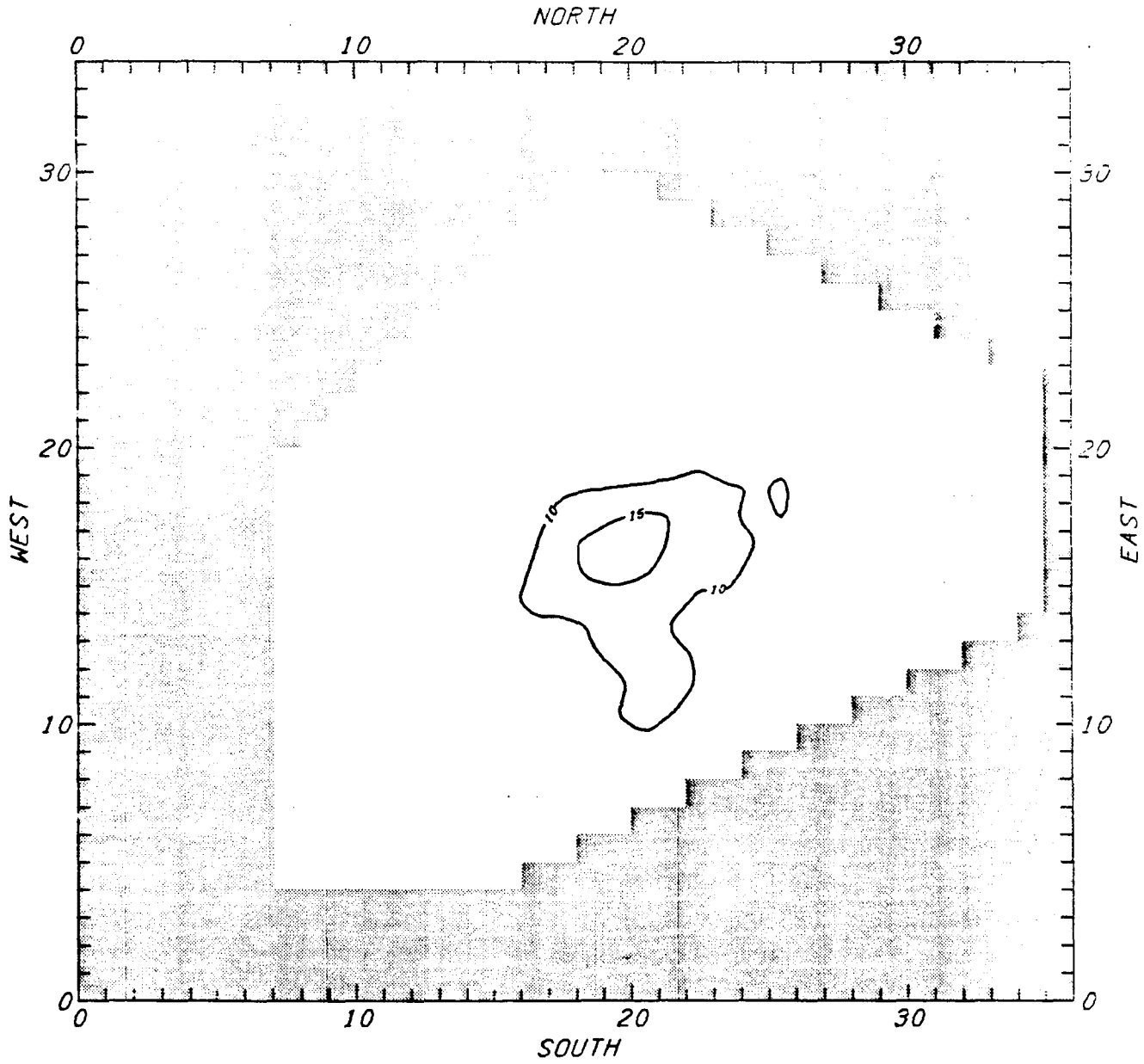

FORMALDEHYDE CONC (JULY 13) IN PPB - YEAR 2000 BASE CASE (LOWER IC)

(i) BETWEEN THE HOURS OF 8 AND 9

FIGURE 12 (continued)

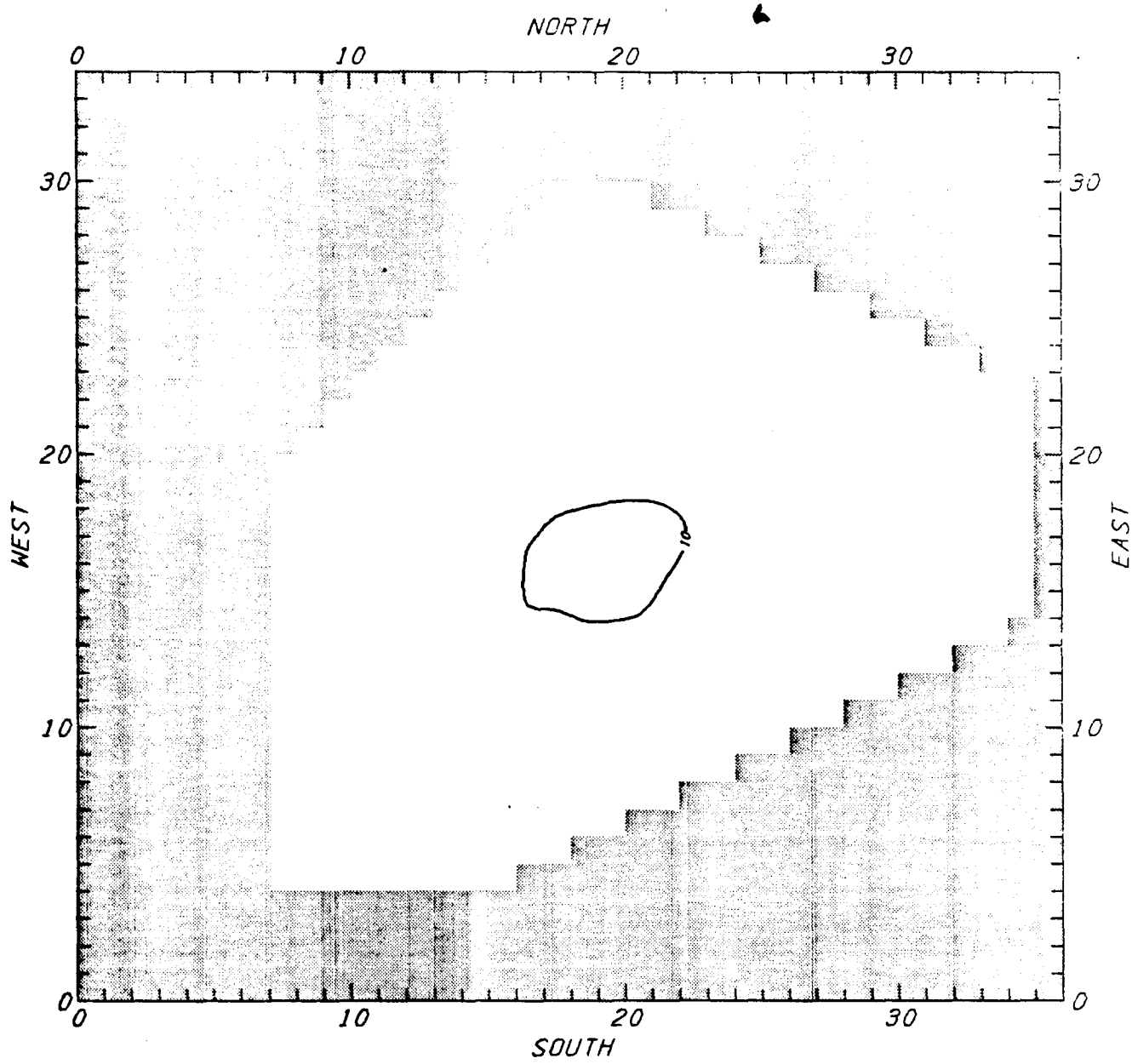

FORMALDEHYDE CONC (JULY 13) IN PPB - YEAR 2000 BASE CASE (LOWER IC)

(j) BETWEEN THE HOURS OF 9 AND 10

FIGURE 12 (continued)

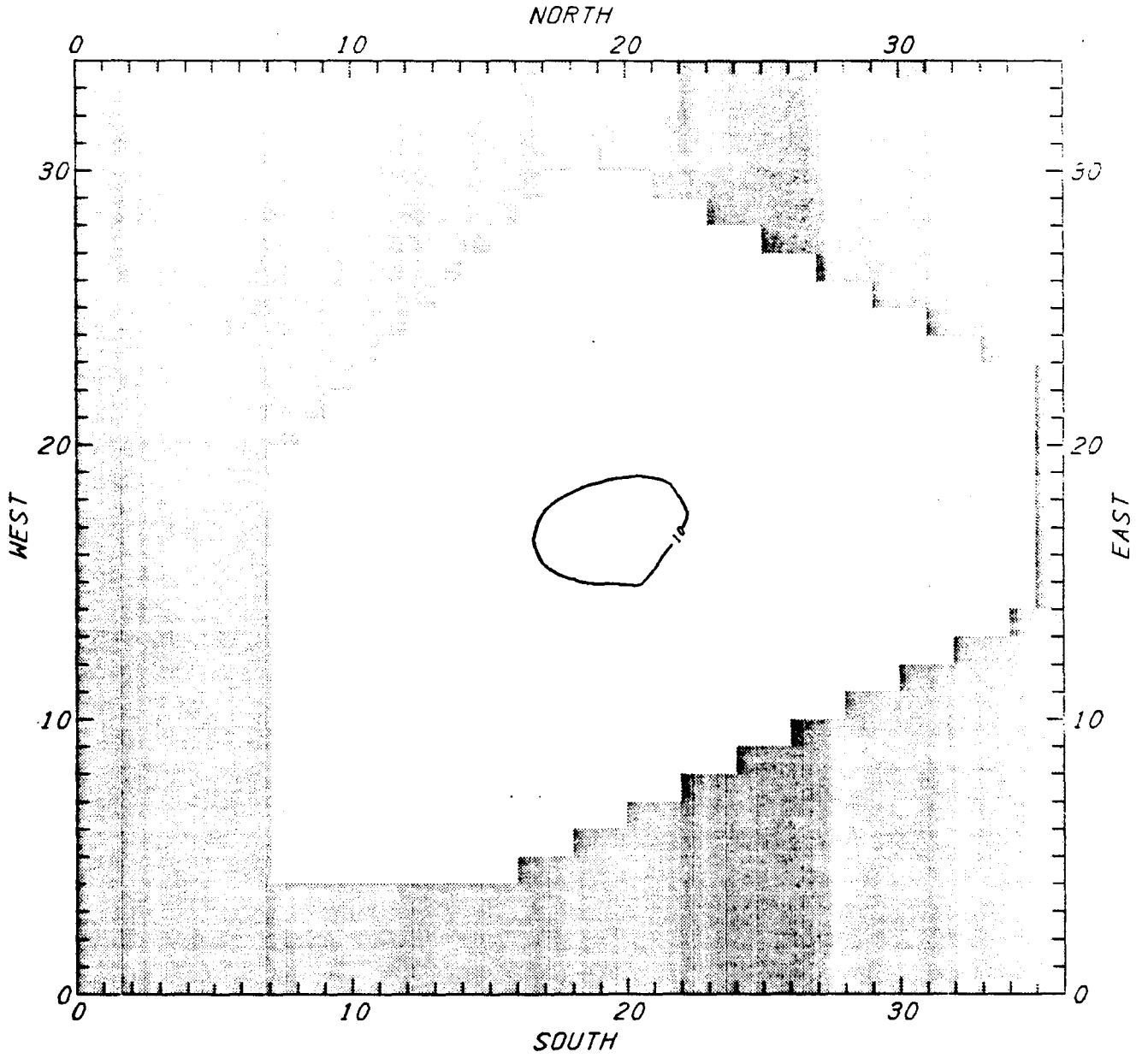

FORMALDEHYDE CONC (JULY 13) IN PPB - YEAR 2000 BASE CASE (LOWER HC)

(k) BETWEEN THE HOURS OF 10 AND 11

FIGURE 12 (continued)

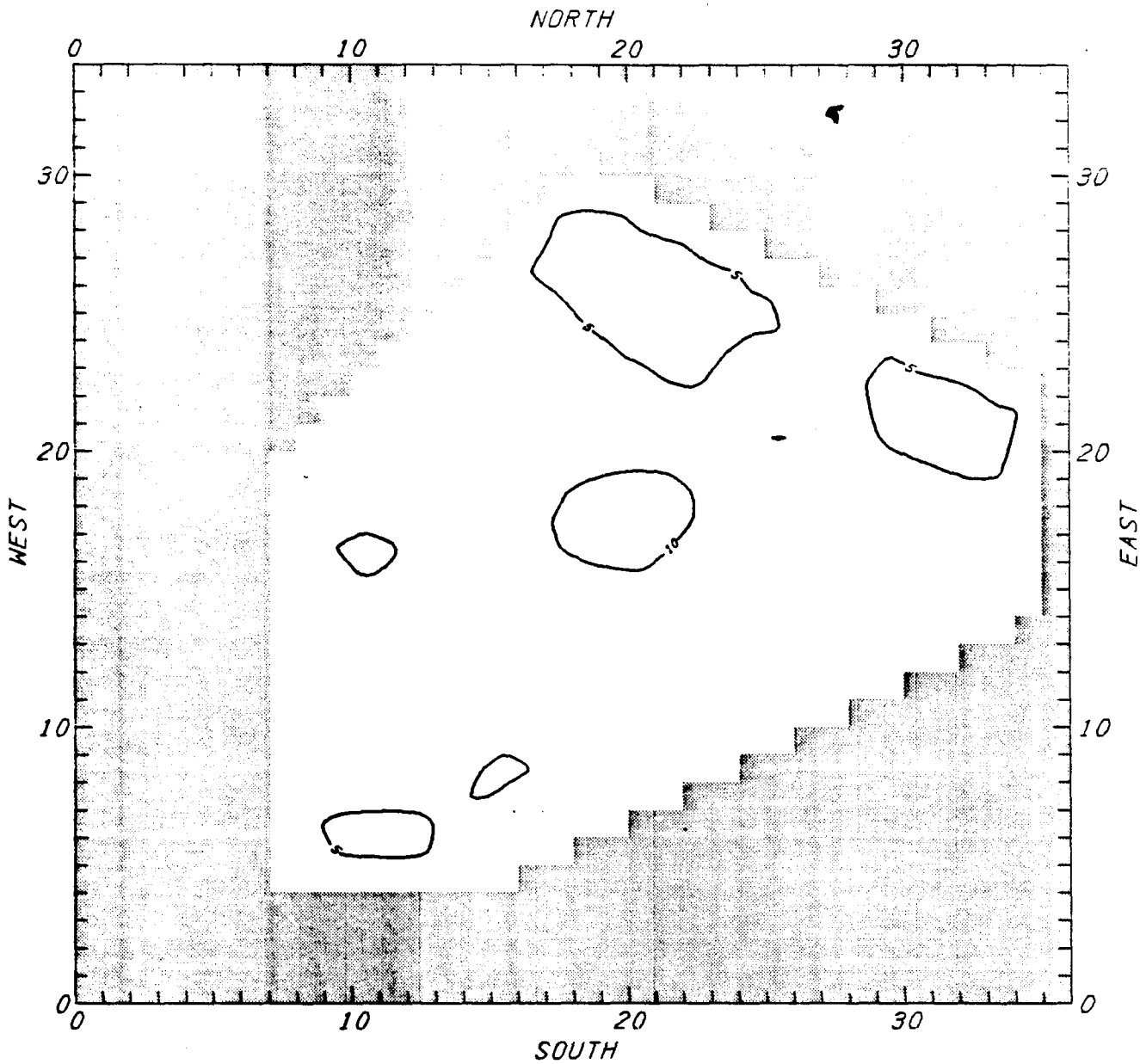

FORMALDEHYDE CONC (JULY 13) IN PPB - YEAR 2000 BASE CASE (LOWER IC)
(1) BETWEEN THE HOURS OF 11 AND 12

FIGURE 12 (concluded)

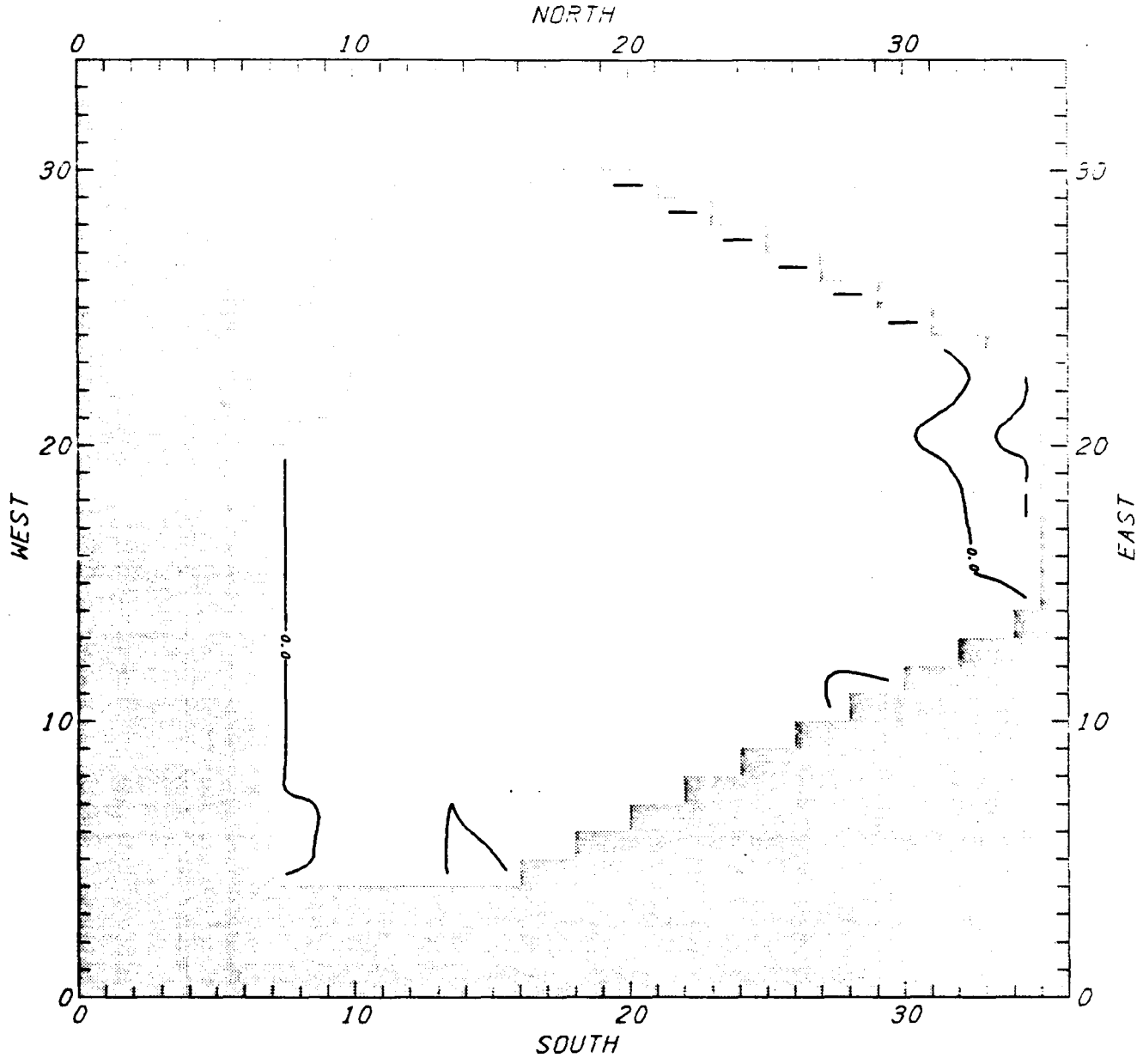

FORMALDEHYDE CHANGE (JULY 13) IN PPB - YR 2000, 2B MINUS BASE

(a) BETWEEN THE HOURS OF 0 AND 1

FIGURE 13

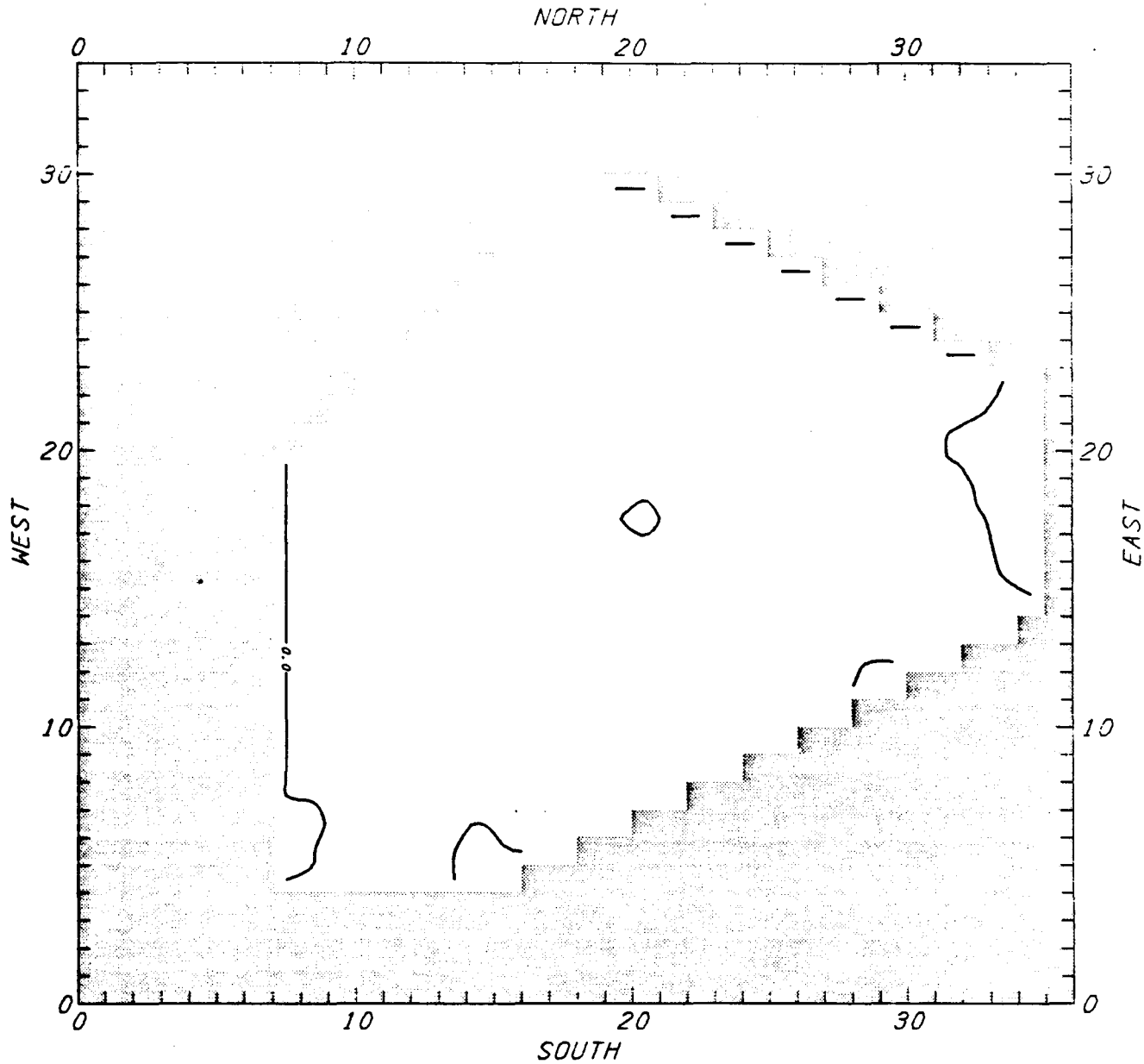

FORMALDEHYDE CHANGE (JULY 13) IN PPB - YR 2000, 2B MINUS BASE

(b) BETWEEN THE HOURS OF 1 AND 2

FIGURE 13 (continued)

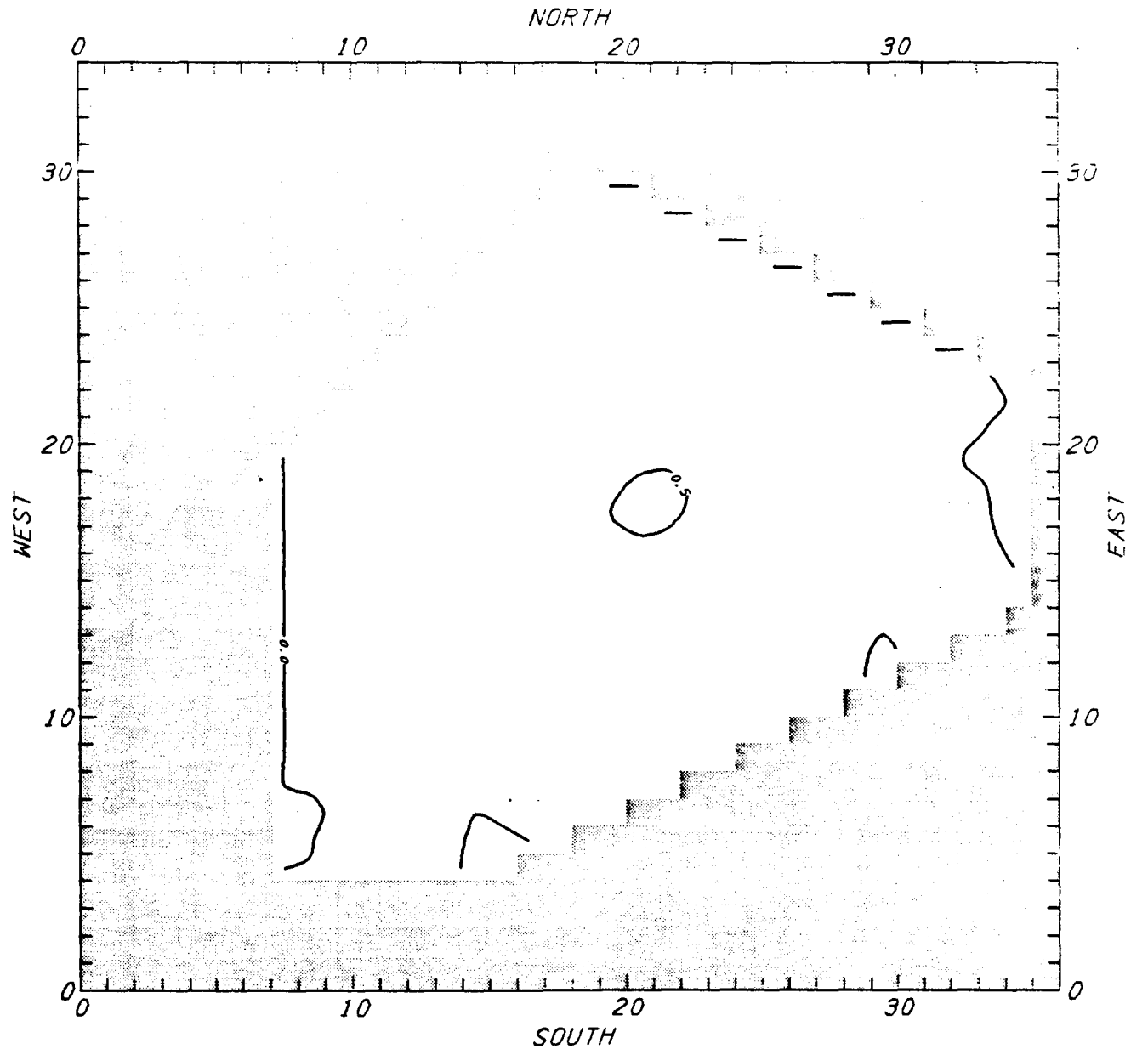

FORMALDEHYDE CHANGE (JULY 13) IN PPB - YR 2000, 2B MINUS BASE

(c) BETWEEN THE HOURS OF 2 AND 3

FIGURE 13 (continued)

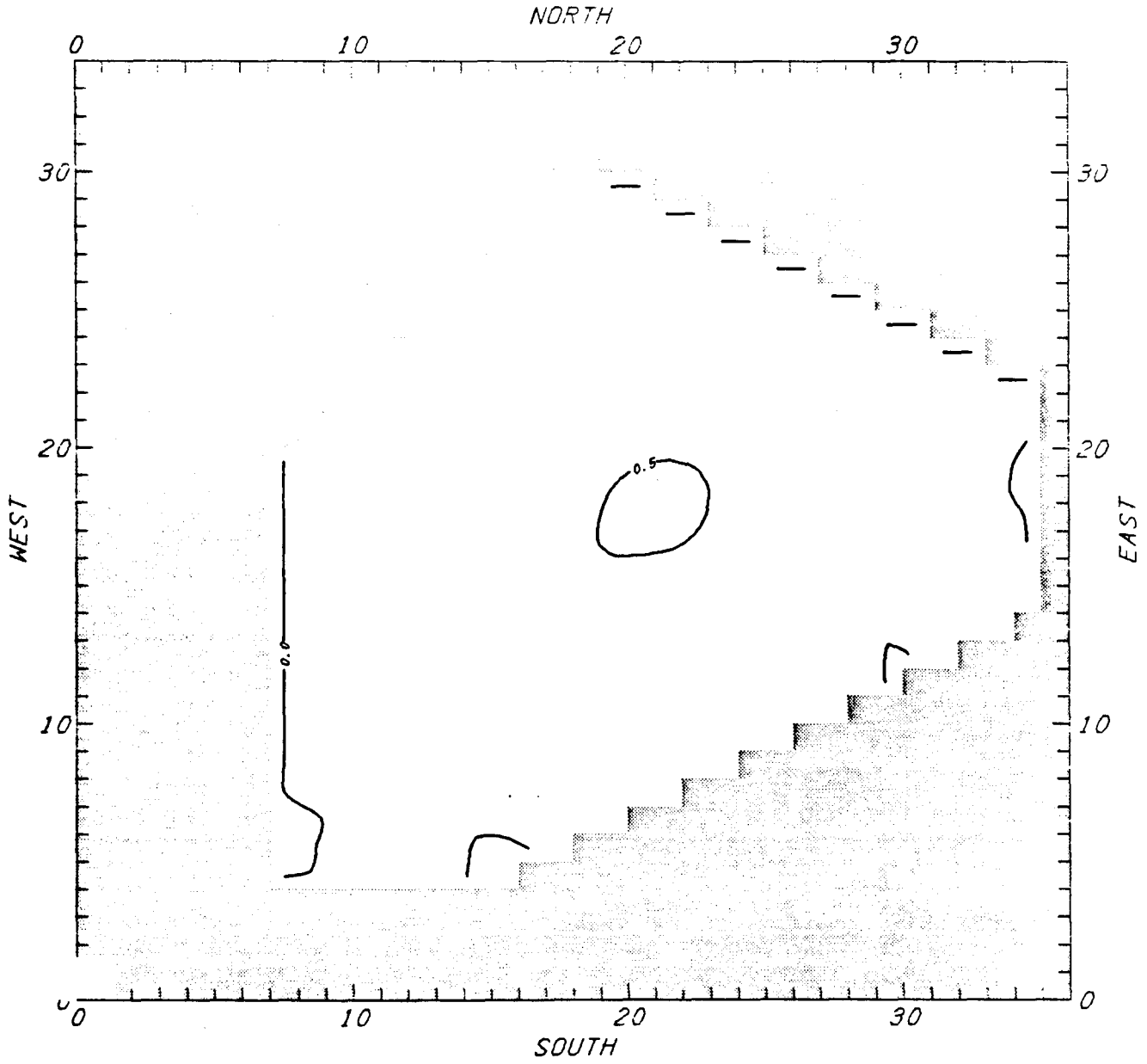

FORMALDEHYDE CHANGE (JULY 13) IN PPB - YR 2000, 2B MINUS BASE

(d) BETWEEN THE HOURS OF 3 AND 4

FIGURE 13 (continued)

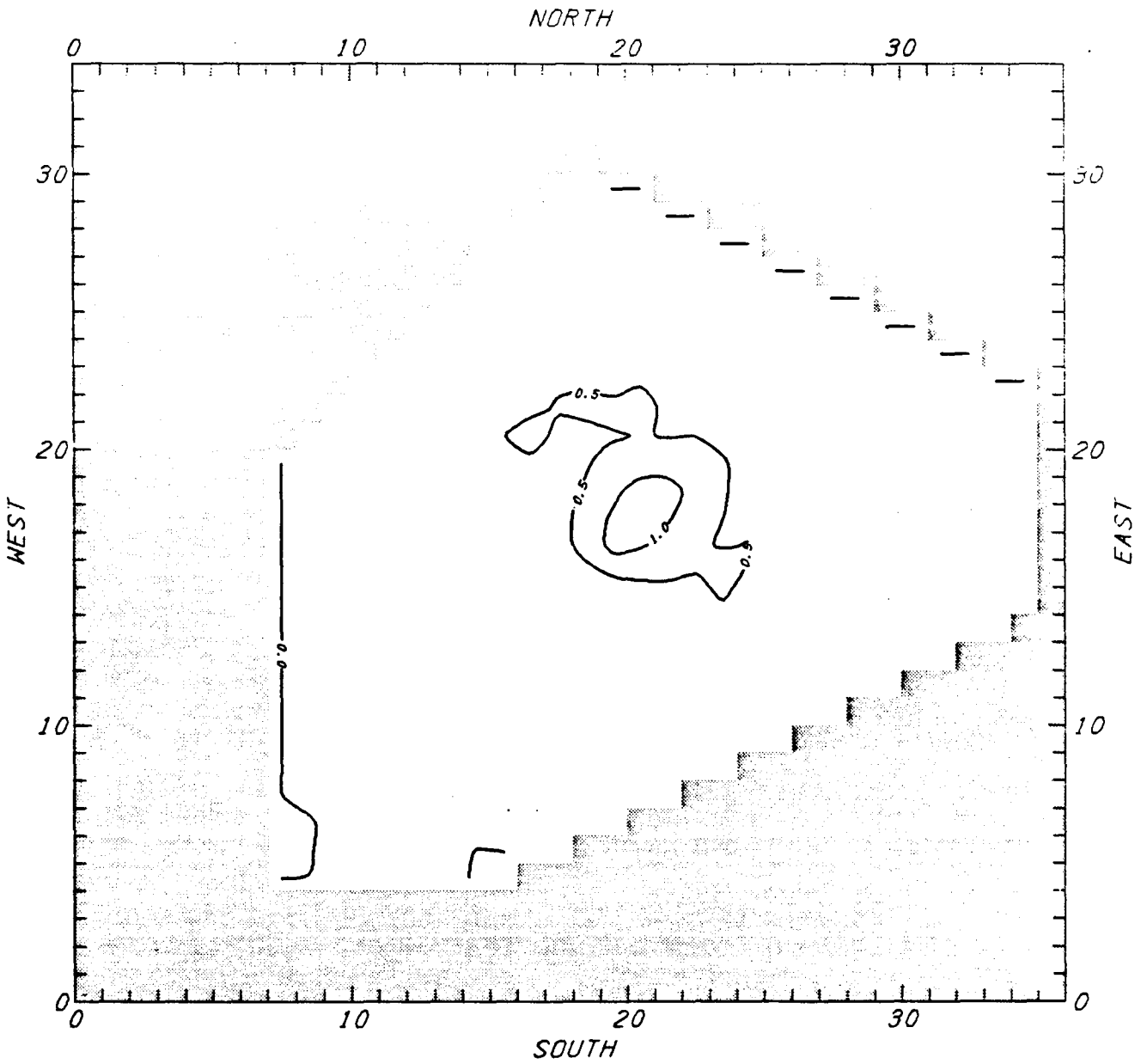

FORMALDEHYDE CHANGE (JULY 13) IN PPB - YR 2000, 2B MINUS BASE.
(e) BETWEEN THE HOURS OF 4 AND 5

FIGURE 13 (continued)

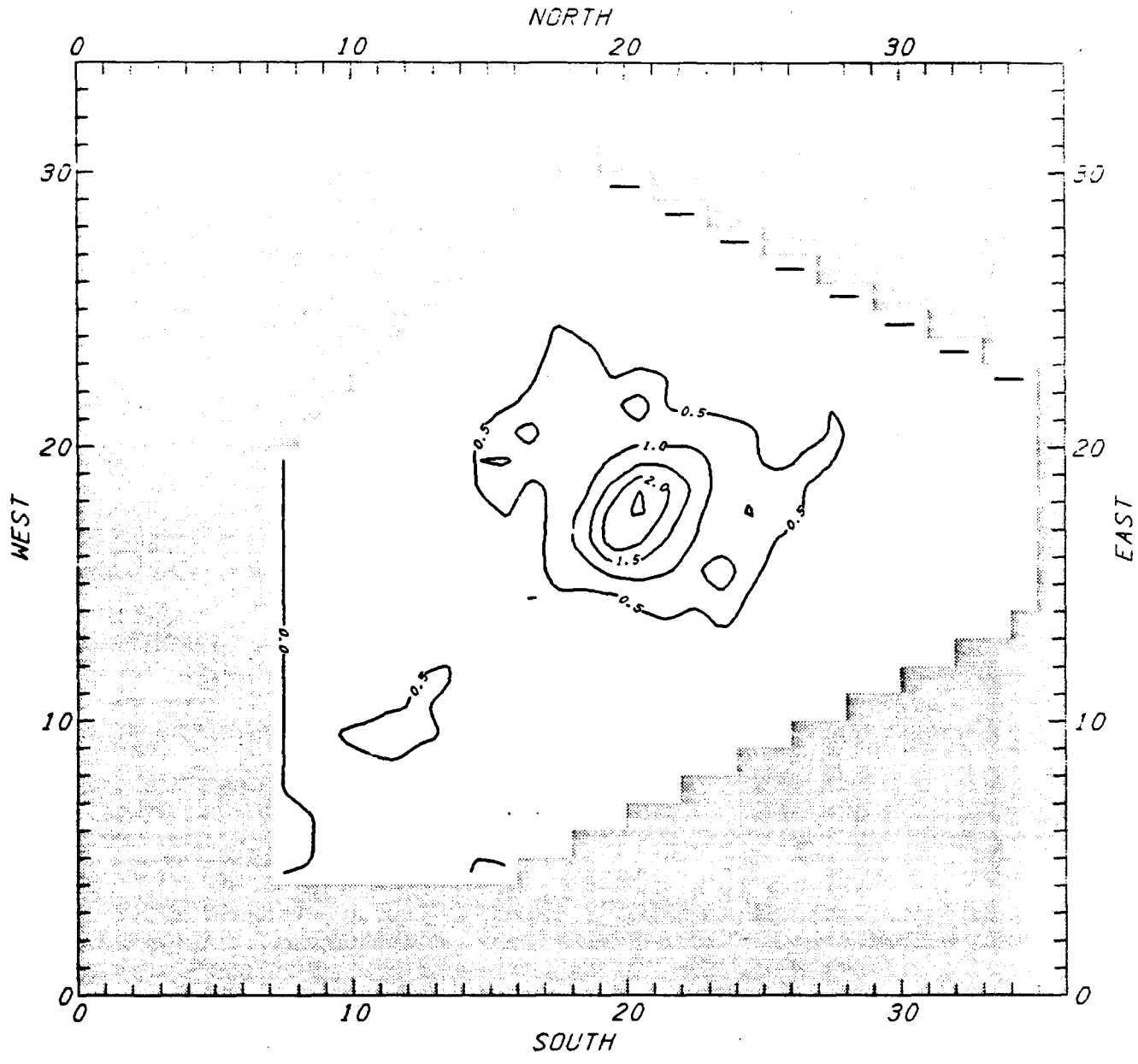

FORMALDEHYDE CHANGE (JULY 13) IN PPB - YR 2000, 2B MINUS BASE

(f) BETWEEN THE HOURS OF 5 AND 6

FIGURE 13 (continued)

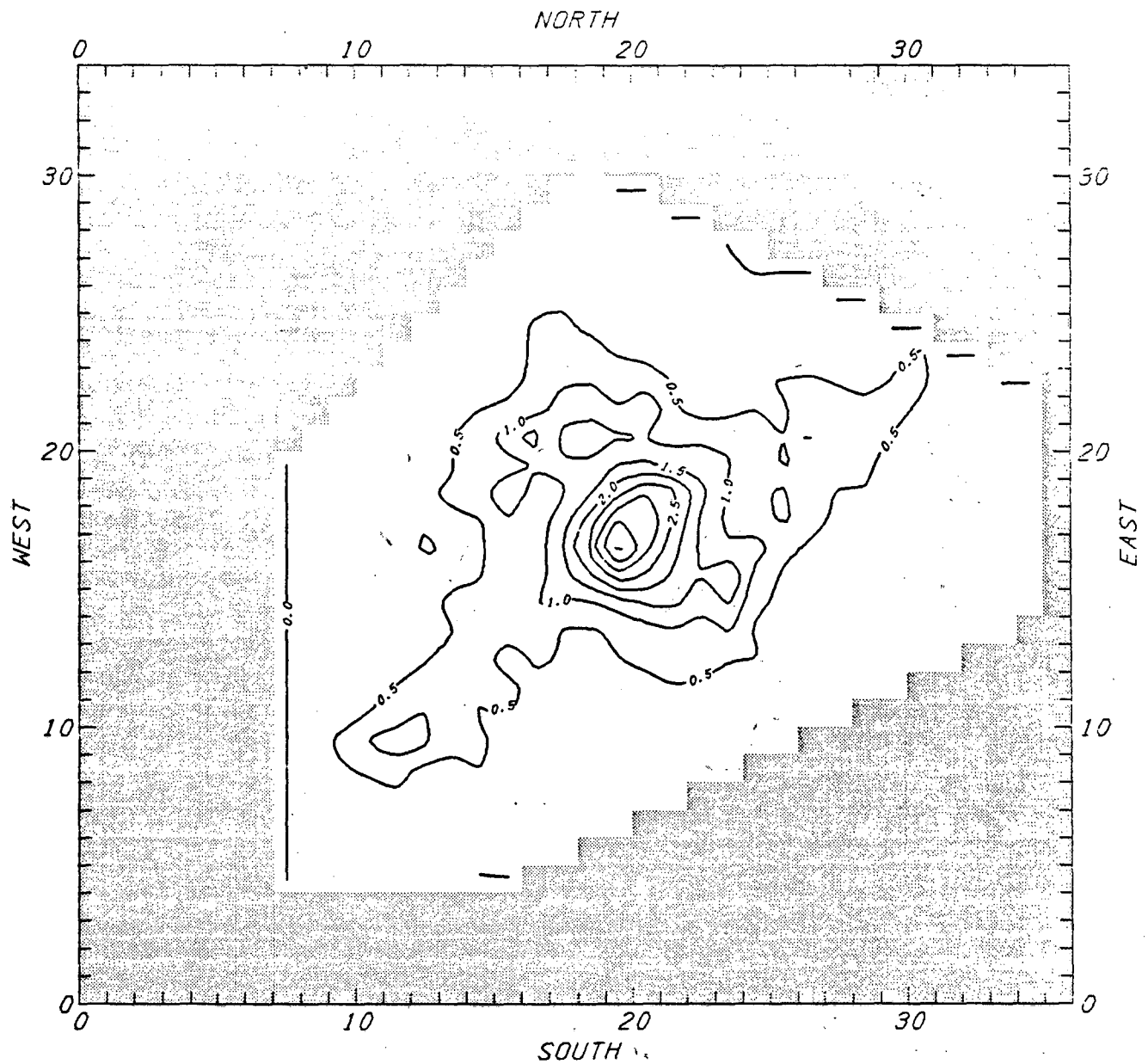

FORMALDEHYDE CHANGE (JULY 13) IN PPB - YR 2000, 2B MINUS BASE

(g) BETWEEN THE HOURS OF 6 AND 7

FIGURE 13 (continued)

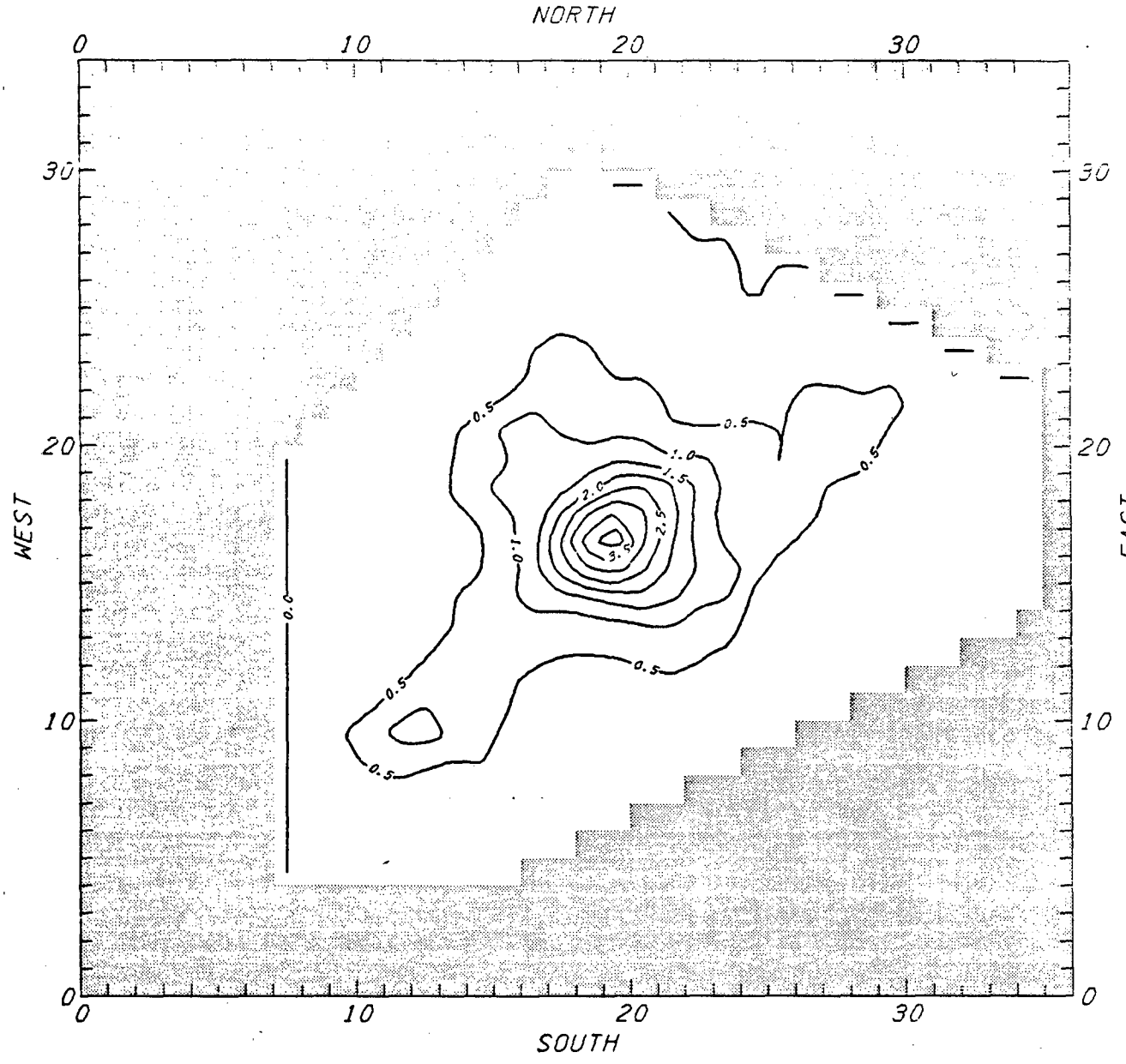

FORMALDEHYDE CHANGE (JULY 13) IN PPB - YR 2000, 2B MINUS BASE

(h) BETWEEN THE HOURS OF 7 AND 8

FIGURE 13 (continued)

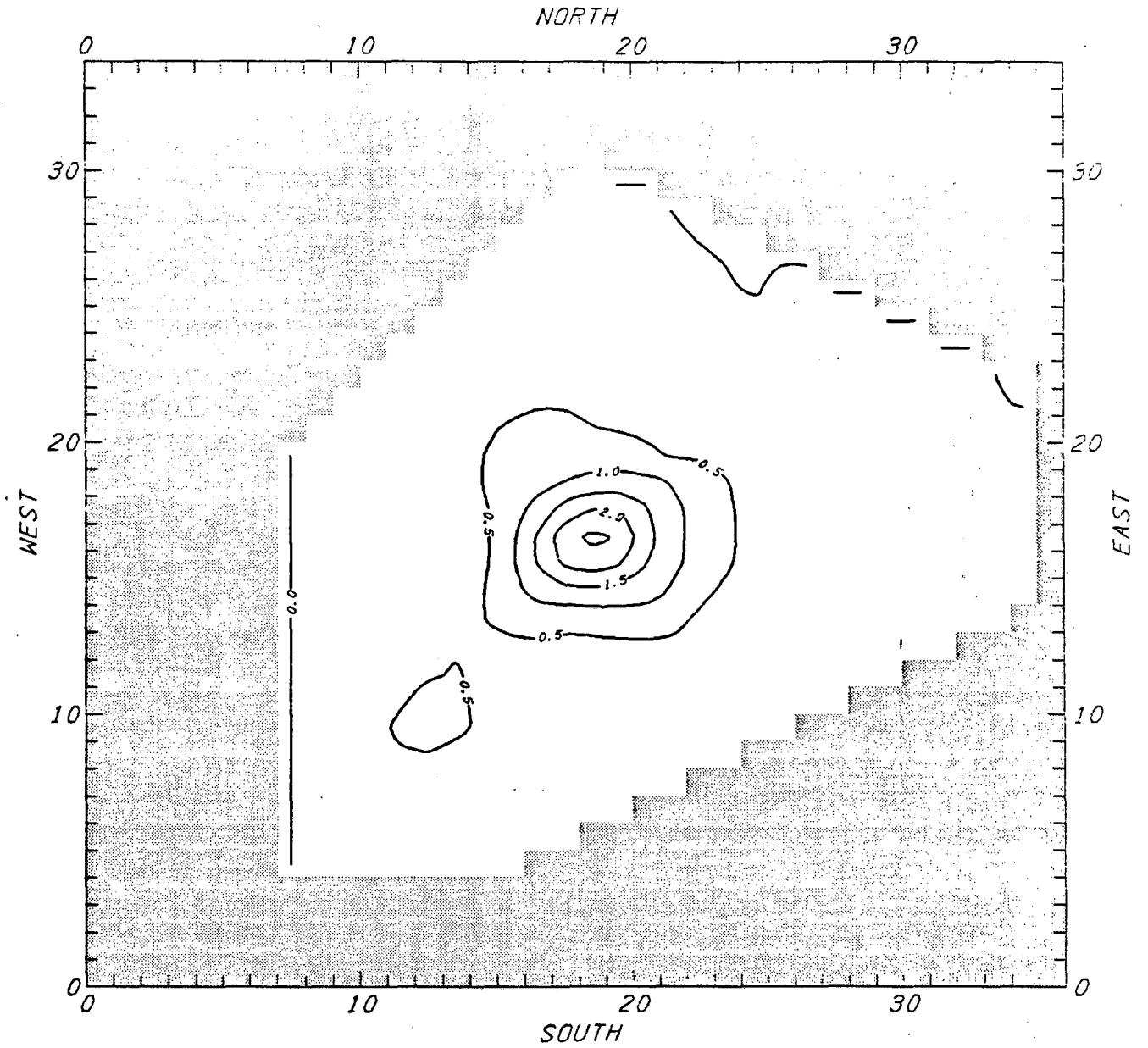

FORMALDEHYDE CHANGE (JULY 13) IN PPB - YR 2000, 2B MINUS BASE

(i) BETWEEN THE HOURS OF 8 AND 9

FIGURE 13 (continued)

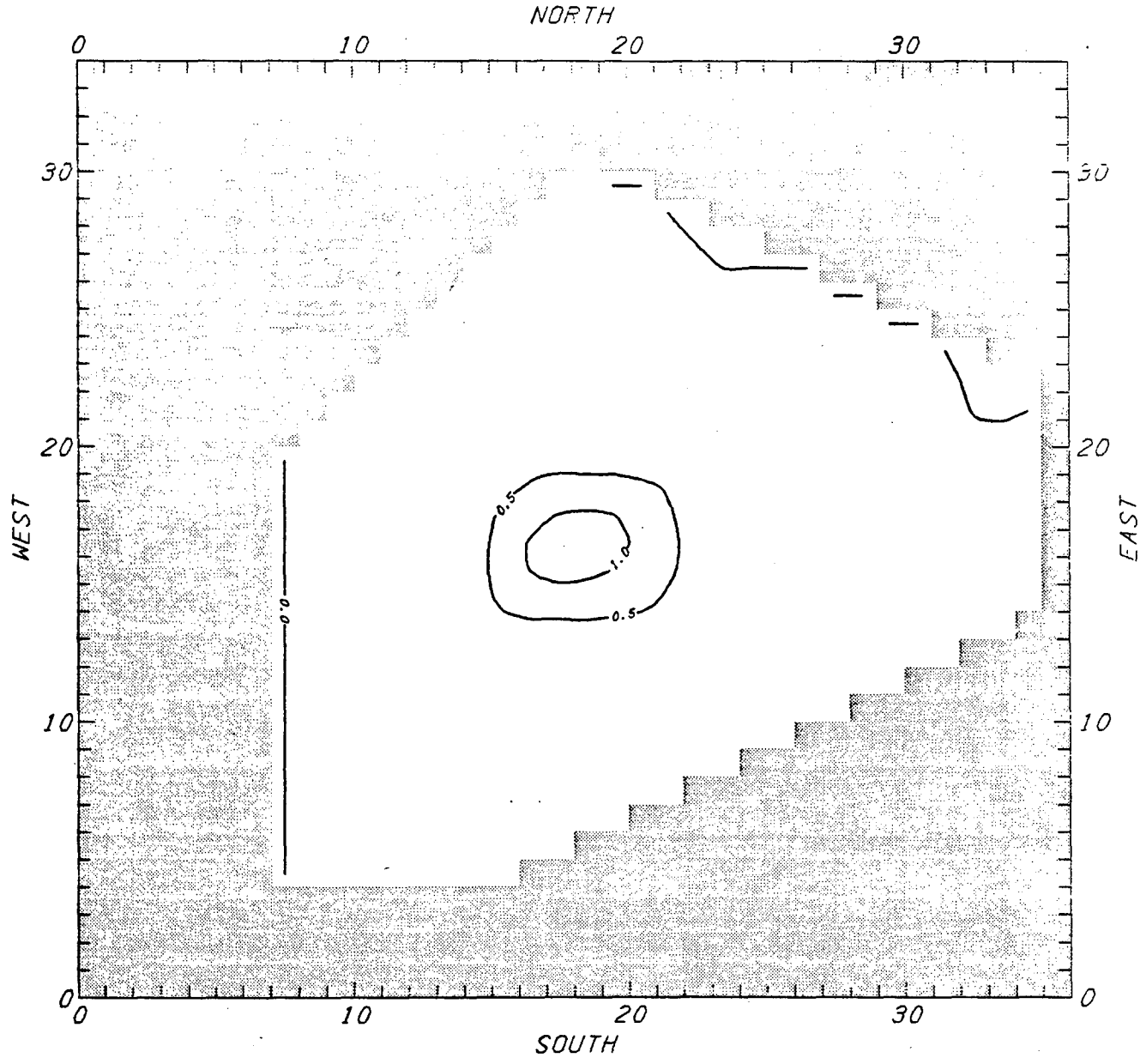

FORMALDEHYDE CHANGE (JULY 13) IN PPB - YR 2000, 2B MINUS BASE

(j) BETWEEN THE HOURS OF 9 AND 10

FIGURE 13 (continued)

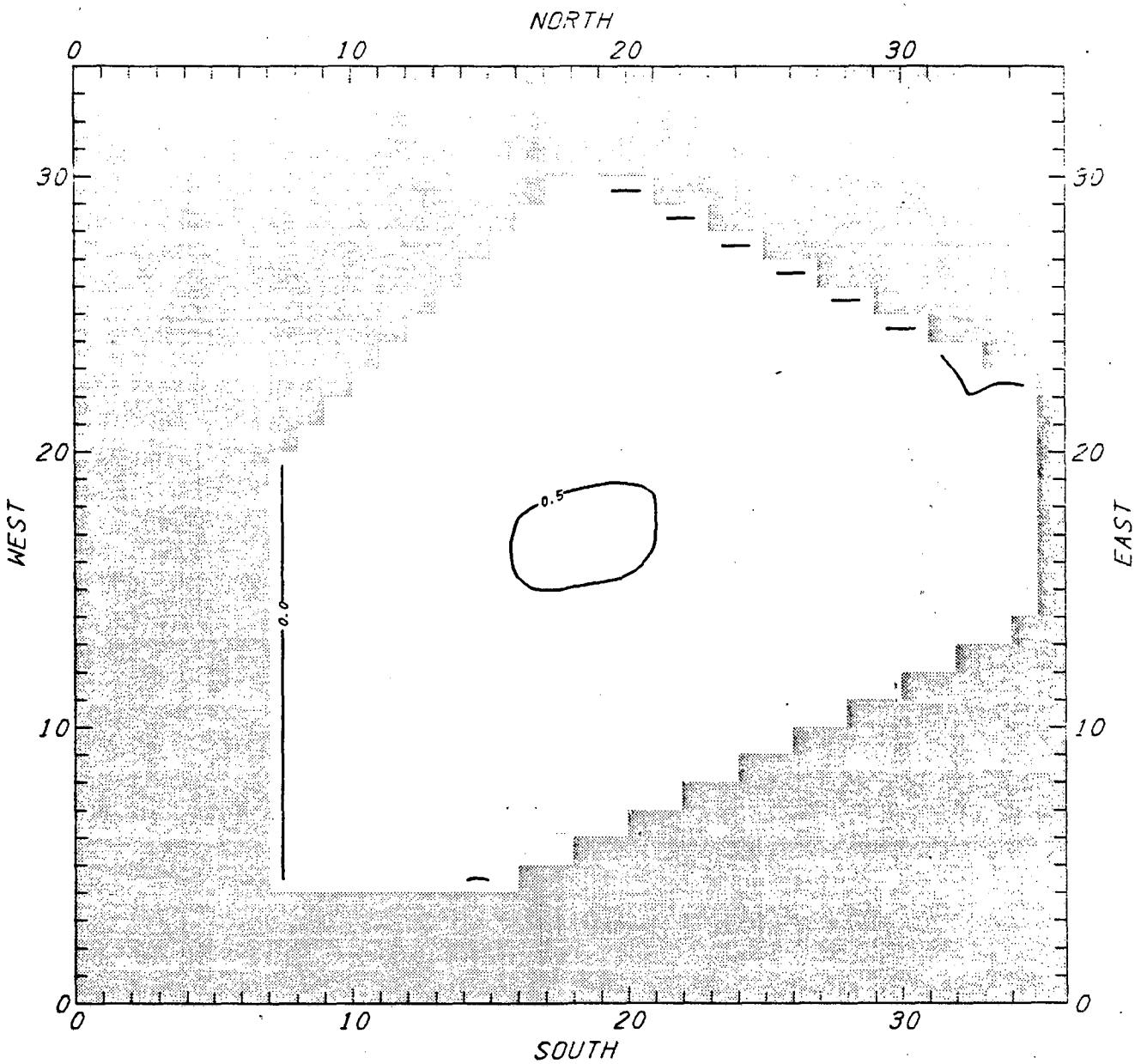

FORMALDEHYDE CHANGE (JULY 13) IN PPB - YR 2000, 2B MINUS BASE.
(k) BETWEEN THE HOURS OF 10 AND 11

FIGURE 13 (continued)

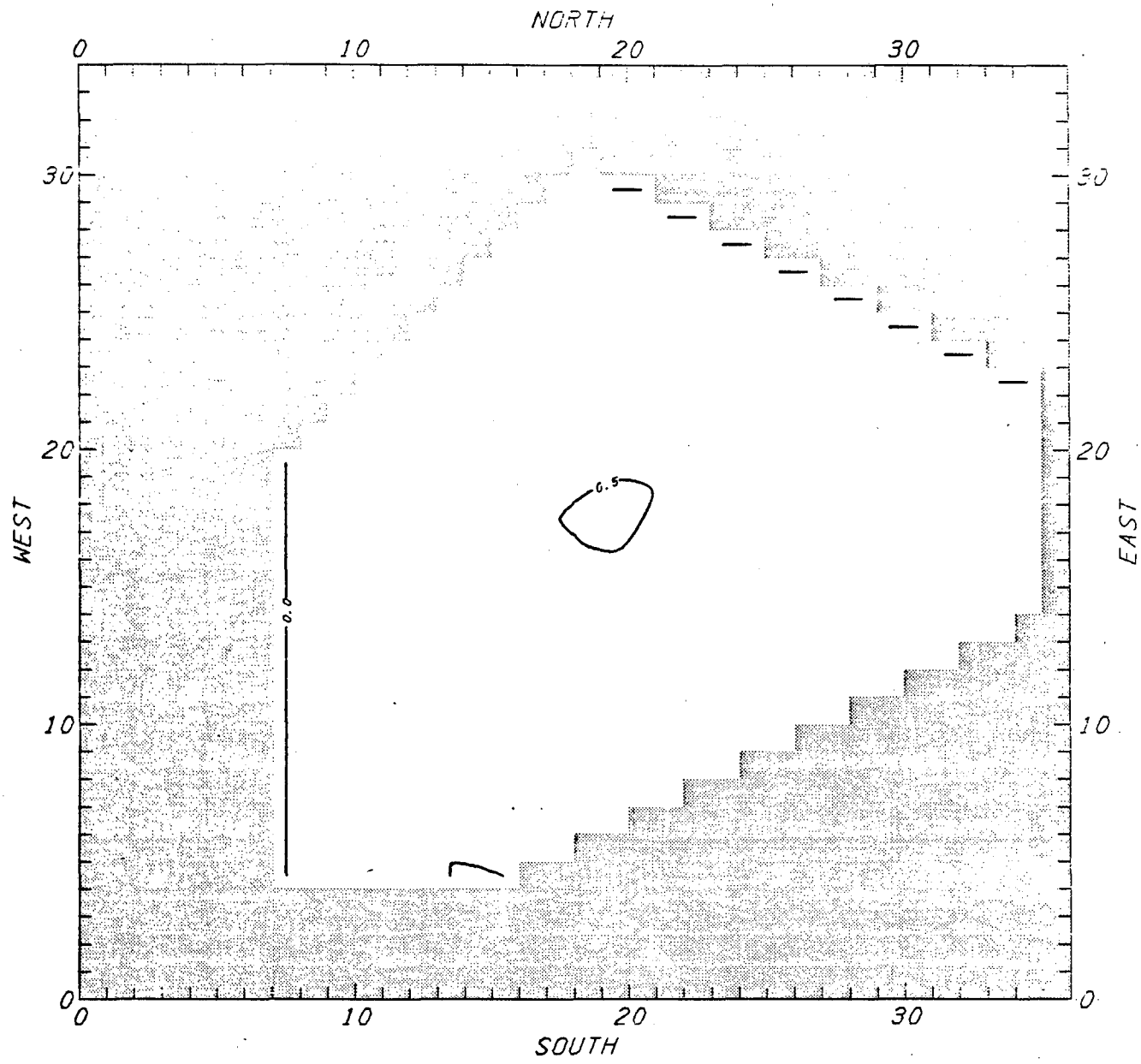

FORMALDEHYDE CHANGE (JULY 13) IN PPB - YR 2000, 2B MINUS BASE

(1) BETWEEN THE HOURS OF 11 AND 12

FIGURE 13 (concluded)

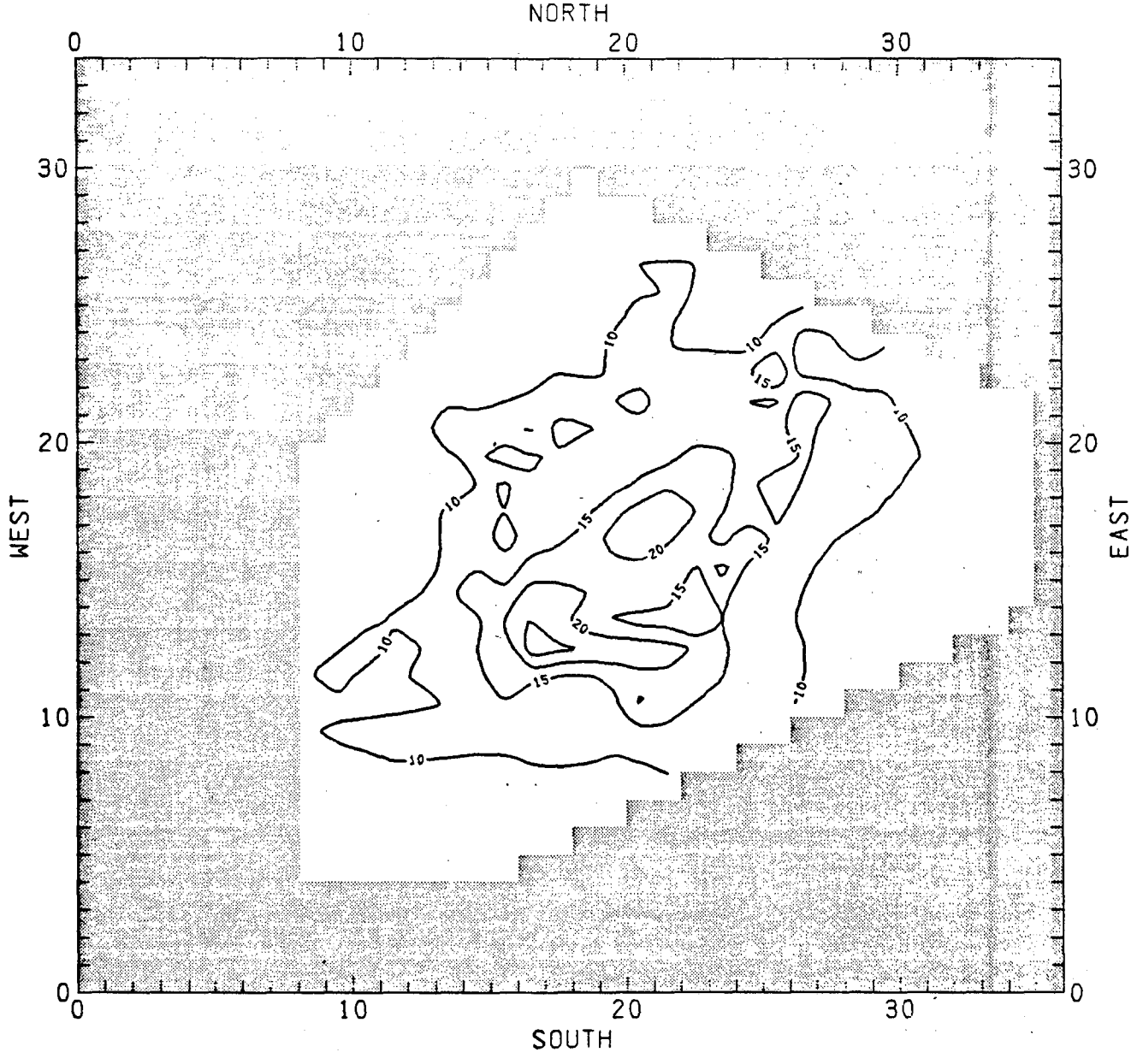

FORMALDEHYDE CONC (JULY 13) IN PPB - YEAR 2000 BASE CASE (LOWER IC)
FOR ALL HOURS

FIGURE 14

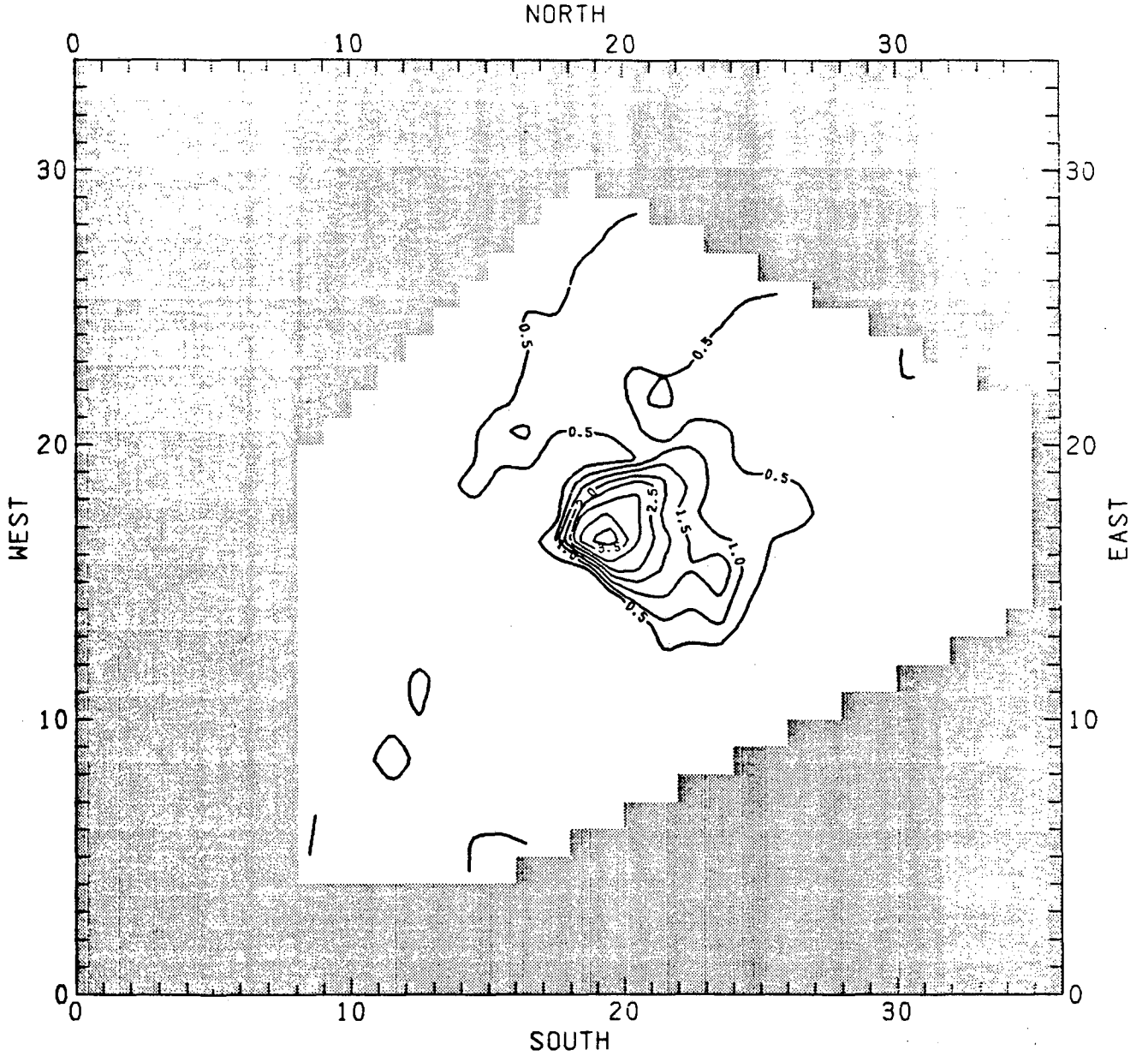

FORMALDEHYDE CHANGE (JULY 13) IN PPB - YR 2000, 2B MINUS BASE FOR ALL HOURS

FIGURE 15

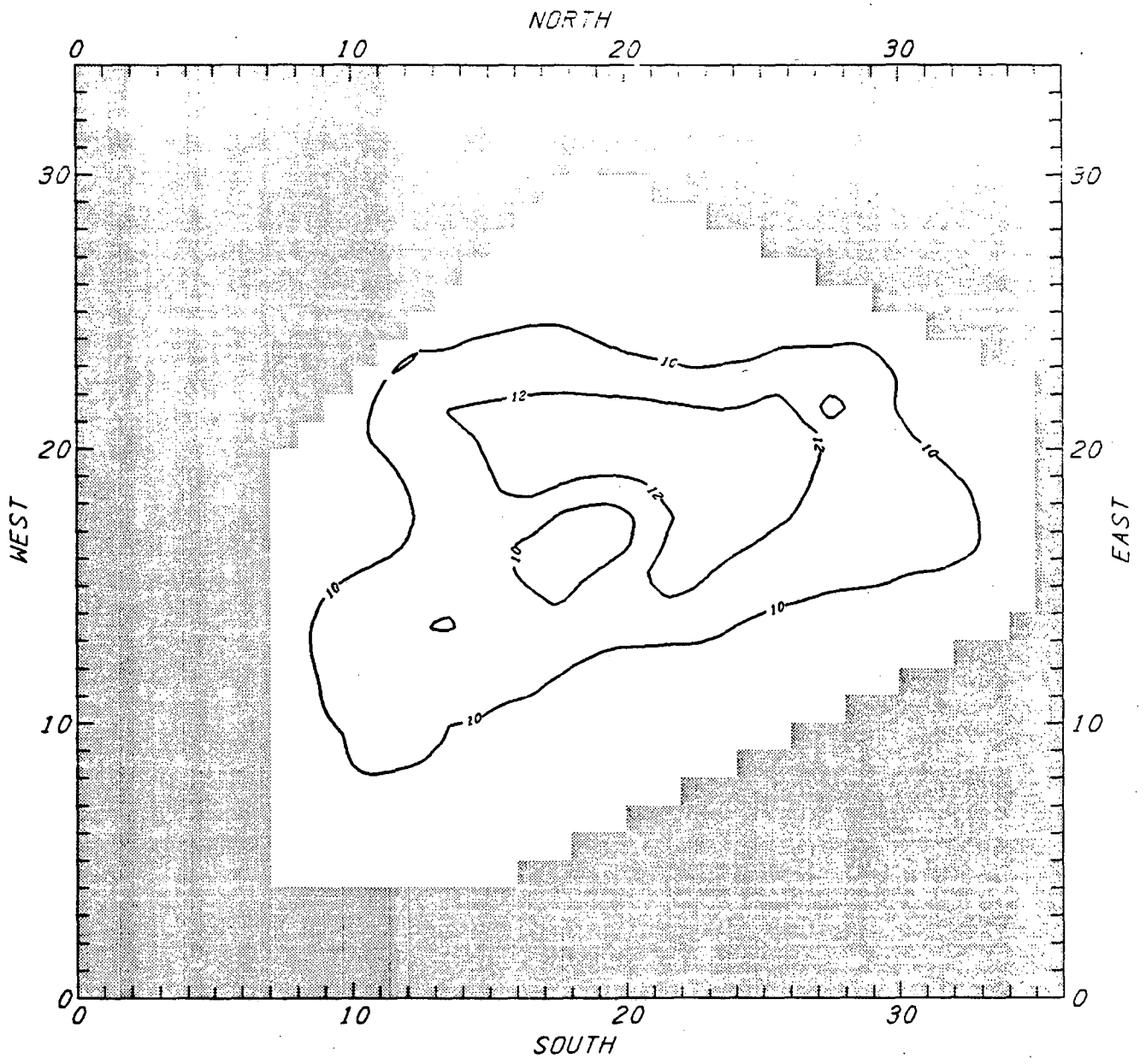

OZONE CONC (JULY 13) IN PPHM - YEAR 2000 BASE CASE (LOWER IC)

(a) BETWEEN THE HOURS OF 12 AND 13

FIGURE 16

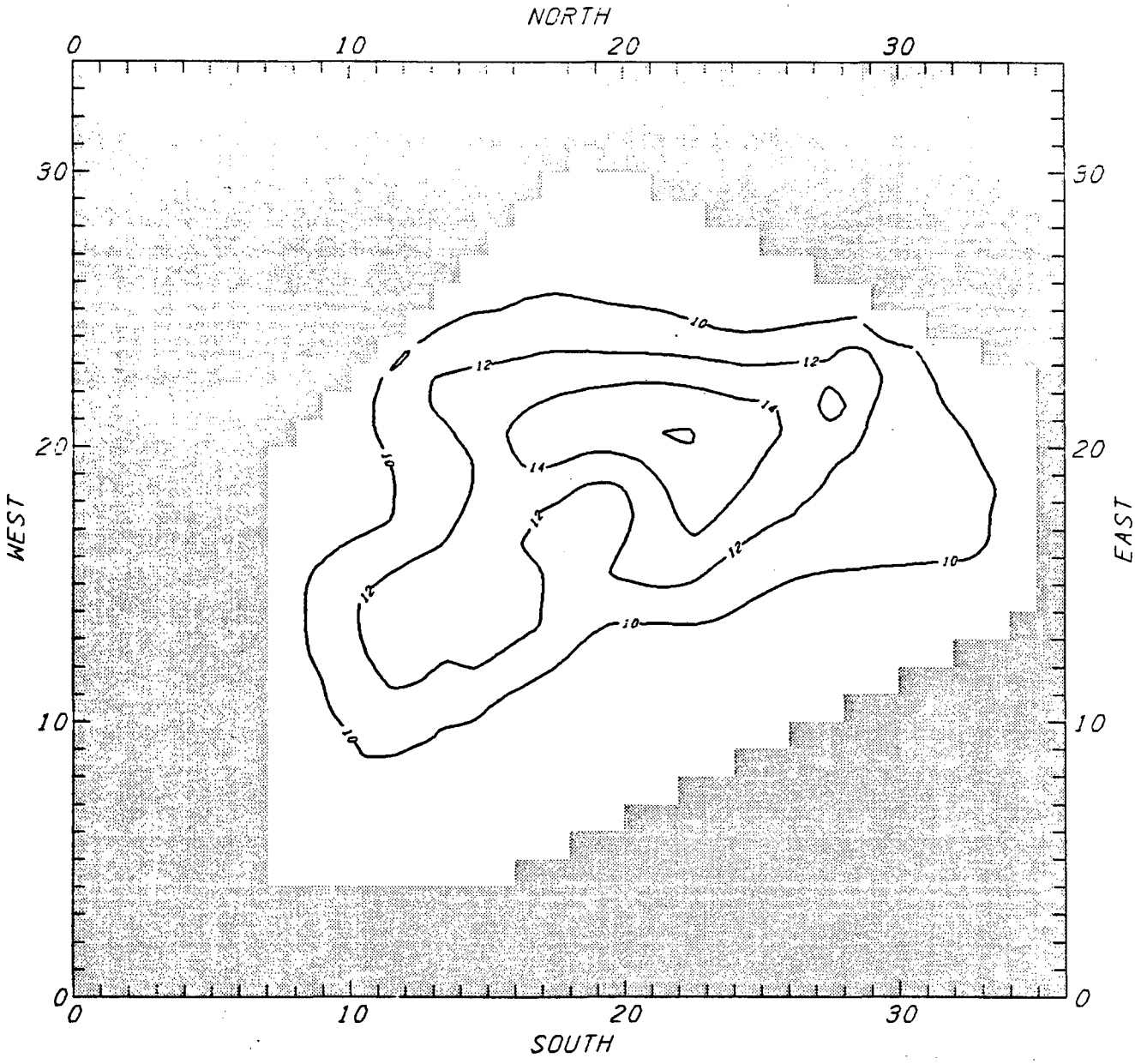

OZONE CONC (JULY 13) IN PPHM - YEAR 2000 BASE CASE (LOWER IC)

(b) BETWEEN THE HOURS OF 13 AND 14

FIGURE 16 (continued)

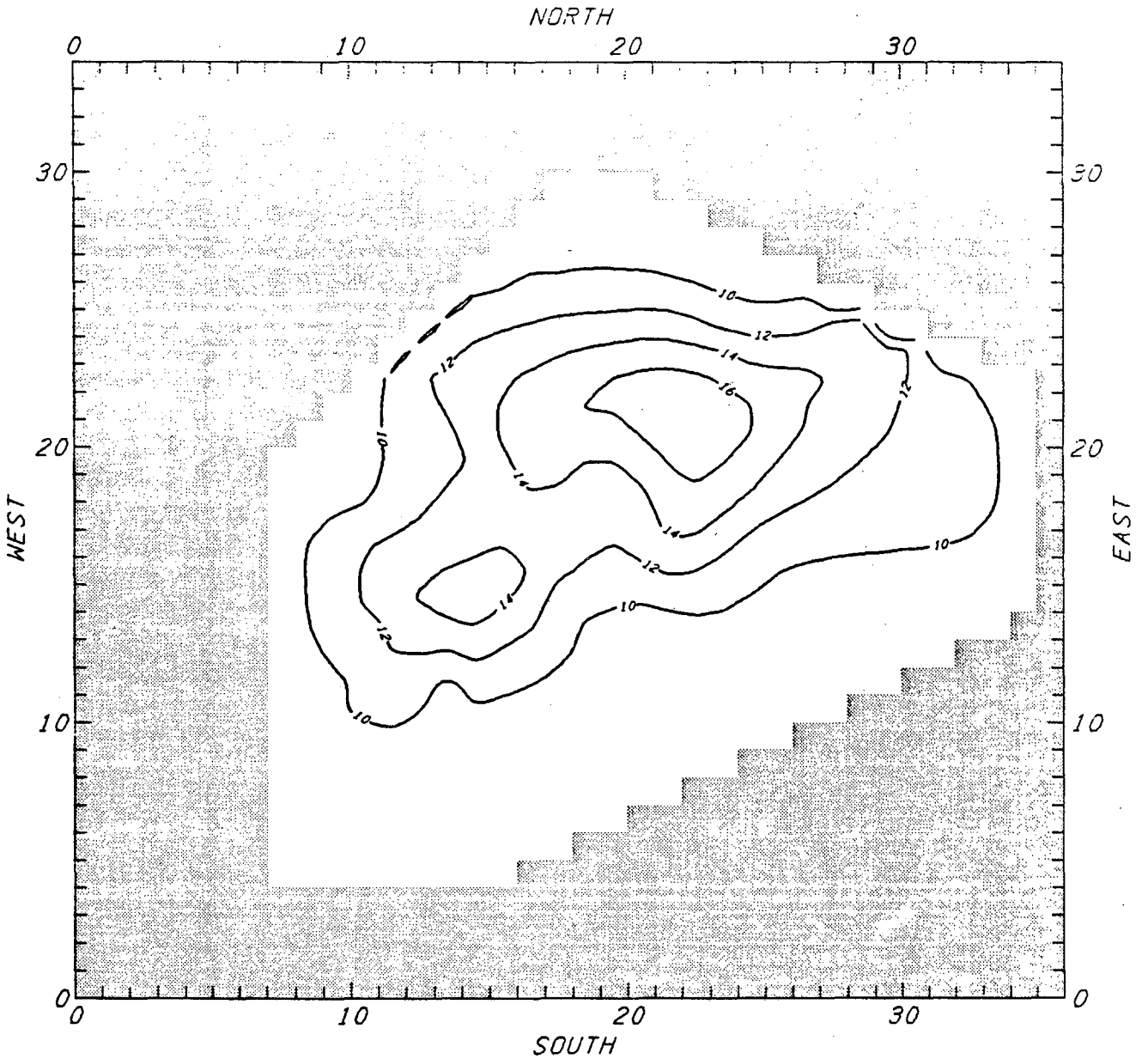

OZONE CONC (JULY 13) IN PPHM - YEAR 2000 BASE CASE (LOWER IC)

(c) BETWEEN THE HOURS OF 14. AND 15

FIGURE 16 (continued)

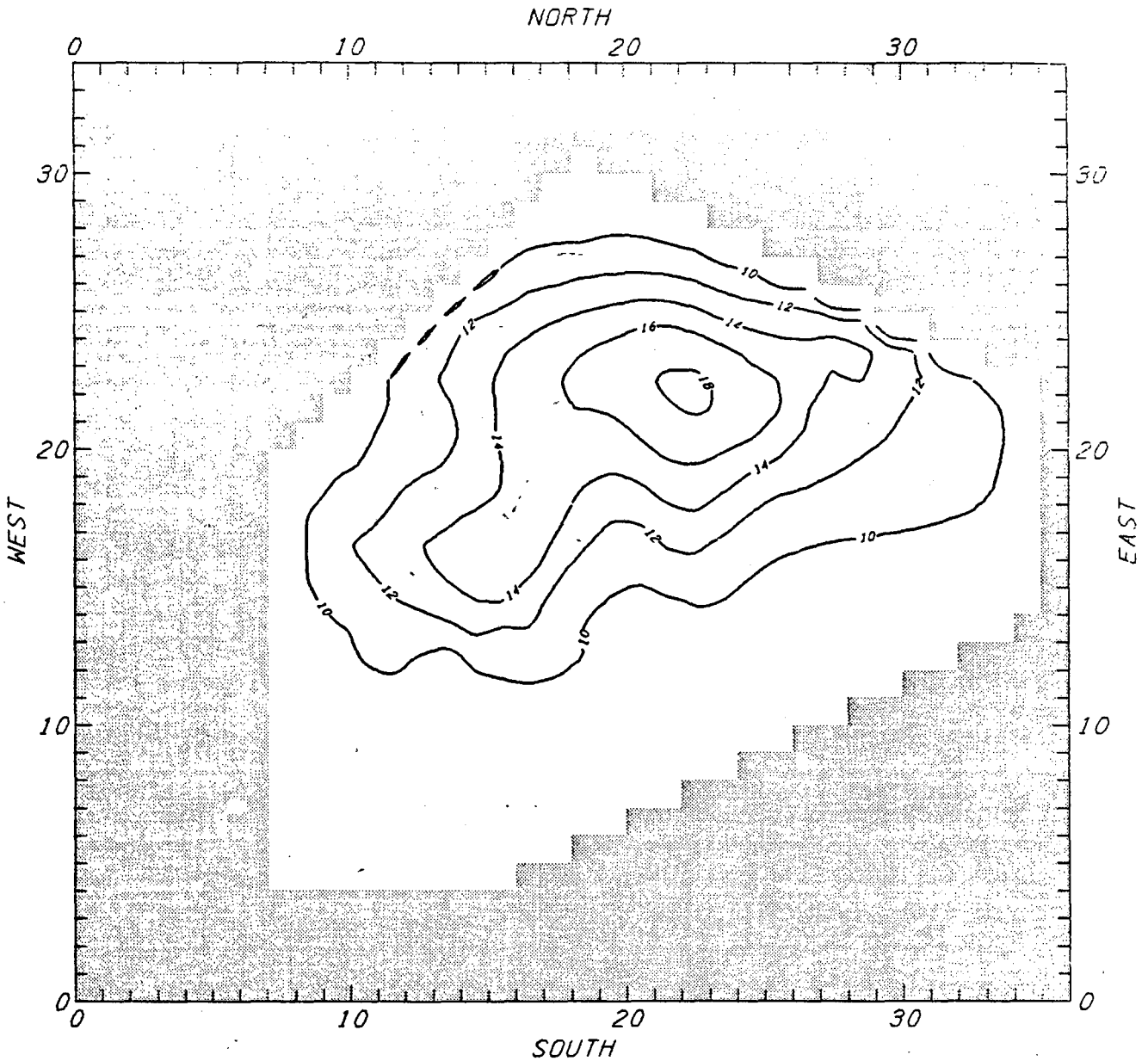

OZONE CONC (JULY 13) IN PPHM - YEAR 2000 BASE CASE (LOWER IC)
(d) BETWEEN THE HOURS OF 15 AND 16

FIGURE 16 (continued)

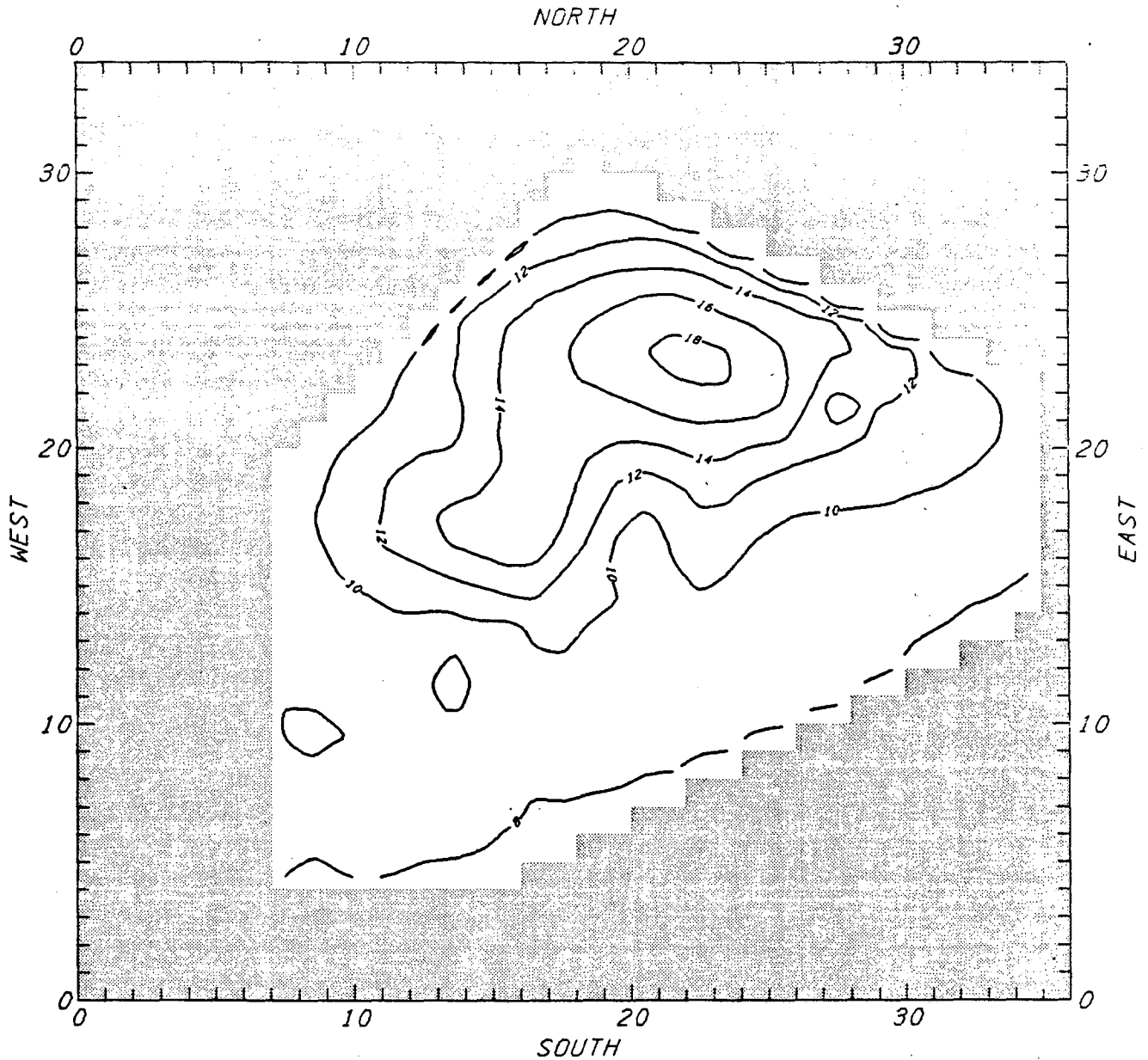

OZONE CONC (JULY 13) IN PPHM - YEAR 2000 BASE CASE (LOWER IC)

(e) BETWEEN THE HOURS OF 16 AND 17

FIGURE 16 (continued)

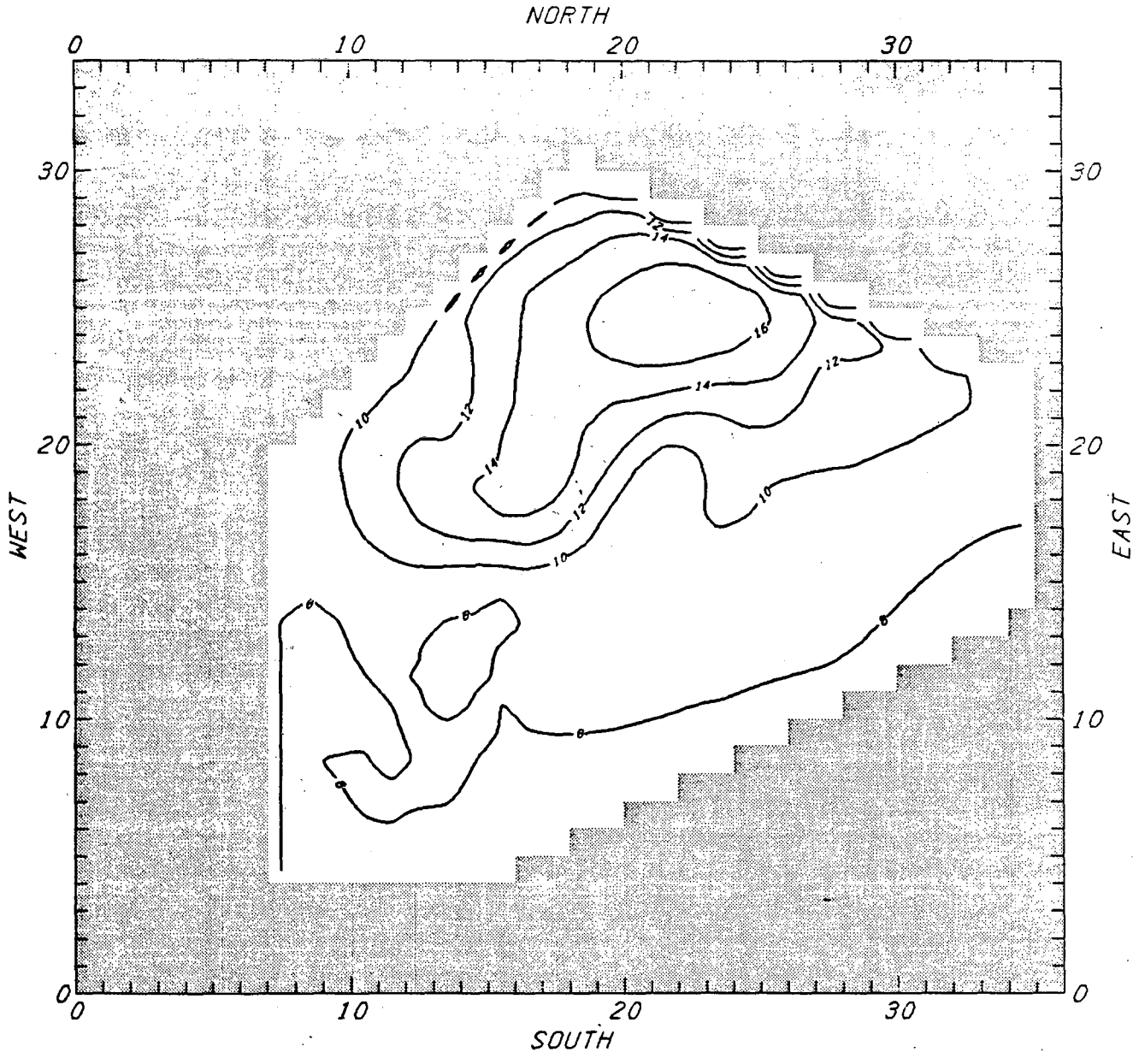

OZONE CONC (JULY 13) IN PPHM - YEAR 2000 BASE CASE (LOWER IC)

(f) BETWEEN THE HOURS OF 17 AND 18

FIGURE 16 (continued)

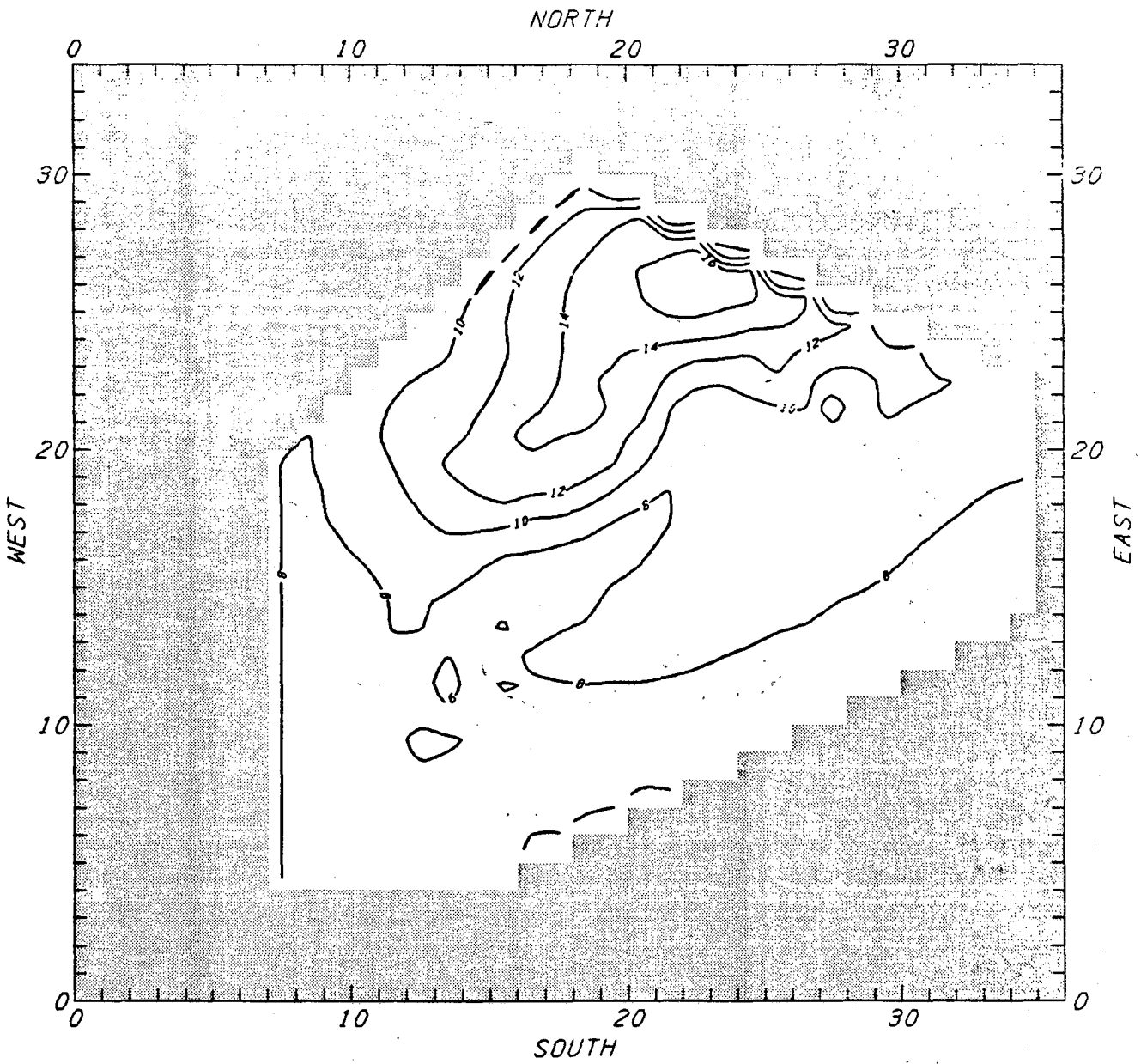

OZONE CONC (JULY 13) IN PPHM - YEAR 2000 BASE CASE (LOWER IC)
(g) BETWEEN THE HOURS OF 18 AND 19

FIGURE 16 (continued)

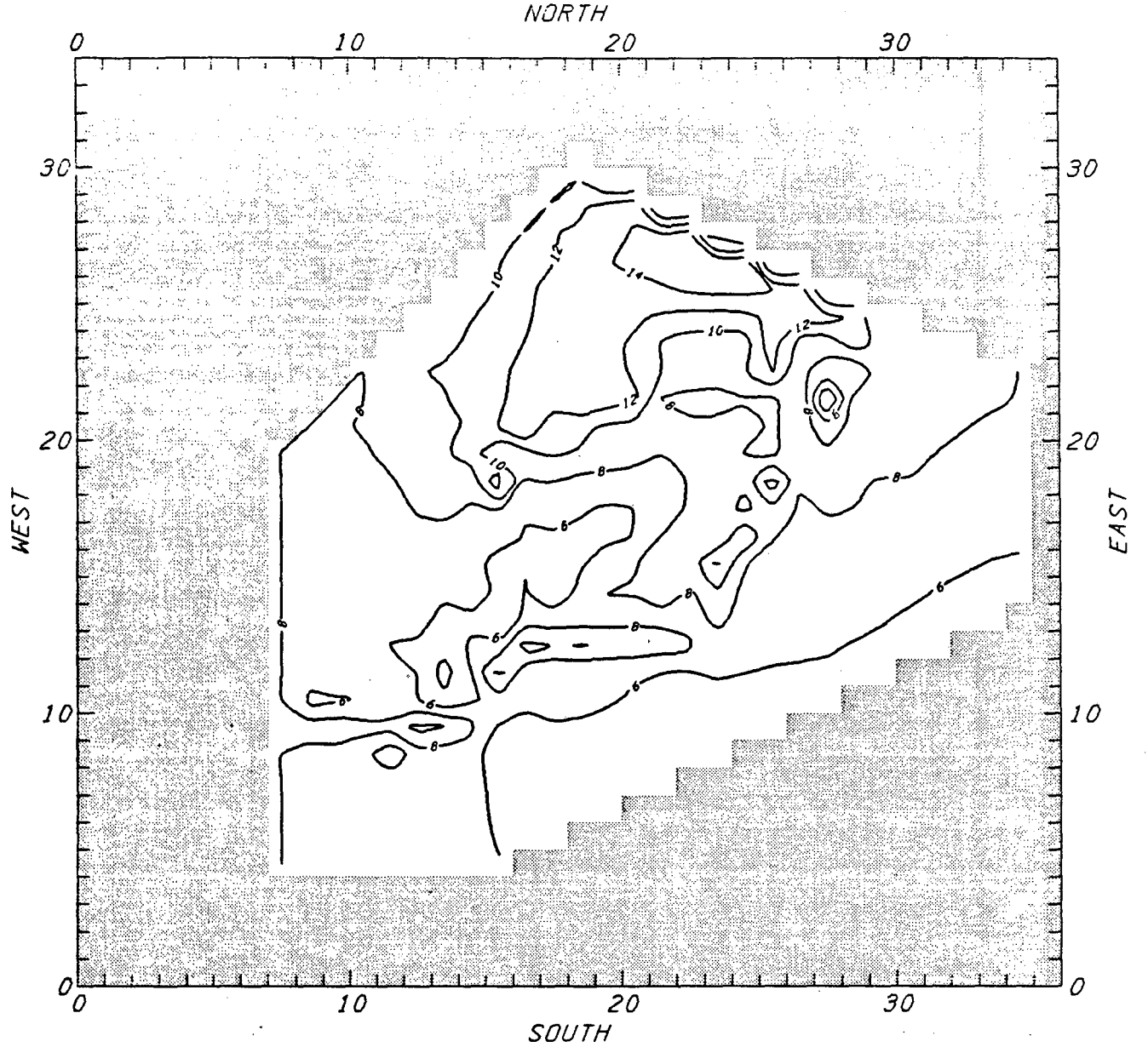

OZONE CONC (JULY 13) IN PPHM - YEAR 2000 BASE CASE (LOWER IC)

(h) BETWEEN THE HOURS OF 19 AND 20

FIGURE 16 (concluded)

REFERENCES

Ames, J., et al. 1978. "A User's Manual for the Airshed Model." U.S. Environmental Protection Agency, Research Triangle Park, North Carolina (SAI NO. EM78-89R2).

DVRPC. 1982. "Year 2000 Transportation Plan for the Delaware Valley Region." Delaware Valley Regional Planning Commission, Philadelphia, Pennsylvania.

DVRPC. 1983. "1982 Revision of the State Implementation Plan for Ozone and Carbon Monoxide for the Pennsylvania Portion of the Philadelphia Air Quality Control Region." Delaware Valley Regional Planning Commission, Philadelphia, Pennsylvania.

EPA. 1978. "User's Manual for Kinetics Model and Ozone Isopleth Plotting Package." U.S. Environmental Protection Agency, Research Triangle Park, North Carolina (EPA-600/8-78-014a).

EPA. 1982. "Emissions Inventories for Urban Airshed Model Application in the Philadelphia AQCR." U.S. Environmental Protection Agency, Research Triangle Park, North Carolina (EPA-450/4-82-005).

EPA. 1984. "Guideline for Using the Carbon-Bond Mechanism in City-Specific EKMA." U.S. Environmental Protection Agency, Research Triangle Park, North Carolina (EPA-450/4-84-005).

ESI. 1982. "Emission Inventories for Urban Airshed Model Application in the Philadelphia AQCR." Engineering-Science, Inc., Fairfax, Virginia (EPA-450/4-82-005).

Haney, J. L. 1985. "Evaluation and Application of the Urban Airshed Model in the Philadelphia Air Quality Control Region." U.S. Environmental Protection Agency, Research Triangle Park, North Carolina (EPA-450/4-85-003).

Killus, J. P., and G. Z. Whitten. 1981. "A New Carbon-Bond Mechanism for Air Quality Simulation Modeling." U.S. Environmental Protection Agency, Research Triangle Park, North Carolina (EPA-600/3-82-041).

Killus, J. P., and G. Z. Whitten. 1984. "Technical Discussions Relating to the Use of the Carbon-Bond Mechanism in OZIPM/EKMA." U.S. Environmental Protection Agency, Research Triangle Park, North Carolina (EPA-450/4-84-009).

Myers, T. C., D. C. Whitney, and S. D. Reynolds. 1979. "User's Guide to the SAI Trajectory Model, Volume II--Appendix E." U.S. Department of Transportation, Washington, D.C. (DOT-FH-11-8529).

Pefley, R. K., B. Pullman, and G. Z. Whitten. 1984. "The Impact of Alcohol Fuels on Urban Air Pollution: Methanol Photochemistry Study." U.S. Department of Energy, Washington, D.C. (DOE/CE/50036-1).

Reynolds, S. D., J. H. Seinfeld, and P. M. Roth. 1973. Mathematical modeling of photochemical air pollution--I. Formulation of the model. Atmos. Environ., 7:1033-1061.

Sigsby, J. E., S. Tejada, W. Ray, J. M. Lang, and J. W. Duncan. 1984. "Volatile Organic Compound Emissions from 46 In-Use Passenger Cars." Submitted for publication.

Whitten, G. Z., H. Hogo, and R. G. Johnson. 1981. "Application of the Empirical Kinetic Modeling Approach (EKMA) to Urban Areas." U.S. Environmental Protection Agency, Research Triangle Park, North Carolina (EPA-450/4-81-005A).

Whitten, G. Z. 1983. The chemistry of smog formation: A review of current knowledge. Environ. Int., 9:447-463.

Whitten, G. Z., and H. Hogo. 1983. "Impact of Methanol on Smog: A Preliminary Estimate." Systems Applications, Inc., San Rafael, California (SYSAPP-83/044).